

Design of Medium Size Blended Wing Body Subsonic Transport Aircraft

a project presented to
The Faculty of the Department of Aerospace Engineering
San José State University

in partial fulfillment of the requirements for the degree
Master of Science in Aerospace Engineering

by

Nishant Patel

May 2018

approved by

Dr. Nikos J. Mourtos
Faculty Advisor



San José State
UNIVERSITY

ABSTRACT

According to studies conducted by Federal Aviation Administration, US airline alone burn 16.2 billion gallons of aviation fuel per year which leads to more than three percent of air pollution of the U.S. The aviation industry contributes more than 1% of global air pollution. These figures may seem to be non-significant when compared to other sources of pollution but the aviation industry accounts for only 0.5% of world trade shipment with a global energy consumption of 2.2%. The current advances in electric battery and motors does not provide a replacement to gas-turbine engines in near future especially for long range aircrafts. This paper presents a conceptual design of a BWB aircraft with a passenger capacity of 160 people for a range of 9200 km with a cruise speed of 0.77 Mach number and is FAR 25 certifiable. The approach for designing an unconventional configuration includes traditional approach for aircraft design as well as novel method. In any range equation, lift to drag ratio plays a prominent role. For a BWB aircraft, this ratio is quite high and with increase in the engine efficiency, the fuel burn per passenger per km can be decreased substantially. The unibody design for BWB aircraft provides a low empty weight when compared to its conventional counterpart with similar passenger capacity and mission profile.

Contents

1. Introduction	8
2. Literature Review	10
3. Configuration Design.....	12
4. Mission Specification and Comparative Study.....	18
5. Weight Sizing and Weight Sensitivities	22
6. Performance Constraint Analysis.....	36
7. Fuselage Design.....	60
8. Wing, High Lift System & Lateral Control Design.....	80
9. Design of Empennage & Longitudinal & Directional Control.....	97
10. Landing Gear Design: Weight and Balance Analysis	108
11. Stability and Control Analysis.....	121
12. Drag Polar Estimation	124
13. Environment/ Economic Trade-off; Safety/ Economic Trade-off.....	129
14. Class II: Landing Gear Design.....	135
15. V-n Diagram	145
16. Class II: Weight Estimation.....	148
17. Future Work	153
References.....	154

List of Figures

Figure 1 Airbus A319	13
Figure 2 Northrop YB-49	13
Figure 3 Boeing X-48B (8.5% Scaled for Conceptual HWB Commercial Aircraft).....	14
Figure 4 Northrop Grumman B-2	14
Figure 5 Bombardier CS300	15
Figure 6 Preliminary Sketch of the proposed design	17
Figure 7 Mission Profile.....	19
Figure 8 Log – Log Chart of Weight Data.....	23
Figure 9 Log – Log Chart of BAE 146-200	23
Figure 10 Weight Inputs of Similar aircrafts for Regression Point	27
Figure 11 Plot of Trend Line for Regression Points	28
Figure 12 Empty Weight Calculation	29
Figure 13 Design Point Plot	30
Figure 14 Empty Weight Calculation.....	32
Figure 15 Trade Study-Range Vs. Payload.....	33
Figure 16 Trade Study- Takeoff Weight Vs. L/D	33
Figure 17 Definition of FAR 25 Take-off distances.	37
Figure 18 Take-off requirement chart for 5000 ft field.....	38
Figure 19 Take-off requirement chart for 6000 ft field.....	39
Figure 20 Take-off requirement chart for 7000 ft field.....	40
Figure 21 Take-off requirement chart for 10000 ft field.....	41
Figure 22 Definition of FAR 25 Landing Distance	42
Figure 23 Wetted Area (SWet) vs. Parasitic drag (f).....	45
Figure 24 Matching plot for manual calculations	51
Figure 25 Stall Speed Parameters	52
Figure 26 Take-off Parameters.....	52
Figure 27 Landing Requirements	53
Figure 28 FAR 25 Climb Requirements.....	53
Figure 29 Cruise Requirement.....	54
Figure 30 Matching Plot	54
Figure 31 Extrapolated Matching Graph.....	55
Figure 32 Optimum Design Point	56
Figure 33 Conceptual “gfan+” engine.	57
Figure 34 Dimension table.	61
Figure 35 Dimensions of standing male crew member	61
Figure 36 Cockpit design parameters.....	62
Figure 37 Wheel type controller-based dimensions	63
Figure 38 Quality of accessibility areas	63
Figure 39 Dimensions and Adjustments for cockpit design	64
Figure 40 Definition of radial eye vector	65
Figure 41 Visibility requirements	67
Figure 42 Cockpit layout	68
Figure 43 Multi-bubble configuration.....	69

Figure 44 Integrated skin and shell Concept.....	69
Figure 45 Oval fuselage.....	70
Figure 46 Definition of fineness ratio.....	70
Figure 47 Fuselage parameters.....	71
Figure 48 Top view of fuselage.....	72
Figure 49 Front view of fuselage.....	72
Figure 50 Rear view of the fuselage.....	73
Figure 51 Side view of the fuselage.....	73
Figure 52 3D view of the fuselage.....	74
Figure 53 Cabin layout 1.....	76
Figure 54 Cabin layout 2.....	76
Figure 55 Seating layout of NASA SUGAR Ray.....	77
Figure 56 Minimum aisle requirements.....	77
Figure 57 Dimensions of seat for different class.....	78
Figure 58 Frame depth, spacing and longeron spacing.....	78
Figure 59 Cabin planform and seating layout of the proposed aircraft.....	79
Figure 60 Database for Wing.....	82
Figure 61 Wing Geometric Data for Conventional Aircraft.....	82
Figure 62 SUGAR RAY Geometric Data.....	83
Figure 63 Mach Number vs Leading Edge Sweep.....	83
Figure 64 Design Mach Number vs Thickness Ratio.....	84
Figure 65 NASA (2)-0714.....	85
Figure 66 NASA(2)- 0012.....	86
Figure 67 NASA (2)-0412.....	86
Figure 68 3-D View of the Wing.....	88
Figure 69 Front View of the Wing.....	88
Figure 70 Side View of the Wing.....	88
Figure 71 Wing planform data.....	89
Figure 72 Wing planform output.....	89
Figure 73 Wing planform.....	89
Figure 74 Elevons input data.....	89
Figure 75 Wing planform with elevons.....	90
Figure 76 Elevons output data.....	90
Figure 77 Slats input data.....	90
Figure 78 Slats output.....	91
Figure 79 wing planform with slats and elevons.....	91
Figure 80 High Lift Devices.....	92
Figure 81 Graphical Representation of the MAC.....	95
Figure 82 Definition of moment arms.....	98
Figure 83 Data of geometric constraints for empennage.....	100
Figure 84 SUAGR RAY Data.....	101
Figure 85 Vertical Tail inputs.....	102
Figure 86 Tail geometric outputs.....	102
Figure 87 Tail geometry.....	103

Figure 88 Vertical tail planform	104
Figure 89 Rudder inputs.....	104
Figure 90 Rudder output.....	104
Figure 91 Vertical tail with rudder	105
Figure 92 2D CAD for Vertical tail	106
Figure 93 Weight distribution of SUGAR Ray.....	109
Figure 94 CG for Wing and Tail.....	110
Figure 95 CG for nacelle and fuselage.....	110
Figure 96 Side View with CG location	112
Figure 97 Top View with CG location	112
Figure 98 Proposed Aircraft: Weight excursion diagram of the proposed aircraft	113
Figure 99 Longitudinal tip over criteria.....	114
Figure 100 Lateral tip over criteria.....	114
Figure 101 Ground clearance requirement	115
Figure 102 Landing gear disposition	116
Figure 103 Geometric definitions for Static load calculation	116
Figure 104 Contact Surface	118
Figure 105 Revised CG excursion diagram of the proposed aircraft	119
Figure 106 X-Plot for Directional Stability.....	122
Figure 107 Wetted area vs equivalent parasite area.....	126
Figure 108 Mach number vs zero lift drag rise	127
Figure 109 Front view of the aircraft	129
Figure 110 Rear view of the aircraft.....	129
Figure 111 Side View of the aircraft.....	129
Figure 112 Top view of the aircraft.....	130
Figure 113 3D view of the aircraft.....	131
Figure 114 Tire Pressure for Various Types of Runway Surfaces	136
Figure 115 Landing Gear Wheel Layouts	136
Figure 116 Effect of Tire Pressure and Tire Load on LCN	137
Figure 117 Types of Aircraft Tires	138
Figure 118 Rake and trail definition.....	141
Figure 119 Trailing Link Mechanism	142
Figure 120 Self Locking Brace Actuator	142
Figure 121 Liquid Spring Shock Absorber	143
Figure 122 Maneuver V-n Diagram Figure 123 V-n Gust Diagram.....	145
Figure 124 V-n Gust Diagram	147
Figure 125 V-n Maneuver Diagram.....	147

List of Tables

Table 1 Comparison of BWB and Conventional Design	10
Table 2 Important Specification Comparison	12
Table 3 Configuration and capabilities of similar aircraft	20
Table 4 Comparison of Parameters.....	21
Table 5 Aircraft type and Weight Data of Similar Aircraft.	22
Table 6 Suggested Values for L/D, C_j , \bar{q}_p and C_p	25
Table 7 Take-off Distance sizing for STOFL=5000 ft at sea-level	38
Table 8 Take-off Distance sizing for STOFL=6000 ft at sea-level	39
Table 9 Take-off Distance sizing for STOFL=7000 ft at 10000 ft.....	40
Table 10 Take-off Distance sizing for STOFL=10,000 ft at 10000 ft.....	41
Table 11 W/STO- results with WL/W-TO=0.60.....	43
Table 12 W/STO- results with WL/W-TO=0.65.....	43
Table 13 W/STO- results with WL/W-TO=0.70.....	44
Table 14 Results from the secondary method	44
Table 15 Correlation Coefficient	46
Table 16 Summary of Drag Polars	46
Table 17 FAR 25.111 (OEI).....	47
Table 18 FAR 25.121 (OEI).....	47
Table 19 FAR 25.121 (OEI).....	48
Table 20 FAR 25.121.....	48
Table 21 FAR 25.119 (AOE)	49
Table 22 FAR 25.121.....	49
Table 23 gfan+ Key Weight, Geometry, Performance.	57
Table 24 Wing Parameters Summary.....	87
Table 25 Data of the Proposed Aircraft.....	92
Table 26 Spar Calculation.....	93
Table 27 Geometric data for proposed tail.....	101
Table 28 Weight distribution of proposed aircraft	109
Table 29 Weights and moment arms of the proposed aircraft	111
Table 30 Wheel dimensions for main landing gear.....	117
Table 31 Wheel dimensions for nose landing gear	117
Table 32 Contact area for nose and main landing gear	118
Table 33 Revised moment arm of the proposed aircraft.....	118
Table 34 Loading Conditions and CG of the proposed aircraft	119
Table 35 Drag increment due to flaps.....	127
Table 36 Drag increment due to landing gear	127
Table 37 Zero lift drag coefficient: Proposed aircraft	128
Table 38 Summary of Drag Polars	128
Table 39 Drag Polars	128
Table 40 Aircraft Details.....	131
Table 41 Load Values	139
Table 42 Sorted Wheel Information	140
Table 43 Summary of Weight Estimation.....	151

1. Introduction

Transportation plays a major role in growth of the country and preserves the well-being of the nation's economy. Aerial transport being a crucial part of this sector, has evolved as fastest and safest with farthest reach of all the mode of transports. Over half the population of the world uses the service provided by air transport, which again provides employment, directly or indirectly, to more than 56 million people around the globe. Around 0.5% of world trade shipments are transported by air but it represents this represent 35% value of the world trade value. The statistics are impressive, but it also consumes 2.2% of world energy.

In last 35 years, there has been 60% improvement in aircraft fuel efficiency and people being affected by aircraft noise has been reduced by 95% but on the same hand, there has been a six-fold increase in the total world commuters by air. Because of the continual growth of demand, the emission of air pollutants from the aviation is increasing and progress in noise reduction is very slow. Due to environmental degradation at an alarming rate, there are increasing constraints being imposed on aviation industry.

In the wake of these problem, FAA is working with its stake holders to find an innovative solution. To motivate companies to research an alternative option, NASA has launched a program named Environmentally Responsible Aviation which strives to reduce the emission of pollutants and overall aircraft sound by 75% by 2025. NASA as a dedicated research team to called Subsonic Ultra Green Aircraft Research (SUGAR), which is compiled to work on advance concepts of aircraft design which meet the stringent constraints imposed on aircrafts for the harmonious and sustainable growth of industry.

SUAGR research team has been working on various project like High, Volt, Ray and High to integrate innovative designs with advance design concepts. This report is based on the work under SUGAR Ray, a project which is dedicated to introducing the blended wing body conceptual design to the commercial airlines. Its main objective is to reduce the emissions by reducing the fuel consumption by 30% and limiting the overall noise level to 42dB. For achievement of the extremely tight limitations, engineers sought help od very unconventional design of hybrid wing body.

A hybrid wing body is an aircraft with no distinguishing line between the fuselage and wing. The wings are smoothly blended into the body. Such an approach is efficient due to high lift producing wings and wide airfoil shaped body. This configuration allows entire body to generate lift and potentially decreasing the drag. As the entire body generates lift, unlike the conventional tube-and-wing configuration in which fuselage leads the drag production hence reducing the efficiency of the aircraft, the wingspan can be reduced as the potential wing area can be reduced to generate same amount of lift. The SUGAR Ray research team has proposed the use of a high bypass 2 spool turboprop engine while the proposed aircraft is designed for the use of gas-

electric hybrid propulsion design for an unconventional hybrid wing configuration for commercial use. The use of hybrid system will decrease the emission of pollutants significantly as for some phases of the aircraft mission profile, purely electric power will be used hence cutting of the emissions.

2. Literature Review

Humans made first aircraft in 1903, The Wright Flyer and after 43 years first swept wing jet, Boeing B-47, took its flight in 1946. The B-47 was the mile stone for the modern-day transport jet. The transition of research from Tube-and-Wing (TW) configuration to Blended-Wing-Body (BWB) began when NASA sponsored study to create a new, more efficient configuration for subsonic transport. Research was focus on increasing the wetted area which would directly increase the aerodynamic efficiency of the aircraft. There were various alternatives were proposed to conventional Tube-and-Wing and one of them was BWB configuration. It was the only design which interested engineers and scientists as it promises to increase in aerodynamic efficiency by 25%^{1,2}.

In 1993, Boeing proposed its first design of Blended-Wing-Body for subsonic commercial transport. In this study, 800 passenger capacity BWB and conventional designs were sized and compared for a range of 7000 nautical miles. Results showed substantial increase in performance of BWB over its conventional counterpart. The takeoff weight was reduced by 15% and 27% reduction in fuel burn per seat. The results were achieved with use of innovative structural concept which became pivotal for the development of BWB. The wetted area was reduced by 33% which resulted in exceptional aerodynamic efficiency as the cruise lift to drag ratio is related to wetted area. LW 102A airfoil was designed for C_l 0.25 and $C_{m/4} = +0.03$ at $M=0.7$ was modified using the method of Ref. 3. The resulting airfoil provided the cross-sectional shape of center body.⁴

Table 1 Comparison of BWB and Conventional Design

Model	BWB	Conventional
Passenger	800	800
Range	7000 nm	7000 nm
MTOGW, lb	823,000	970,000
OEW, lb	421,000	470,000
Fuel burned	213,000	294,000
L/D at Cruise	23	19
Thrust, total lb	3 x 61,600	4 x 63,600

The initial studies for BWB configuration by Boeing motivated further research in the field and subsequently yielded the development of a family of BWB subsonic aircraft ranging from 200 to 600 passenger capacities with a high level of parts commonality and manufacturing efficiency. An 8.5% scale model of a commercial subsonic BWB aircraft by Boeing called X-48B. There are 3 variants to the design each model designed for specific goal. X-48A was the first and most preliminary design which was canceled before production. X-48B was designing to study the aircraft dynamics and aerodynamic of a 450 passenger BWB aircraft. X-48C is designed to test the capability of BWB in lowering the noise level of aircrafts.

Surplus resources are available for designing a conventional TW aircraft. Many off the shelf software with user-friendly environment are also available for analysis of a conventional aircraft.

BWB being an unconventional and innovative configuration, there is lack of any established design methodology or analysis software. NASA Langley Research Center has updated the Flight Optimizing System (FLOPS) for analysis of BWB⁵. The algorithms created for traditional TW configurations were modified to make FLOPS compatible to layout and size HWB cabin. Northwestern Polytechnical University collaborated with Commercial Aircraft Corporation of China to introduce high fidelity aerodynamics analysis tools and CFD- driven optimization and inverse design⁶. Such methods were not implemented in designing BWB aircraft as it pursues high cruise efficiency while satisfying a unique set of design requirements and constraints. Using high fidelity aerodynamic analysis tool in optimization design leads to high computational cost, which is a major obstacle to incorporation of CFD-driven optimization in BWB design. A new module was created in MATLAB and was validated for a 150 passenger BWB, which is the smallest in the current researches.

3. Configuration Design

1. Introduction

The previous report provided a brief preview of the aircraft that was proposed to design. The next step in design process is to define the configuration of the aircraft. The proposed aircraft is a hybrid wing body aircraft which a very unconventional design, so the configuration will differ from the traditional tube-and-wing configuration.

2. Comparative Study of Airplanes with Similar Mission Performance

2.1 Comparison of Weights, Performance and Geometry of Similar Airplanes

Table 2 Important Specification Comparison

Table 2: Comparison of Parameters	Northrop YB-49	Boeing X-48	Northrop Grumman B-2	Airbus A319	Bombardier CS300
Take- off weight	87,969 kg	227 kg	170,600 kg	75,500 kg	63,095 kg
Aspect Ratio	7.2	4.1	5.87	10.47	10.97
Thrust/Weight	0.23	NA	0.205	1.59	
Range	16,057 km	NA	11,100 km	6,950 km	11,100 km
Service ceiling	13,900 m	3,000 m	15,200 m	11,900-12,500 m	12,497m
Cruise Speed	587 kmph	219 kmph	900 kmph	829 kmph	829 kmph
Wing Span	52.43 m	NA	52.4 m	35.8 m	35.1 m
Wing Area	371.6 m ²	NA	478 m ²	122.4 m ²	112.3 m ²

22 Configuration Comparison of Similar Airplanes

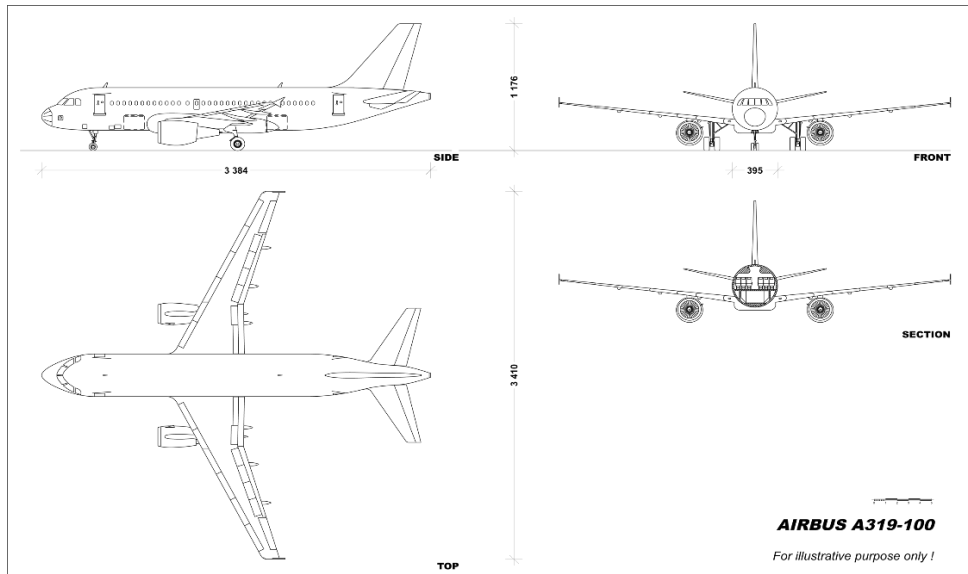


Figure 1 Airbus A319

NORTHROP YB-49

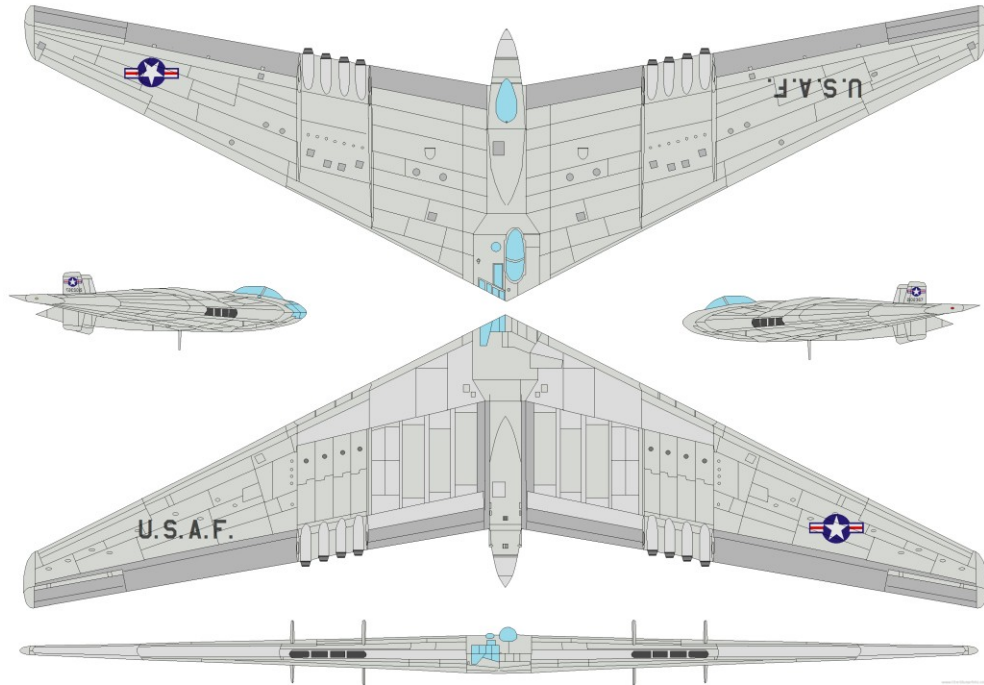


Figure 2 Northrop YB-49



Figure 3 Boeing X-48B (8.5% Scaled for Conceptual HWB Commercial Aircraft)

United States Patent [19]

Waaland et al.

[54] AIRCRAFT

[11] Patent Number: **Des. 314,366**

[45] Date of Patent: **Feb. 5, 1991**

[73] Assignee: **Northrop Corporation, Hawthorne, Calif.**

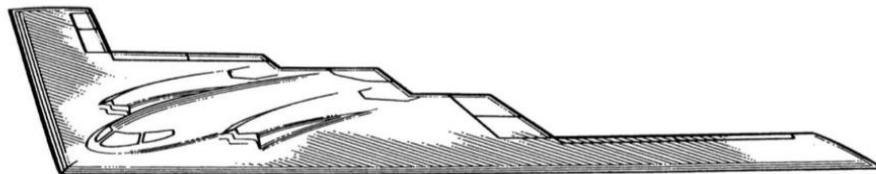


FIG. 1

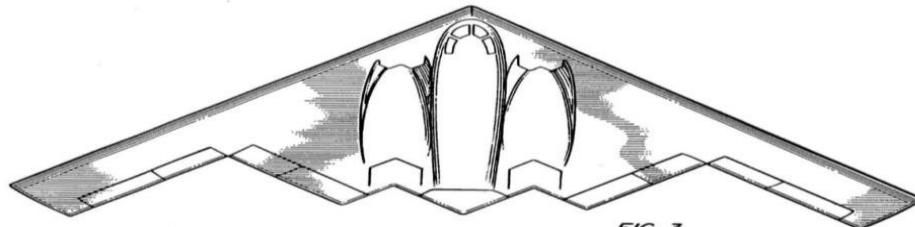


FIG. 3



FIG. 4



FIG. 6

Figure 4 Northrop Grumman B-2

CS300 External Dimensions

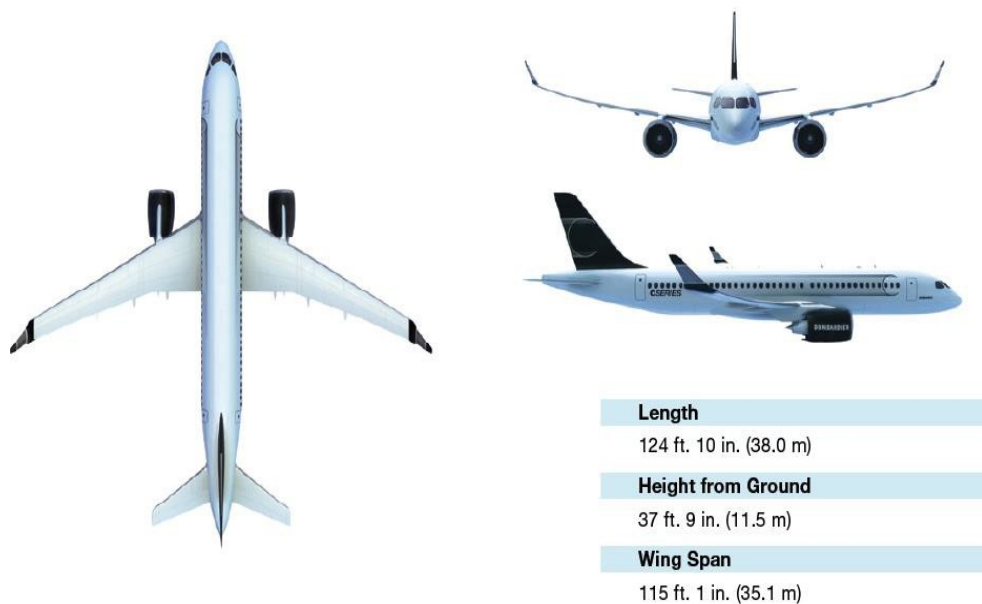


Figure 5 Bombardier CS300

23 Discussion

The above list includes two conventional configurations aircraft and two hybrid wing configurations. Boeing X-48 is an 8.5% sub scaled model of a conceptual aircraft that uses blended wing design for commercial aircraft.

Conventional Configuration:

- The tube-and-wing design airplanes have a pair of swept back wings to reduce drag at the speed of 0.8 Mach with a conventional tail plane design for simplicity and ease of maintenance.
- Powered by twin jet turbine engine hanging from the wing which helps it to counter the lift generated by the wing and prevent failure of it. The empennage features standard tail.

Unconventional Configuration:

- The two-unconventional design aircraft feature blended wing which provides a high range and high aerodynamic efficiency. The listed airplanes were used for military purpose with stealth capabilities.
- Other difference is missing vertical stabilizer. The directional stability is provided by cranking the wing tips at an angle and use spoilers for yaw control.
- Northrop Grumman B-2 has engine mounted in the structure of the delta wing which reduces the drag and is important for the stealth operation, while YB-49 has series of engines at the rear of plane with two pairs of vertical stabilizers providing the directional stabilizer.

Boeing X-48 is a delta wing design which has engines mounted at the rear of airplane and has a vertical stabilizer which has the same effect on stability and control as the conventional design.

3. Configuration Selection

3.1 Overall Configuration

The overall configuration depends on the mission specification of the proposed aircraft. The aircraft to be designed has a mission specification that allows it to be used in for commercial airlines as a passenger transport carrier. It is a land-based aircraft. It infuses a military use blended wing body to the commercial airplanes.

3.2 Wing Configuration

The conventional configuration has a straight or swept back wings and the aircraft can be high-winger, mid-winger or low-winger. As it is a blended wing configuration, there is no differentiable fuselage and wing like that of tube-and-wing design. A swept back wing for drag reduction when it flies at its maximum speed.

3.3 Empennage Configuration

Blended wing body does not have an empennage. The horizontal wing is integrated with the body and the vertical stabilizers can be present at the rear of the body or can be integrated in the winglets. With much more advance design concepts and augmented controls, the tail plane can be eliminated but it has not been tested in any of the commercial aircrafts. The aircraft would be inherently unstable which contrasts with the conventional commercial aircrafts which are designed inherently stable. The response of the innovative rudder would be slower when compared to its processors.

3.4 Integration of the Propulsion System

The position of the propulsion system plays a major role in efficiency and noise experiment within the cabin of the aircraft. To reduce the aircraft the engines would be placed at the rear of the airplane. A hybrid power house is to be used. The gas-powered engines would provide the necessary power for take-off and landing, while during cruise, the aircraft will switch to electric motor or an engine powered by a fuel cell. This would create a problem to balance the aircraft around the center of gravity as well as the weight would increase due to battery for the electric motors.

3.5 Landing Gear Disposition

All passenger planes must successfully clear the safety regulations as it would be a matter of hundreds of lives. The safest landing gear configuration is the tricycle configuration, as it provides

ease of landing and a perfectly horizontal surface which is essential for comfort of passengers as well as crew. The horizontal orientation of the airplane makes it easy to load cargo and freight. As well with the advantages, the weight of the aircraft would increase as the nose landing wheel would have to be made stronger in comparison with others as it would support 20-30% weight of the aircraft. Positioning the landing gears should be precise with respect to center of gravity else there is fear of toppling the airplane during braking.

3.6 Proposed Configuration

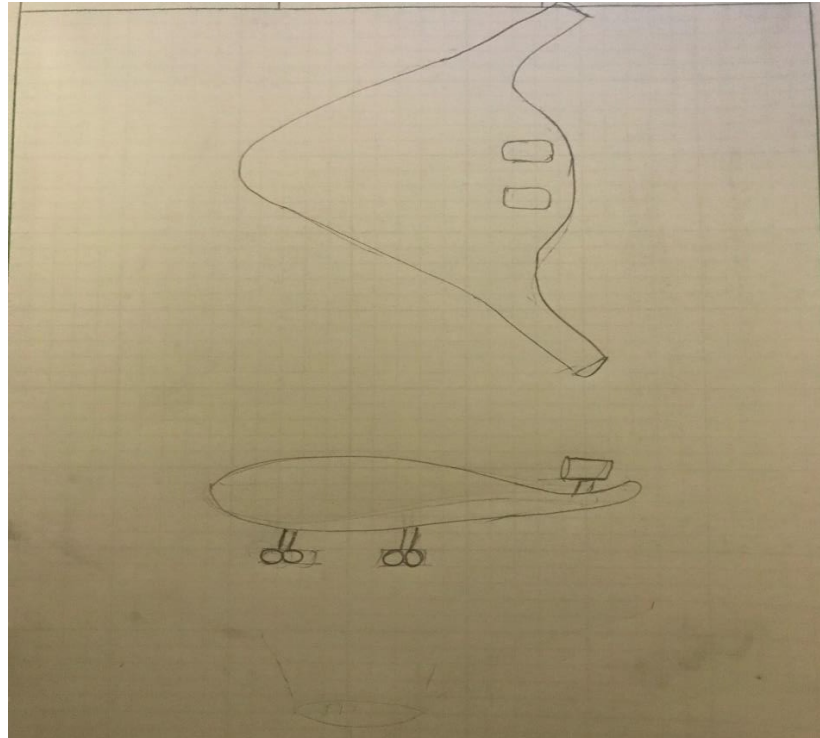


Figure 6 Preliminary Sketch of the proposed design

4. Mission Specification and Comparative Study

1. Introduction

The hybrid wing configuration has been a subject of study over past several decades with as a potential of subsonic commercial transport and cargo aircraft. The aerodynamic efficiency of the new and advance configuration tends to increase the fuel efficiency and noise reduction. An 800 passenger HWB design was introduced by Liebeck, et. al¹ which provided 27% of fuel burn advantage compared to its conventional tube and wing design. Another study was carried out for a 450 passenger HWB aircraft, but no comparative study based on performance was included in research. Liebeck used this study to compare it with Airbus A-380 aircraft and estimated that a 32% of fuel burn advantage can be gained from the HWB configuration, however no comparisons to advance TW concepts were provided². Different studies have shown that there is decrease in 27 – 30% of fuel consumption. A study was carried out for which ten new vehicle concepts were developed; five advance TW aircraft and five equivalent HWBs. Even after research and development of the HWB configuration for over three decades, it is not being used in the commercial flights because for equivalent passenger capacity, the wingspan of HWB aircraft is significantly higher due to which it cannot be accommodated at the existing airport around the world. Another reason being it does not meet the stringent safety regulations imposed by FAA, with less number of gates for entering and evacuating the aircraft, the proposed designs cannot be abandoned within 90 seconds of time. The configuration depends on the many of new advance technologies which are currently under research and development. Still technology is amateur and there is a high degree of risk in using it for commercial aircrafts.

2. Mission Specification

The goal of the design is to introduce the HWB configuration to commercial aircrafts which is more efficient and meeting all the safety requirements which are proposed by FAA. The benchmark of the design would be the specifications laid by the ERA program of NASA.

- Payload: 160 passengers with a total weight carrying capacity of 25000 kg.
- Number of crew members: 4
- Range: 3000 nm
- Cruise speed and Mach number: 0.85
- Take-off field length: 2744 m
- Landing field length: 1900 m
- Approach speed: <150 knots
- Noise requirements: 42 dB

2.1 Mission Profile

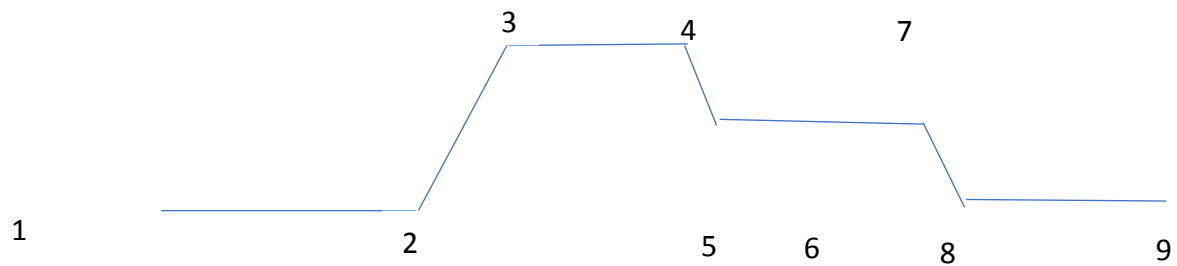


Figure 7 Mission Profile

- 1: Engine Start and warm up
- 1-2: Taxi
- 2: Take-off
- 2-3: Climb
- 3-4: Cruise
- 4-5: Descent

2.2 Market Analysis

Global warming and depletion of fossil fuels is the most critical problem that is being faced by the world. The environment related problems led to the foundation of ERA by NASA which aims for greener aircrafts. Extensive research is going on the alternative fuels and power houses, but it will take a significant amount of time to develop a technology which is as reliable as current aircraft configurations and aviation engines. The HWB configuration for commercial aviation can be developed in much lesser time and from existing technologies. NASA agreed to give away a prize money of \$11 million dollars for the company which comes up with most feasible and efficient HWB design for the commercial aircraft.

2.3 Technical and Economic Feasibility

Innovative design or product requires a lot of research. The designing process necessitates many iterations which requires a lot of time and financial investments. Developing a new HWB commercial aircraft is not simple and require decades of research, which was true of any simple or advance TW aircrafts. Modern technologies and advance carbon structures make it feasible to develop such aircraft.

2.4 Critical Mission Requirements

The HWB design has the tendency of increasing the wing span which makes it impossible to accommodate it in the current airports. The critical factors that would dominate the design of the aircraft:

- Payload
- Range
- Wing span
- Safety norms for evacuation
- Fuel consumption

The above-mentioned factors have the weight to change the shape and design of the aircraft.

3. Comparative Study

HWB for commercial aircrafts have not been introduced. All the designs are under study so there are no exactly same aircrafts with similar mission specifications to compare with. But there are BWB aircrafts which are developed by the military for their sole purposes or the scaled down models which are developed by the commercial aircraft manufacturing companies.

3.1 Mission Capabilities and Configuration Selection

Table 3 Configuration and capabilities of similar aircraft

Northrop Grumman YB-49	Boeing X-48B	Northrop Grumman B-2
 <p data-bbox="224 1402 331 1436">Figure 2</p>	 <p data-bbox="634 1402 742 1436">Figure 3</p>	 <p data-bbox="1062 1402 1169 1436">Figure 4</p>
<p data-bbox="224 1518 607 1703">It was a prototype of jet powered heavy bomber with a configuration of a flying wing. The aircraft was never put in production.</p>	<p data-bbox="634 1518 1036 1703">It is a BWB configuration and have developed as a subscaled model for ERA program. It is explicitly developed for commercial aircraft.</p>	<p data-bbox="1062 1518 1403 1665">A flying wing design developed as a stealth bomber for anti-aircraft defense.</p>

3.2 Comparison of Important Parameters

Table 4 Comparison of Parameters

Table Comparison of Parameters	2: of	Northrop YB-49	Boeing X-48	Northrop Grumman B-2
Take- off weight		87,969 kg	227 kg	170,600 kg
Aspect Ratio		7.2	4.1	5.87
Thrust/Weight		0.23	NA	0.205
Range		16,057 km	NA	11,100 km
Service ceiling		13,900 m	3,000 m	15,200 m
Cruise Speed		587 kmph	219 kmph	900 kmph

Boeing X-48B is a scaled down model of a proposed idea, hence it is a UAV that is being tested for aerodynamic properties hence the data cannot be compared to the other two aircraft which are bombers. None of the above-mentioned aircrafts are used for commercial purpose which is the aim of the report. Preliminary studies show that the HWB configuration provide high aerodynamic efficiency which is the main motive behind developing it for a commercial use. The world is facing a huge crisis of depleting natural resources which forces us to innovate contemporary designs and technologies which are more fuel efficient or use alternative fuel. The HWB results in more fuel-efficient design which decrease the fuel consumption by 30% and reduces the release of nitrous oxide which is the major cause for environmental degradation.

5. Weight Sizing and Weight Sensitivities

1. Introduction

The purpose of the report is to calculate the preliminary weight of the proposed aircraft and to provide sensitivity analysis. To satisfy the mission requirements such as payload, cruise speed and range, the estimation of the takeoff weight is important. Maximum takeoff weight is calculated using data from the similar aircraft and it is kept constant. The regression coefficients are also calculated based on the similar aircrafts. Calculations are made following the weight estimation method provided in the Aircraft Design book by J. Roskam. The following weights are estimated in this report:

- Empty Weight
- Fuel Weight
- Payload

AAA program is also used to estimate the weights and sensitivity and the manual calculations are compared with the results from software to check the deviation. Takeoff weight sensitivities are calculated in with respect to Payload, Empty weight, Range, Endurance and Specific fuel consumption.

2. Mission Weight Estimates

2.1 Database for Takeoff and Empty Weights of Similar Aircrafts

Table 5 Aircraft type and Weight Data of Similar Aircraft.

Aircrafts	Takeoff Weight (lb)	Empty Weight (lb)	Airplane Type
Northrop YB-49	193939	104142	Combat BWB
NASA SUGAR Ray	182500	104142	Commercial BWB
Airbus A319 neo	141100	89950	Commercial TW
Airbus A320 neo	162040	93920	Commercial TW
Bombardier CS300	149040	81750	Commercial TW
Boeing 737-100	109950	62020	Commercial TW
Northrop Grumman B2	376110	158070	Stealth BWB Bomber

22 Determination of Regression Coefficient A and B

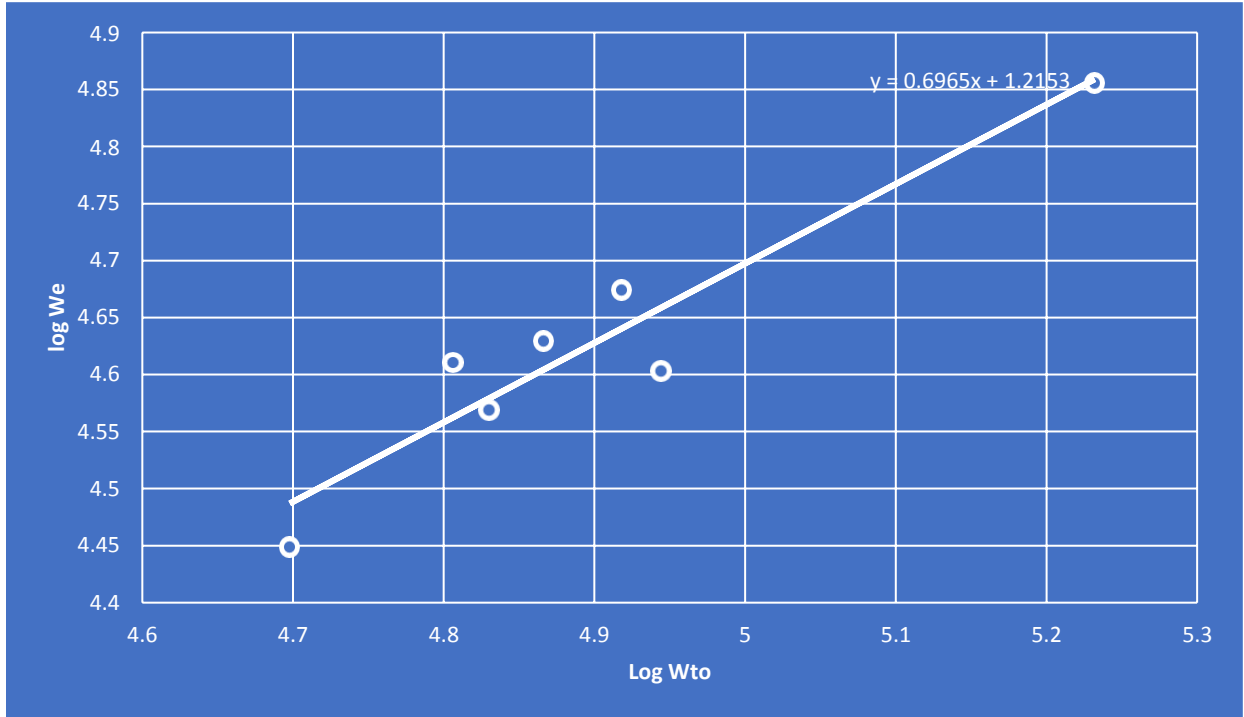


Figure 8 Log – Log Chart of Weight Data

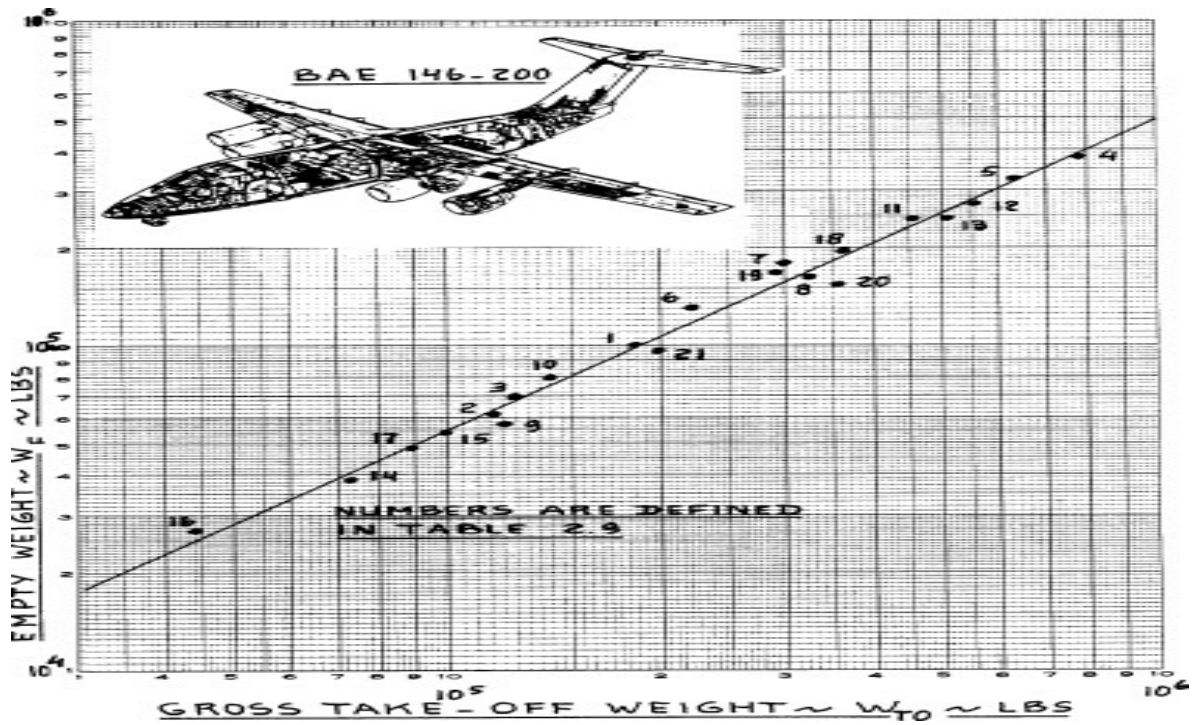


Figure 9 Log – Log Chart of BAE 146-200

The regression points are based on the similar aircraft that are used to compare the proposed airplane. It acts as a guide post in determining the preliminary weight sizing of aircraft by providing a limiting value for empty weight of aircraft from which the tentative empty weight can be determined with one percent tolerance. The regression points provided in book "Aircraft Design" by J. Roskam are for older versions of airplanes. So, for designing aircraft with more advanced composites and materials, a new log-log chart for aircrafts is generated and has been compared with the closest available chart in book. It can be observed that a linear relation for $\log_{10}(W_{TO})$ and $\log_{10}(W_E)$ holds for the newly generated chart. This provides me with the regression points that can be used to accurately estimate the empty weight according to new advanced materials and technology available.

The regression coefficients A and B can be calculated by comparing the trend line equation from the graph of generated and by comparing the equation used for calculating the allowable empty weight.

$$y = 0.6965x + 1.2153$$

$$\log_{10} W_E = \frac{\log_{10} W_{TO}}{B} - \frac{A}{B}$$

Comparing the equations

$$A = -1.745 \text{ and } B = 1.436$$

2.3 Determination of Mission Weights

2.3.1 Manual Calculation of Mission Weight

Assumptions:

- 1) The efficiency of the aircraft engine remains constant.
- 2) The long and short cruise both are at same velocity.

Assumed data for calculations

Range: 5000 nm

W_{TO} : 150800 lb

$$\text{Payload calculation: } (175 + 30) * 160 + (175 + 30) * 6 = 34030 \text{ lb}$$

Fuel Fraction for various Mission Phases

Phase 1: Engine Start and Warm Up- 0.990

Phase 2: Taxi- 0.990

Phase 3: Takeoff- 0.995

Phase 4: Climb- 0.980

Phase 5: Descent 1- 0.990

Phase 6: Cruise- 0.980
 Phase 7: Loiter- 0.985
 Phase 8: Cruise- 0.980
 Phase 9: Descent 2- 0.990
 Phase 10: Landing, Taxi, Shutdown: 0.995

Table 6 Suggested Values for L/D, C_j , η_p and C_p

	Cruise	Loiter
L/D	26.611	30.782
C_j	0.8	0.6
η_p	0.4	0.5
C_p	0.85	0.8

Calculations for Fuel Fraction for Cruise

Cruise speed: 0.8 Mach @ 41,000 ft = 527.84 mph
 Cruise Range: 4604 miles
 Short Cruise Range: 346 miles
 Loiter Time: 0.75 hours

$$R_{cr} = \frac{V}{C_j} \times \left(\frac{L}{D}\right)_{cr} \times \ln\left(\frac{W_4}{W_5}\right)$$

$$4606 = \frac{527.84}{0.8} \times 26.611 \times \ln\left(\frac{W_4}{W_5}\right)$$

$$\frac{W_5}{W_4} = 0.769$$

$$346 = \frac{527.84}{0.8} \times 26.611 \times \ln\left(\frac{W_5}{W_6}\right)$$

$$\frac{W_6}{W_5} = 0.980$$

Calculation for Fuel Fraction for Loiter

$$E_{ltr} = \frac{1}{e} \times \left(\frac{L}{D} \right)_{ltr} \times \ln \left(\frac{W_7}{W_8} \right)$$

$$0.75 = \frac{1}{0.6} \times 30.782 \times \ln \left(\frac{W_7}{W_8} \right)$$

$$\frac{W_8}{W_7} = 0.985$$

Maximum Fuel Fraction:

$$M_{ff} = \frac{W_1}{W_{TO}} \times \frac{W_2}{W_1} \times \frac{W_3}{W_2} \times \frac{W_4}{W_3} \times \frac{W_5}{W_4} \times \frac{W_6}{W_5} \times \frac{W_7}{W_6} \times \frac{W_8}{W_7} \times \frac{W_9}{W_8} \times \frac{W_{10}}{W_9}$$

$$= 0.684$$

Calculation for Weight of Fuel

$$W_F = (1 - M_{ff}) \times W_{TO} = (1 - 0.684) \times 150800 = 47637.32 \text{ lb}$$

$$W_{F \text{ res}} = 5\% \text{ of } W_F = 2381.87 \text{ lb}$$

$$W_T = W_F + W_{F \text{ res}} = 50019.19 \text{ lb}$$

Tentative Empty Weight of Proposed Aircraft:

$$W_{E \text{ tent}} = W_{TO} - W_T - W_{Pl} = 66750.81 \text{ lb}$$

Calculating W_E allowable from the regression coefficients

$$A = -1.745 \text{ and } B = 1.436$$

$$W_e = \frac{\log_{10} W_{TO}}{B} - \frac{A}{B}$$

$$W_e = \frac{\log_{10} 150800}{1.436} + 1.2135 = 66382.95 \text{ lb}$$

Difference between tentative W_E and allowable $W_E = 0.55\%$

2.3.2 Calculating Mission Weights using AAA Program

Advanced Aircraft Analysis 3.7 - Project1.aaa - Flight Condition 1 - [Take-off and Empty Weight Regression Coefficient Calculation: Flight Condition 1]

File Edit Window Airfoil Help

Weight Aerodynamics Performance Geometry

Take-off and Empty Weight Regression Coefficient Calculation: Flight Condition 1

Calculate Plot Clear Out Import Table Export

Input Parameters

W_{TO} lb W_E lb Number

Empty Weight - Take-off Weight Table

#	Airplane Name	W_{TO} lb	W_E lb
1	A319 neo	141095.7	89948.5
2	A320 neo	162039.6	93916.8
3	CS300	149032.3	81749.5
4	737-100	109942.2	61993.9
5	YB-49	193938.2	88440.5
6	SUGAR Ray	182500.6	104142.0
7	B2 Spirit	376108.2	158071.3

Output Parameters

A B

Figure 10 Weight Inputs of Similar aircrafts for Regression Point

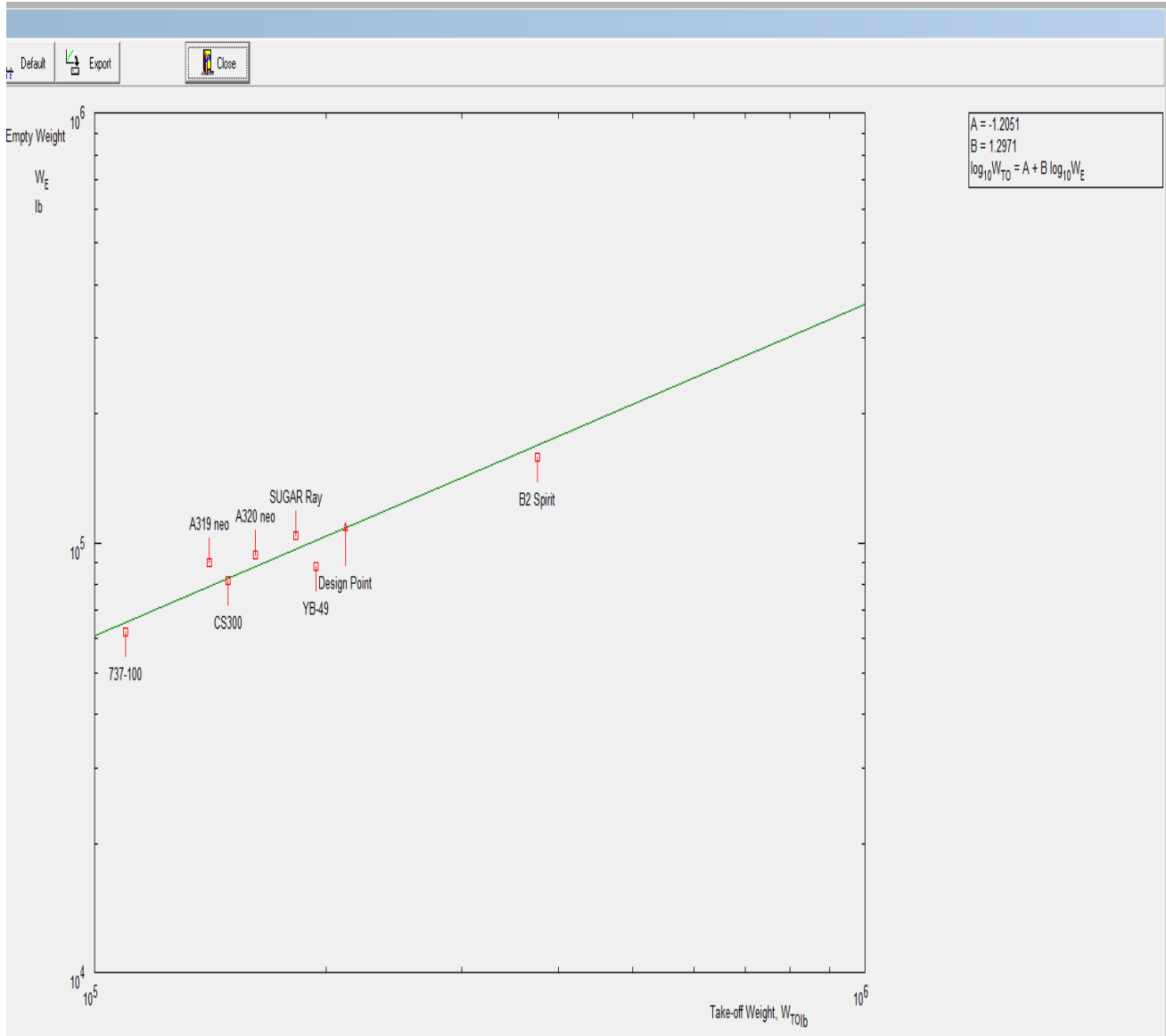


Figure 11 Plot of Trend Line for Regression Points

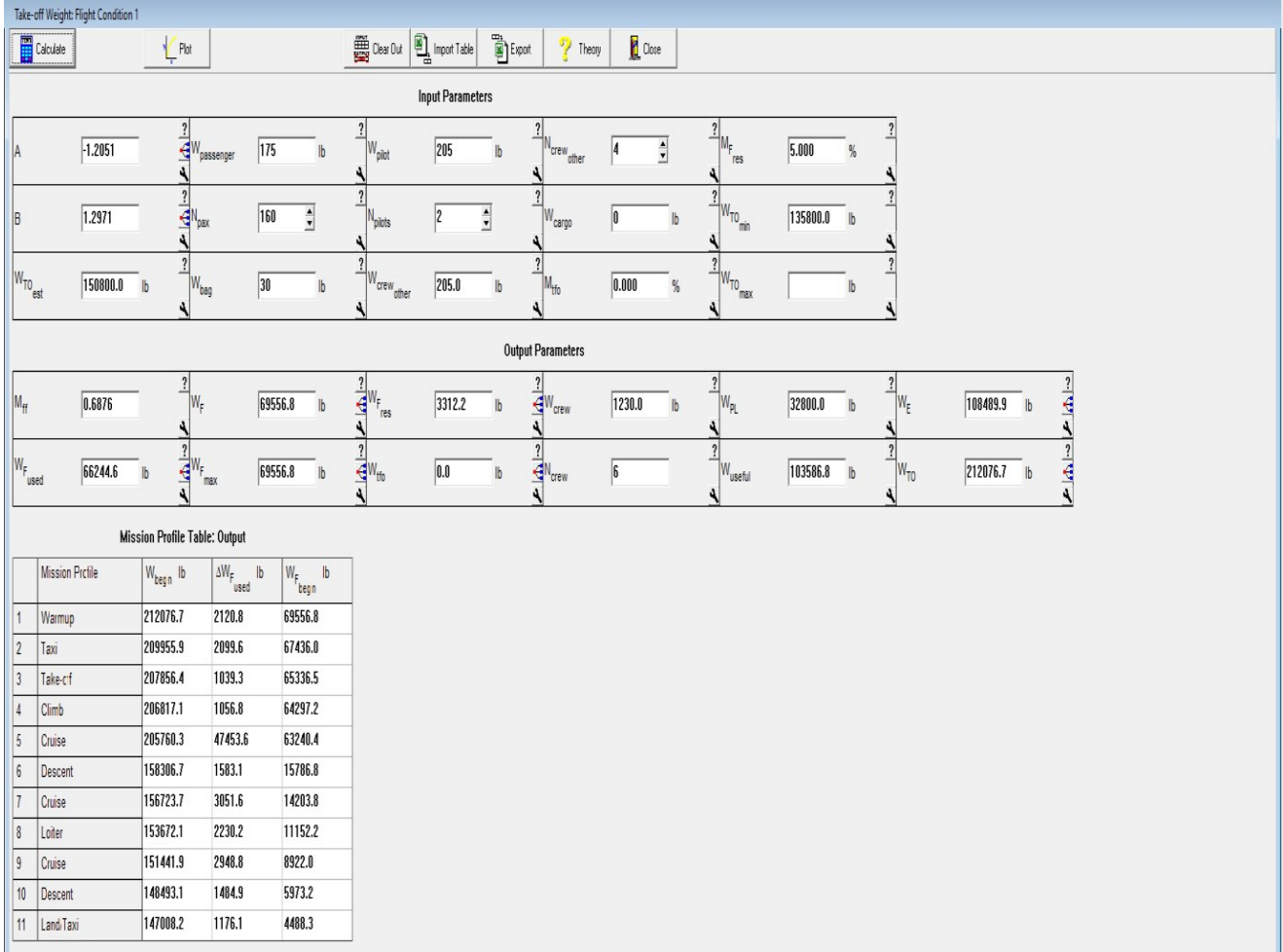


Figure 12 Empty Weight Calculation

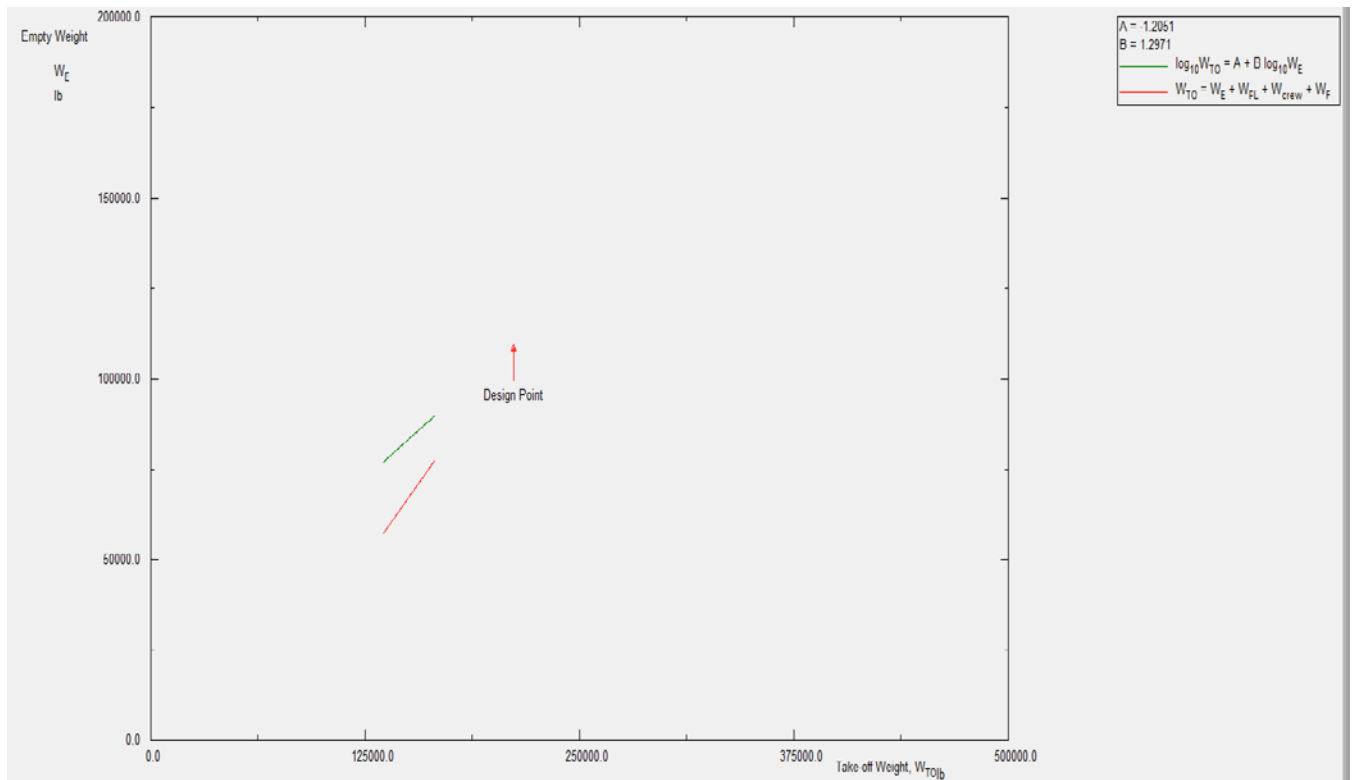


Figure 13 Design Point Plot

It is observed that there is difference between the empty weights calculated by hand and by AAA. This is due to the estimation of regression points using different software for hand-calculations.

3. Takeoff Weight Sensitivities

3.1 Manual Calculation of Takeoff Weight Sensitivities

$$W_{PI} = 32800 \text{ lb}$$

$$W_{Crew} = 1230 \text{ lb}$$

$$\text{Range} = 5754 \text{ miles}$$

$$C = 1 - (1 + M_{res})(1 - M_{ff}) - M_{tfo} = 1 - (1 + 0.05)(1 - 0.684) - 0 = 0.668$$

$$D = W_{PI} + W_{crew} = 34030 \text{ lb}$$

$$F = \frac{-BW_{TO}^2 (1 + M_{res})M_{ff}}{(CW_{TO}(1 - B) - D)}$$

$$= \frac{-1.436 * (150800)^2 * (1 + 0.05) * 0.684}{(0.668 * 150800 * (1 - 1.436) - 34030)} = 300886.31$$

$$\text{Sensitivity of } W_{TO} \text{ to } W_{PI} = \frac{BW_{TO}}{(D-C(1-B)W_{TO})} = 2.778$$

$$\text{Sensitivity of } W_{TO} \text{ to } W_E = \frac{BW_{TO}}{(inv \log_{10}\{(\log_{10} W_{TO}-A)/B\}} = 3.261$$

$$\text{Sensitivity of } W_{TO} \text{ to Range} = \frac{FC_j}{V * \frac{L}{D}} = 17.137 \frac{lb}{mile}$$

$$\text{Sensitivity of } W_{TO} \text{ to Endurance} = \frac{FC_j}{L/D} = 5864.50 \text{ lb/hr}$$

Sensitivity of W_{TO} to Specific Fuel Consumption and L/D Range case:

$$\frac{\partial W_{TO}}{\partial C_j} = \frac{F * R}{V * \frac{L}{D}} = \frac{123256.2 \frac{lbs}{hr}}{\frac{lbs}{hr}}$$

$$\frac{\partial W_{TO}}{\partial L/D} = - \frac{F * R * C_j}{V * \frac{L^2}{D}} = -3705.421$$

Endurance Case:

$$\frac{\partial W_{TO}}{\partial C_j} = \frac{FE}{L/D} = \frac{7331.061 \frac{lbs}{hr}}{lbs}$$

$$\frac{\partial W_{TO}}{\partial L/D} = - \frac{FEC_j}{L/D} = 4398.696$$

32 Calculation of Takeoff Weight Sensitivities using the AAA Program

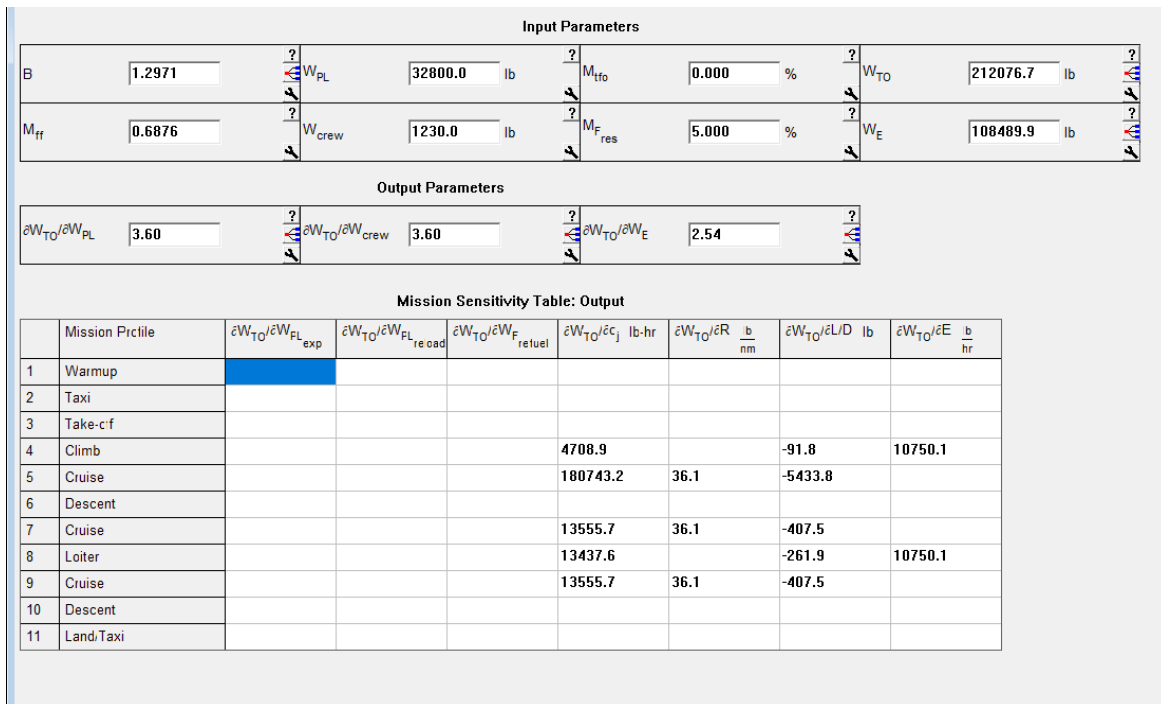


Figure 14 Empty Weight Calculation

33 Trade Studies

Trade studies are done between Range vs Payload and Takeoff weight and L/D which are one the critical parameters for the aircraft. For first trade study, payload was calculates using Breguet's Range equation while keeping the maximum takeoff weight constant for proposed aircraft. The best design point is obtained from the manual calculation.

From the graph, it is observable that with increase in payload the range decreases and vice-versa. Depending upon the mission profile, the aircraft can be designed for higher or lower payloads. The actual design is based on the requirements of the customer.

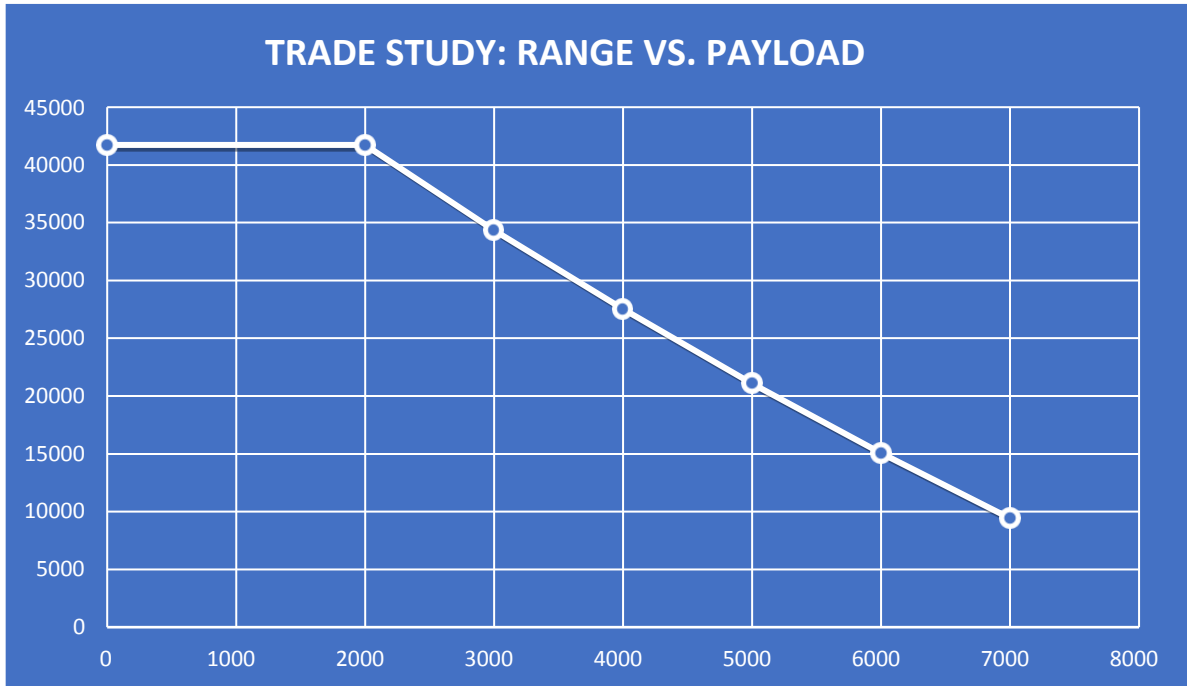


Figure 15 Trade Study-Range Vs. Payload

With the decrease in lift to drag ratio, the efficiency of the aircraft decreases hence giving rise to the need for more fuel. Keeping the empty weight constant, the extra fuel weight is accounted from the total takeoff weight. The inverse is also possible if the lift to drag ratio increases.

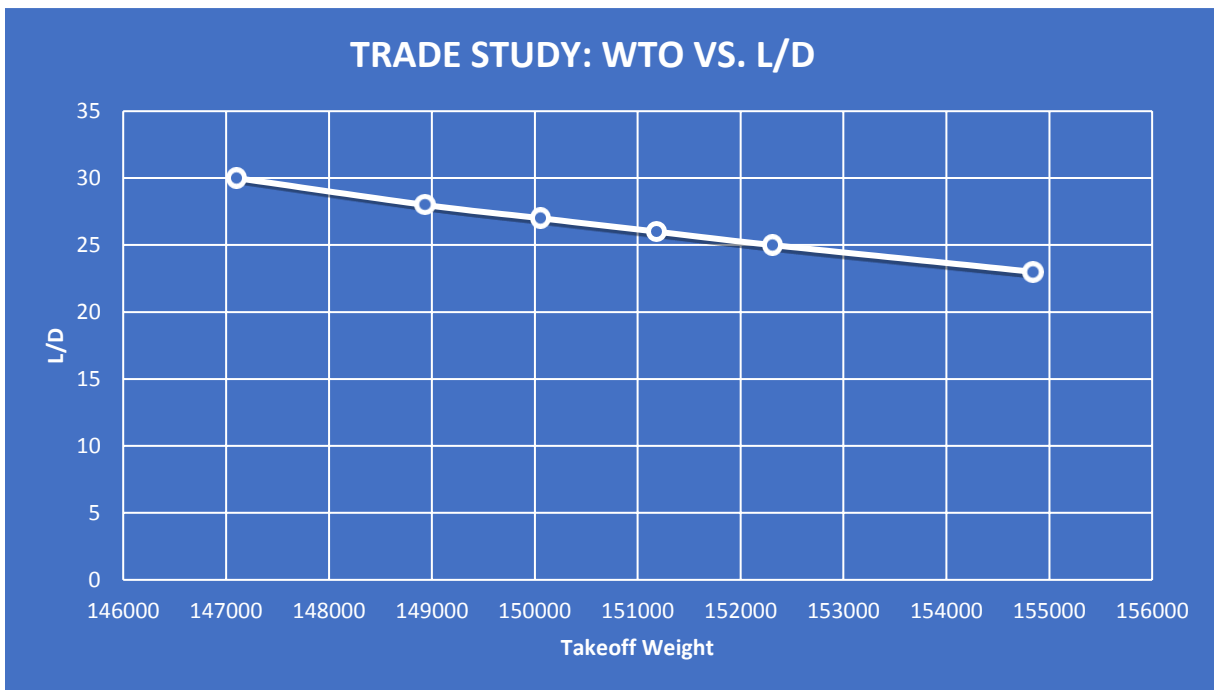


Figure 16 Trade Study- Takeoff Weight Vs. L/D

4. Discussion

This is the third report in the series which covers the class 1 preliminary weight sizing for a BWB commercial transport. The weight sizing method depend upon the regression points which are calculated based on the trend line of the log-log chart of wrights of similar aircraft. The initial part of the report thoroughly covers the weight estimation of the proposed aircraft.

Form the manual calculations, it is observed that there is a difference of 0.55% between the estimated empty weight and allowable empty weight, which is acceptable at this stage of aircraft design. There are assumptions made in the Breguet's range equation, especially on the lift to drag ratio of the aircraft. A high value is considered for L/D ratio as it is a BWB configuration. For cruise, the lift to drag ratio is 26.61 which is large when compared to conventional configurations.

The sensitivity study governs the key parameters with respect to takeoff weight which is oversensitive to the change in endurance and lift to drag ratio which is validated by the trade study. The manually calculated values for weight estimation and sensitivity studies differ by a large margin which is due to different regression points. Manual calculations provide the values: $A = -1.745$ and $B = 1.436$ while the values obtained from the software are $A = -1.205$ and $B = 1.297$.

The sensitivity values from the above calculations mean:

- The takeoff weight will increase by 2.78 lbs. for per pound increase in payload.
- The takeoff weight will increase by 3.26 lbs. for per pound increase in empty weight.
- The takeoff weight will increase by 17.14 mile for per mile increase in range.
- The takeoff weight will increase by 5864.50 lbs. for per hour increase in endurance time.
- Takeoff weight will differ by 123256.2 lb for unit change in specific fuel consumption for cruise.
- Takeoff weight will differ by 3705.42 lb for unit change in lift to drag ratio for cruise.

5. Conclusion

5.1 Conclusion

The calculations show that it is safe to calculate preliminary weights and sensitivity study according to the conventional methods used for TW configuration. In this report, the weight sizing and sensitivity studies are calculated based on the validated method used for TW aircraft from the book by J. Roskam. The gasoline aircrafts are susceptible to change in CG position as the weight of the aircraft changes continuously as the fuel is consumed, so it is important to calculate fuel fractions of each segment of mission profile very precisely.

The calculated sensitivity is compared with sensitivity values in Aircraft Design book and it is within the acceptable range. So, the calculated weights can be used for future stages of the design process.

52 Recommendations

Recent Studies from NASA have resulted further high lift to drag ratio for BWB aircraft. Empty weight calculation includes assumptions which can be replaced by the exact values and more accurate results can be obtained. Detailed analysis of trade studies between different parameter would provide more optimized design points.

6. Performance Constraint Analysis

1. Introduction

Pre-World War I era was recognized with rapid development in the field of aviation. The performance study of the aircraft became very important. Previous reports proposed, mission specification, configuration selection and weight sizing of the aircraft. This chapter introduces performance constraint sizing. The aircraft would be sized and designed according to the FAR 25 regulations for lift, drag, thrust and weight.

In addition to meeting the range, endurance and cruise speed requirements, it is important to meet the constraints for

- Stall Speed
- Take-off field length
- Landing field length
- Cruise Speed
- Climb rate (with all engines operating and one engine operating)
- Time to Climb

The main objective of the report is to provide a rapid methodology of determination of values of the wing loading, thrust to weight ratio and maximum coefficient of lift. A matching plot will be provided to represent, the maximum wing loading and minimum thrust to weight ratio which still meet the all the performance requirements at the lowest cost.

The proposed aircraft is a BWB configuration. The conventional methods must be modified in to provide an accurate and precise performance estimations. Some of the data do have very unconventional values.

2. Manual Calculations of Performance Constraints

Stall Speed

Stall is a condition which is marked by a decrease in lift generated by an airfoil which is due to flow separation from the surface. As per FAR 25 regulations, there is no specific criteria for stall speed. Comparing the data from the aircraft with similar passenger capacity, the stall speed is assumed to be 80 knots.

Take-off Distance:

The methodology provided in the book Aircraft Design, the take-off distance depends upon the following factors:

- Take-off weight
- Take-off speed
- Thrust to Weight ratio

- Aerodynamic lift coefficient
- Ground friction
- Pilot technique

For proposed aircraft, it is assumed that take-off takes place from a hard surface.

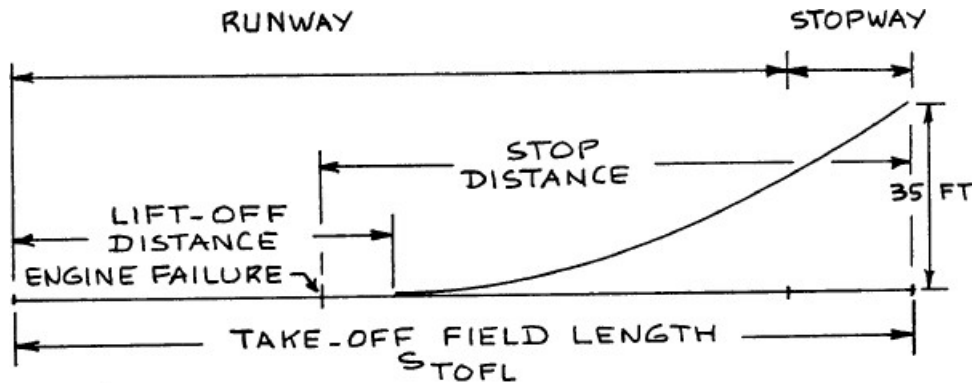


Figure 17 Definition of FAR 25 Take-off distances.

The above figure provides the definition of FAR 25 Take-off distances used in process of sizing the aircraft.

Some of the parameters are assumed to be fixed while others are varied to determine the thrust loading for maximum lift coefficient and wing loading.

The following equation provides the relation between the various parameters and take-off field distance:

$$S_{TOFL} = 37.5 \frac{(W/S)_{TO}}{\left\{ \sigma C_{L \max TO} \left(\frac{T}{W} \right)_{TO} \right\}} = TOP_{25}$$

From the above equation, it is observed that the field length is directly proportional to the wing loading and inversely proportional to the thrust loading. The equation is modified to render thrust to weight ratio depending on the different take-off field length considered. Considering that the runway is at sea-level and for sample calculation assuming the values of $C_{L \max} = 1$ and $(W/S)_{TO} = 45 \text{ lb/ft}^2$, the values are substituted in the equation:

$$\left(\frac{T}{W} \right)_{TO} = 37.5 \frac{45}{(1 * 1) * (5000)} = 0.337 \text{ lb/lbf}$$

The following tables summarizes the values of wing loading with varying coefficient of lift and take-off field length

Table 7 Take-off Distance sizing for STOFL=5000 ft at sea-level

	1	1.1	1.2	1.3
40	0.3	0.272727	0.25	0.230769
60	0.45	0.409091	0.375	0.346154
80	0.6	0.545455	0.5	0.461538
100	0.75	0.681818	0.625	0.576923
110	0.825	0.75	0.6875	0.634615

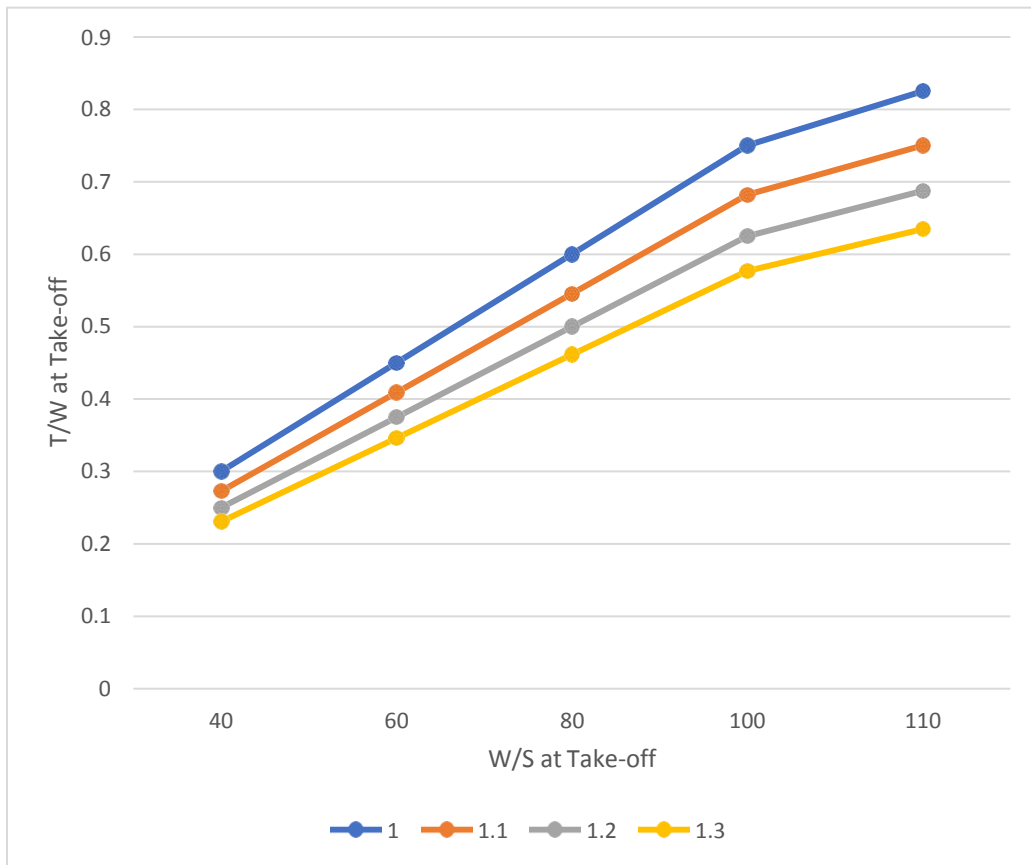


Figure 18 Take-off requirement chart for 5000 ft field

Table 8 Take-off Distance sizing for STOFL=6000 ft at sea-level

	1	1.1	1.2	1.3
40	0.25	0.227273	0.208333	0.192308
60	0.375	0.340909	0.3125	0.288462
80	0.5	0.454545	0.416667	0.384615
100	0.625	0.568182	0.520833	0.480769
110	0.6875	0.625	0.572917	0.528846

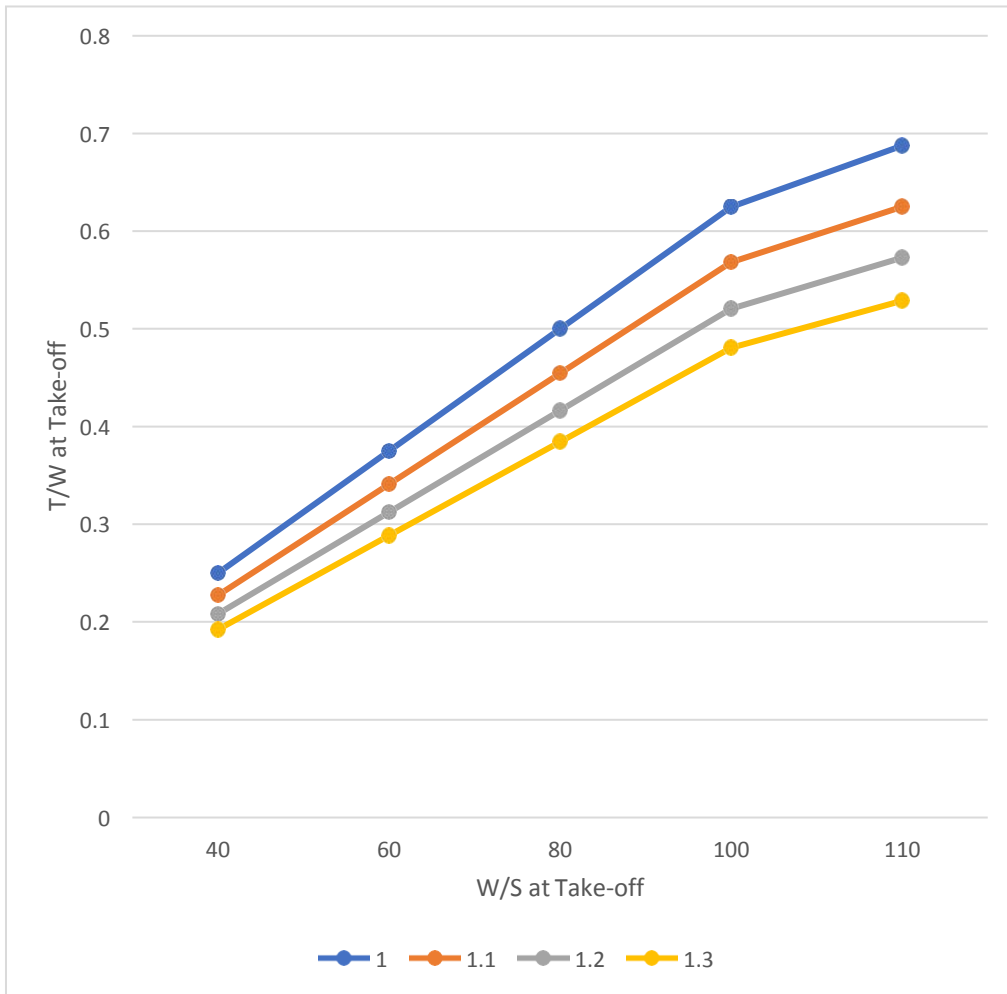


Figure 19 Take-off requirement chart for 6000 ft field

Table 9 Take-off Distance sizing for STOL=7000 ft at 10000 ft

$C_{L \max}$	1	1.1	1.2	1.3
W/S				
40	0.24871	0.2261	0.207258	0.191315
60	0.373064	0.339149	0.310887	0.286973
80	0.497419	0.452199	0.414516	0.38263
100	0.621774	0.565249	0.518145	0.478288
110	0.683951	0.621774	0.569959	0.526116

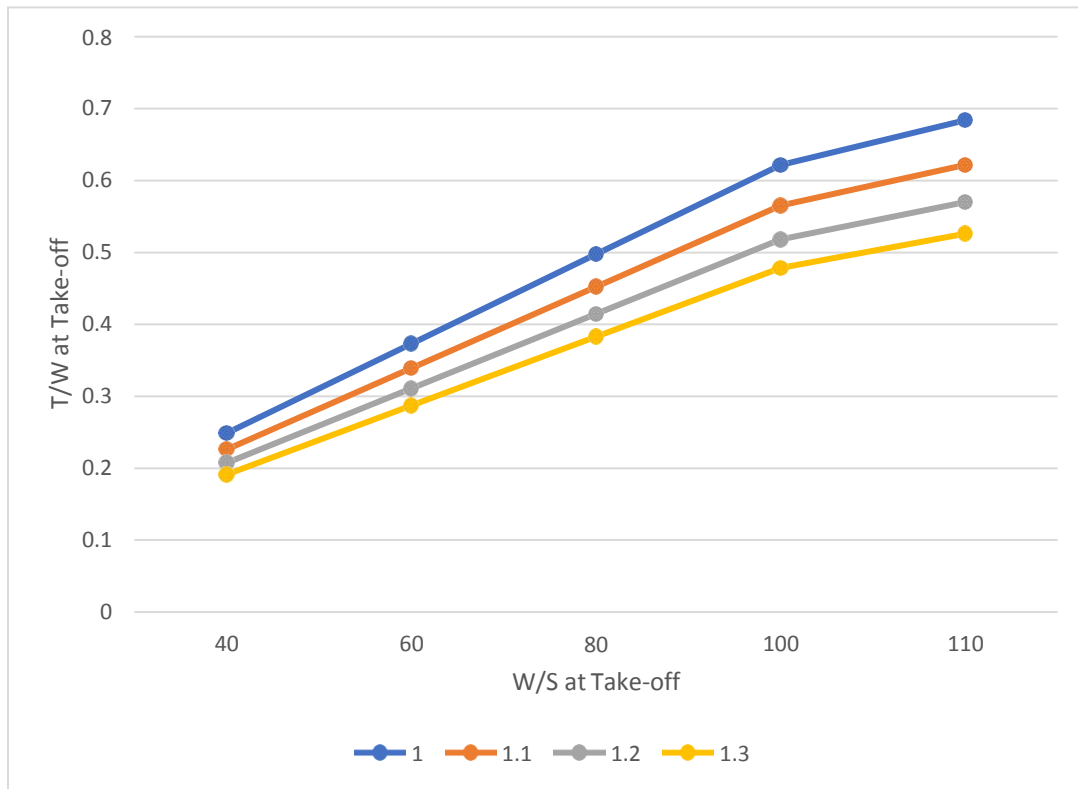


Figure 20 Take-off requirement chart for 7000 ft field

Table 10 Take-off Distance sizing for STOFL=10,000 ft at 10000 ft.

$C_{L\ max}$	1	1.1	1.2	1.3
W/S	1	1.1	1.2	1.3
40	0.190383	0.173076	0.158653	0.146449
60	0.285575	0.259614	0.237979	0.219673
80	0.380767	0.346152	0.317306	0.292898
100	0.475958	0.43269	0.396632	0.366122
110	0.523554	0.475958	0.436295	0.402734

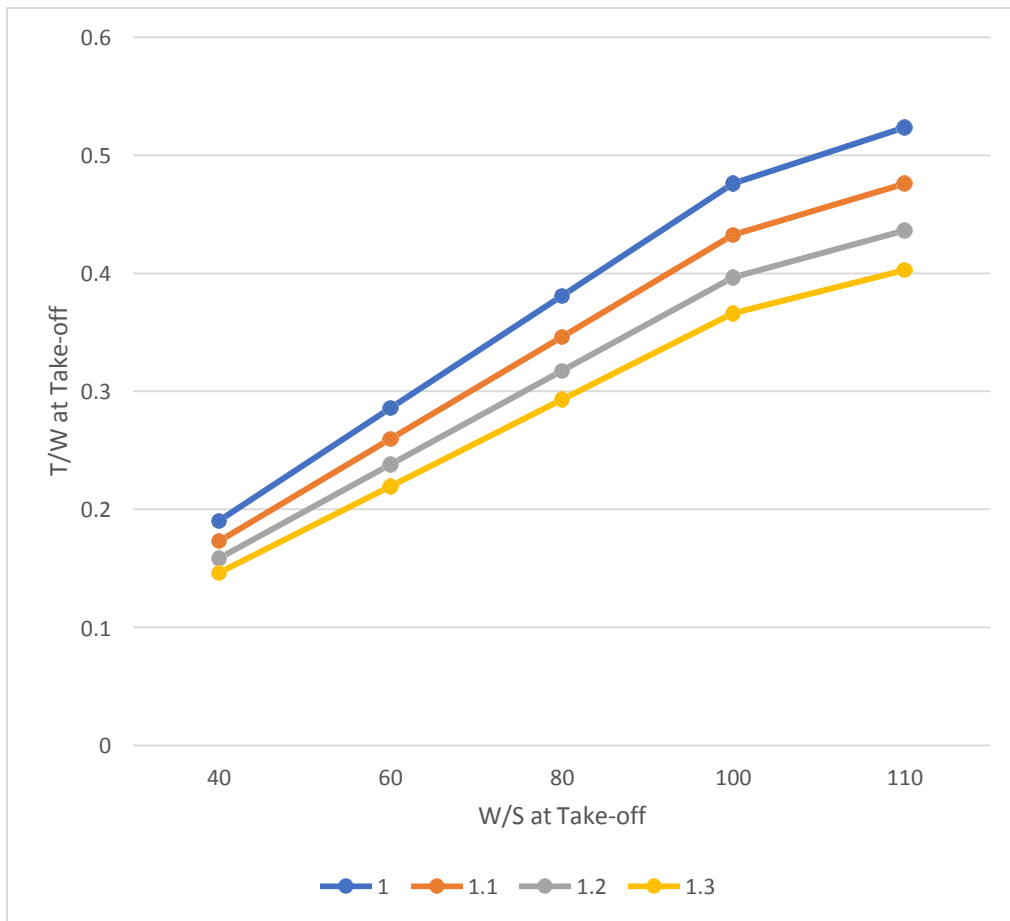


Figure 21 Take-off requirement chart for 10000 ft field

3. Landing Distance

The parameters that affect the landing distance of an aircraft are:

- Landing Weight
- Approach Speed
- Deceleration method used
- Flying quantities of the airplane
- Pilot technique

The following figure provides a definition of FAR 25 landing distances

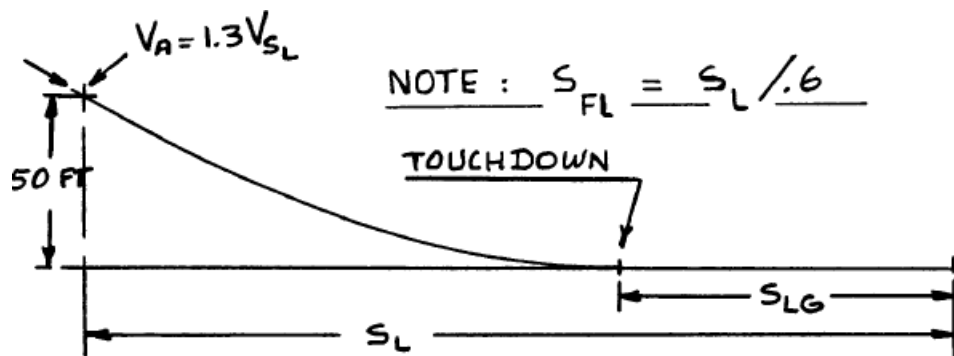


Figure 22 Definition of FAR 25 Landing Distance

The following assumptions are made for the landing distance sizing: standard conditions during landing, the brakes are applied immediately, and the take-off weight of the aircraft is 150800 lb. Using the optimum approach speed, the field length can be calculated as:

$$S_{FL} = 0.3V_A^2$$

$$V_A = 1.3V_{S_L}$$

Comparing the data available from the conceptual design of SUGAR Ray, the approach speed is 103 knots. It was assumed that the ratio of landing weight to take-off weight (W_L/W_{TO}) is 0.85. Then, the $(W/S)_L$ results from

$$\left(\frac{W}{S}\right)_L = \frac{V_{S_L}^2 * \rho}{2} * C_{L \max_L}$$

$$\left(\frac{W}{S}\right)_{TO} = \left(\frac{W}{S}\right)_L / 0.85$$

Substituting the values in the above equation:

$$2 * \frac{\left(\frac{W}{S}\right)_L}{(0.002378 * C_{L \max_L})} = (117.50 * 1.688)^2$$

$$\left(\frac{W}{S}\right)_{S_L} = 93.54 \frac{lb}{ft^2}$$

$$\left(\frac{W}{S}\right)_{TO} = \frac{93.54}{0.85} = 110.05 \frac{lb}{ft^2}$$

The following table summarizes the values of wing loading during take-off calculated with the help of varying maximum lift coefficient during landing and landing field length.

Table 11 W/STO~ results with WL/W-TO=0.60

S _{FL}	V _A	V _{SL}	1.2	1.5	1.7	1.9	2	2.2
7000	152.7525	117.5019	155.9178	163.7136	171.5095	179.3054	187.1013	194.8972
6000	141.4214	108.7857	133.6438	140.326	147.0082	153.6904	160.3725	167.0547
5500	135.4006	104.1543	122.5068	128.6321	134.7575	140.8828	147.0082	153.1335
5000	129.0994	99.30727	111.3698	116.9383	122.5068	128.0753	133.6438	139.2123
4000	115.4701	88.82312	89.09586	93.55065	98.00544	102.4602	106.915	111.3698
3500	108.0123	83.08642	77.95888	81.85682	85.75476	89.65271	93.55065	97.4486

Table 12 W/STO~ results with WL/W-TO=0.65

S _{FL}	V _A	V _{SL}	1.2	1.5	1.7	1.9	2	2.2
7000	152.7525	117.5019	143.9241	151.1203	158.3165	165.5127	172.7089	179.9051
6000	141.4214	108.7857	123.3635	129.5317	135.6998	141.868	148.0362	154.2044
5500	135.4006	104.1543	113.0832	118.7374	124.3915	130.0457	135.6998	141.354
5000	129.0994	99.30727	102.8029	107.9431	113.0832	118.2234	123.3635	128.5036
4000	115.4701	88.82312	82.24233	86.35445	90.46656	94.57868	98.6908	102.8029
3500	108.0123	83.08642	71.96204	75.56014	79.15824	82.75635	86.35445	89.95255

Table 13 W/STO- results with WL/W-TO=0.70

S _{FL}	V _A	V _{SL}	1.2	1.5	1.7	1.9	2	2.2
7000	152.7525	117.5019	133.6438	140.326	147.0082	153.6904	160.3725	167.0547
6000	141.4214	108.7857	114.5518	120.2794	126.007	131.7346	137.4622	143.1898
5500	135.4006	104.1543	105.0058	110.2561	115.5064	120.7567	126.007	131.2573
5000	129.0994	99.30727	95.45985	100.2328	105.0058	109.7788	114.5518	119.3248
4000	115.4701	88.82312	76.36788	80.18627	84.00467	87.82306	91.64145	95.45985
3500	108.0123	83.08642	66.82189	70.16299	73.50408	76.84518	80.18627	83.52737

The method is accurate for conventional aircraft but as there is no established method to calculate the wing loading for a Blended Wing Body aircraft, a secondary method from the book of Leland M. Nicolai was used to give comparative data for the landing sizing.

Table 14 Results from the secondary method

FL (FT)	1.2	1.5	1.7	1.9
7000	83.89831	89.49153	95.08475	100.678
6000	71.18644	75.9322	80.67797	85.42373
5500	64.83051	69.15254	73.47458	77.79661
5000	58.47458	62.37288	66.27119	70.16949
4200	48.30508	51.52542	54.74576	57.9661
3200	35.59322	37.9661	40.33898	42.71186

The secondary method seems to be less accurate as it does not account for the change in weight due to the consumption of the fuel.

4. Sizing to Climb Requirements

Method for Estimating Drag Polar

All airplanes must meet certain climb rate or climb gradient requirements. The jet transport of the proposed size should meet the requirements in according to the FAR 25 regulations. The calculations are based on one all engine operative as well as one engine operative conditions. A minimum thrust to weight ratio is provided for the conditions. For estimation of thrust loading, it is necessary to find drag polar.

$$C_D = C_{D0} + C_L^2/\pi A e$$

Table 15 Correlation Coefficient

c	d	a	b
0.0199	0.7531	-2.522	1

The relation between coefficients and parasitic drag and wetted area is given by

$$\log_{10}(f) = a + b * \log_{10} S_{wet}$$

$$f = 25.77 \text{ sq ft}$$

$$\log_{10}(S_{wet}) = c + d * \log_{10}(W_{TO})$$

$$S_{wet} = 8313 \text{ sq ft}$$

The drag polars are calculated based on the following equations:

$$C_D = C_{D_0} + \frac{C^2_{Lmax}}{\pi A e}$$

The results are summarized in the table below for different configurations:

Table 16 Summary of Drag Polars

Configuration	C _{D0}	C _{DI}
Low Speed, Clean	0.00596	0.05011
Take-off gear up	0.01096	0.051020825
Take-off gear down	0.01696	0.051020825
Landing gear up	0.02596	0.054422213
Landing, gear down	0.03196	0.054422213

5. FAR 25 Requirements

The book summarizes the FAR requirements for takeoff in the following way:

1. FAR 25.111 (OEI)
 - CGR > 0.012
 - Gear up
 - Take-off flaps engaged
 - Take-off thrusts on remaining engine
 - Ground effect
 - 1.2 V_{S TO}

Table 17 FAR 25.111 (OEI)

Effective Cl max	0.694444
Cd	0.035565
L/D	19.52609
(T/W) _{TO}	0.126427
(T/W) _{TO} modified for +50 ⁰ C	0.158034

2. AR 25.121 (OEI)

- CGR > 0
- Gear Down
- Take-off flaps
- Take-off thrust on remaining engine
- Ground effect
- Speed between V_{LOF} and 1.2V_{STO}

Table 18 FAR 25.121 (OEI)

Effective Cl	1.07438
Cd	0.075853
L/D	14.16398
(T/W) _{TO}	0.141203
(T/W) _{TO} modified for +50 ⁰ C	0.176504
At V2	
Effective Cl	0.694444
Cd	0.041565
L/D	16.70745
T/W	0.119707

3. FAR 25.121 (OEI)

- CGR > 0.024
- Gear up
- Take-off flaps engaged
- No ground effects
- Maximum continuous thrust on remaining engine
- $1.2V_{TTO}$

Table 19 FAR 25.121 (OEI)

Effective Cl	0.694444
Cd	0.035565
L/D	19.52609
$(T/W)_{TO}$	0.150427
$(T/W)_{TO}$ modified for +50° C	0.200036

4. FAR 25.121 (OEI)

- CGR > 0.012
- Gear up
- Flaps up
- Enroute climb altitude
- Maximum continuous thrust on remaining engines
- $1.25 V_S$

Table 20 FAR 25.121

Effective Cl	0.512
Cd	0.019096
L/D	26.81185
$(T/W)_{TO}$	0.098594
$(T/W)_{TO}$ modified for +50° C	0.123242

For Landing:

- 5. FAR 25.119 (AEO)
 - CGR > 0.032
 - Gear Down
 - Landing Flaps
 - Take-off thrust on all engines
 - 1.25V_s

Table 21 FAR 25.119 (AOE)

Effective Cl	0.887574
Cd	0.074833
L/D	11.86071
(T/W) _{TO}	0.116312
(T/W) _{TO} modified for +50° C	0.14539

- 6. FAR 25.121 (OEI)
 - CGR > 0.021
 - Gear down
 - Approach flaps engaged
 - Take-off thrust on remaining engines
 - 1.5V_s

Table 22 FAR 25.121

Effective Cl	0.577778
Cd	0.050128
L/D	11.52614
(T/W) _{TO}	0.215519
(T/W) _{TO} modified for +50° C	0.269398

Sizing to Climb Requirement		
Rate of Climb at altitude h (ft/min)	RC _h	322.71
Rate of Climb at Sea-level (ft/min)	RC ₀	3630.55
Height (ft)	h	41000
Absolute Ceiling (ft)	h _{abs}	45000
Time to Climb (min)	t _{cl}	30
Rate of Climb (ft/min)	RC	3450
	V	701
	L/D	29.55
	W/S	48.5

Sizing to Maneuvering Requirements

Maneuver sizing is important for military, acrobat, utility and agricultural aircraft. Since the proposed aircraft is a transport jet which lacks the ability for hard maneuvers so, it is not important to size the aircraft for maneuvering.

Sizing to Cruise Speed Requirements

For cruise speed requirement, the following equation is used from the book by Roskam.

$$T_{req} = C_D \bar{\rho} = C_{D_0} \bar{\rho} + \frac{C_L^2 \bar{\rho}}{\pi A e}$$

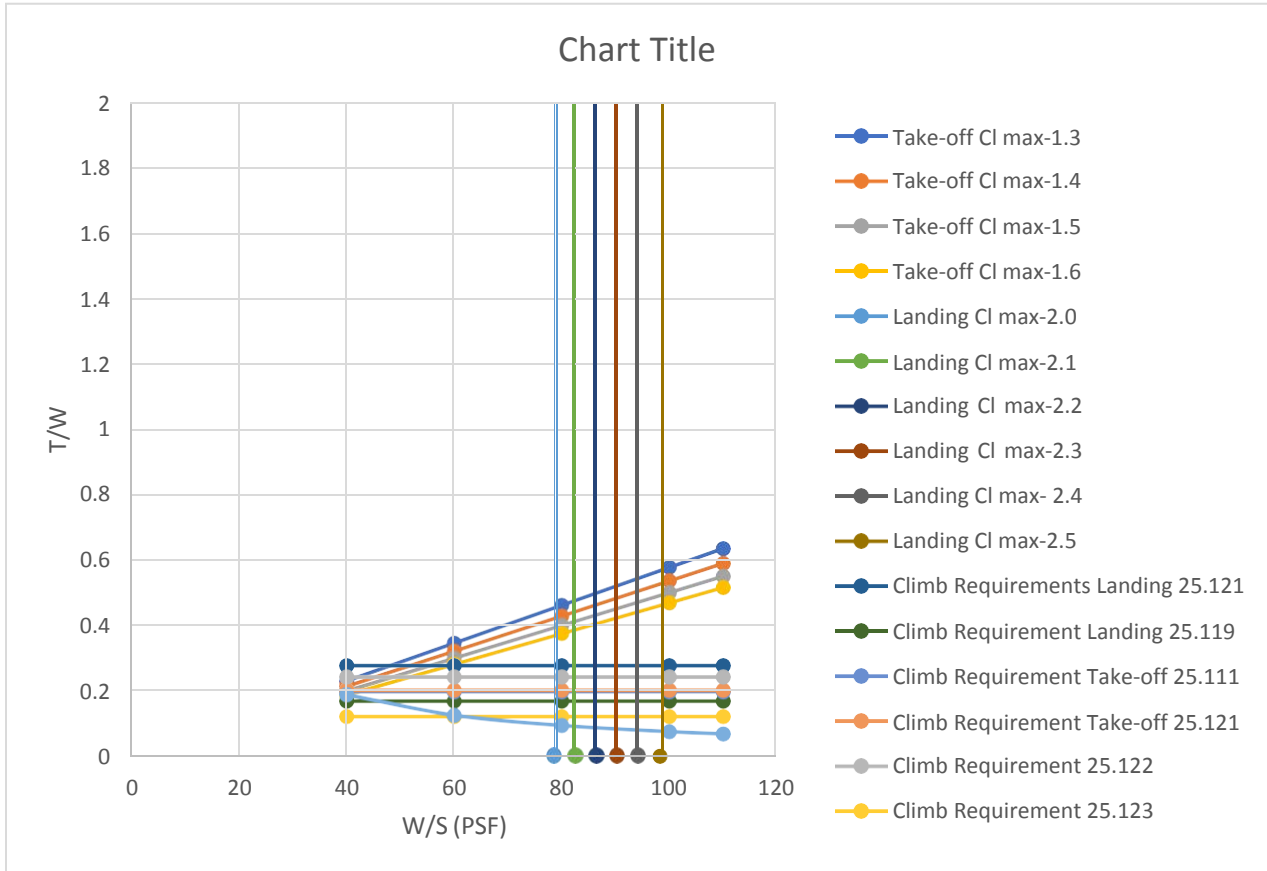
$$W = C_L \bar{\rho}$$

Combing the two equation yields

$$\frac{T}{W_{req}} = \frac{C_D \bar{\rho}}{W} + \frac{C_L^2 \bar{\rho}}{W \pi A e} = \frac{\bar{\rho}}{W} \left[C_{D_0} + \frac{C_L^2}{\pi A e} \right]$$

$$\frac{T}{W} = 1.4654 * \left[0.00596 + \frac{0.3^2}{20.8287} \right] = 0.015$$

7. Matching Plot



8. Results for Performance Sizing using AAA Program

h_S	41000 ft	ΔT_S	-69.7 deg F	$V_{S_{clean}}$	170.00 kts	V_S	180.00 kts
W_S / W_{TO}	0.700	$C_{L_{max_{S_{cln}}}}$	1.600	$C_{L_{max_S}}$	2.300		
Output Parameters							
$(W/S)_{TO_{S_{cln}}}$	48.94 $\frac{lb}{ft^2}$	$(W/S)_{TO_S}$	78.88 $\frac{lb}{ft^2}$				

Figure 25 Stall Speed Parameters

h_{TO}	5000 ft	F_{TO}	0.800	ΔT_{TO}	1.0 deg F
S_{TO}	5000 ft	$C_{L_{max_{TO}}}$	1.600	Plot $\Delta C_{L_{max}}$	0.100

Figure 26 Take-off Parameters

h_L	5000 ft	ΔT_L	50.0 deg F	W_L / W_{TO}	0.650
$C_{L_{max_L}}$	2.500	Plot $\Delta C_{L_{max}}$	0.100	S_L	2546 ft
Output Parameters					
S_{FL}	4243 ft	$(W/S)_L$	86.57	$\frac{lb}{ft^2}$	

Figure 27 Landing Requirements

$F_{MaxCont}$	0.940	$C_{L_{max_A}}$	2.100	e_{clean}	0.8500
F_{8sec}	0.800	$C_{L_{max_L}}$	2.500	$C_{D_{0_{clean,M}}}$	0.0060
$C_{L_{max_{clean}}}$	0.300	W_L / W_{TO}	0.650	e_{TO}	0.8000
$C_{L_{max_{TO}}}$	1.600	AR_w	7.80	$C_{D_{0_{TO_down}}}$	0.0170
e_L	0.7500	CGR	FAR 25	$CGR_{25.121_{ER}}$	0.012
$C_{D_{0_{L_down}}}$	0.0320	$CGR_{25.111}$	0.012	$CGR_{25.121_L}$	0.021
$\Delta C_{D_{0_A}}$	0.0140	$CGR_{25.121_T}$	0.000	$CGR_{25.119}$	0.032
$C_{D_{wm}}$	0.0000	$CGR_{25.121_{SS}}$	0.024		
Output Parameters					
$B_{DP_{clean}}$	0.0480	$B_{DP_{TO_down}}$	0.0510	$B_{DP_{L_down}}$	0.0544

Figure 28 FAR 25 Climb Requirements

h_{Cr}	41000 ft	?	F_{Cr}	0.800	?	$V_{Cr_{max}}$	441.21 kts	?
Output Parameters								
W_{Cr}/W_{TO}	0.900	?	AR_w	7.80	?	$C_{D0_{clean,M}}$	0.0060	?
Output Parameters								
e_{clean}	0.8500	?						
Output Parameters								
$M_{Cr_{max}}$	0.769	?	$B_{DP_{clean}}$	0.0480	?			

Figure 29 Cruise Requirement

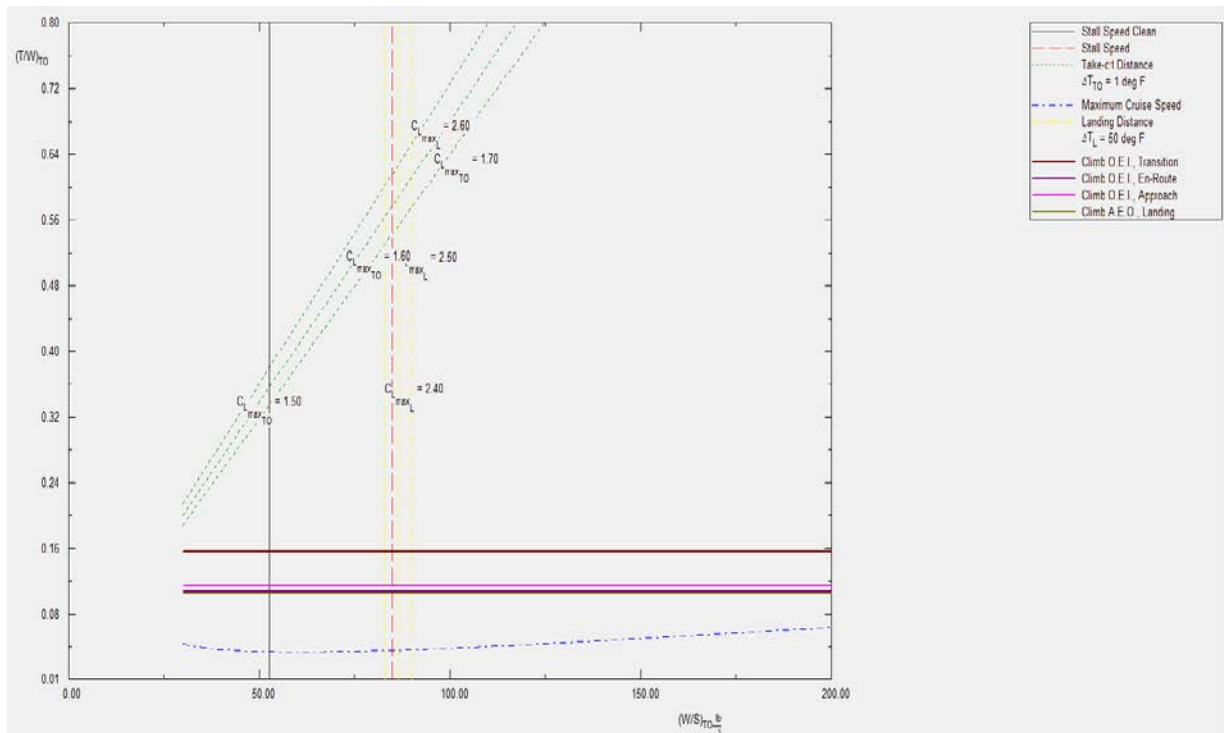


Figure 30 Matching Plot

The coefficients of lift and drag of a BWB are substantially low which reflects its effect on lower wing loading compared to the traditional TW design. The Thrust to weight ratio is very small hence the matching plot is extrapolated to the origin to get the complete picture.

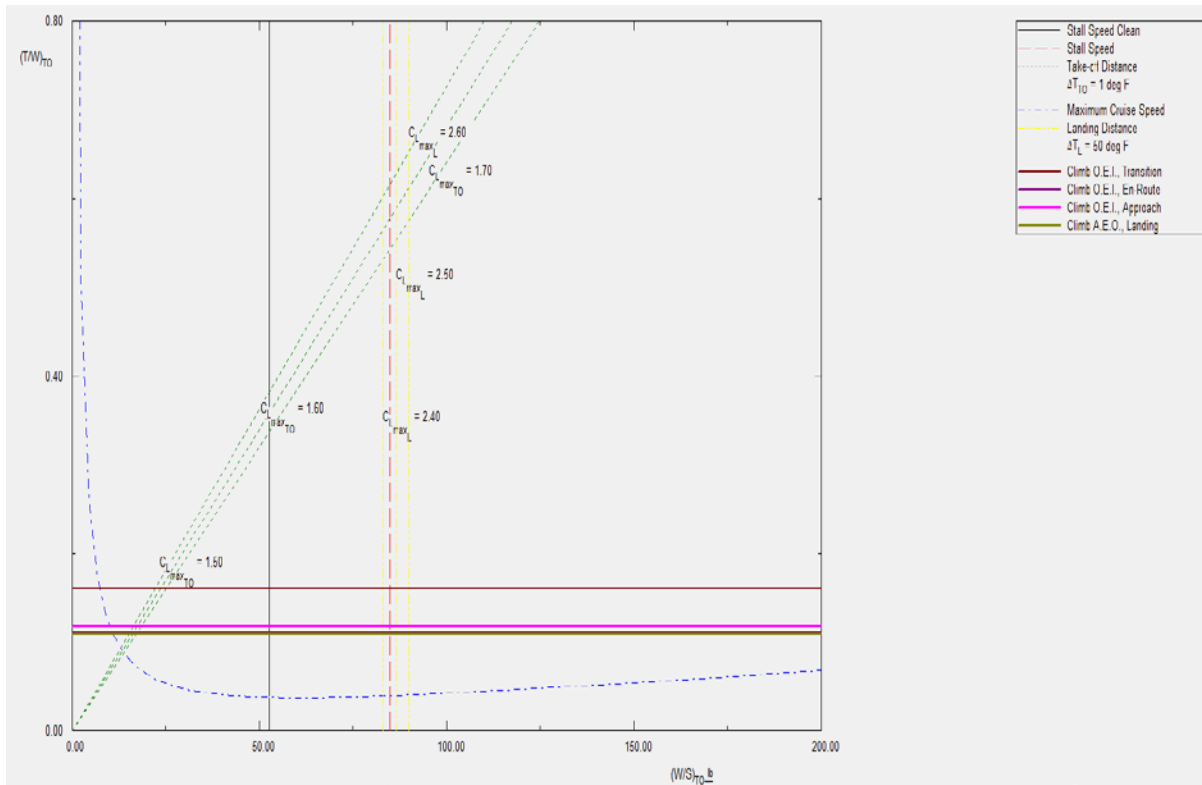


Figure 31 Extrapolated Matching Graph

It can be observed that with maximum values of coefficients of lift and drag the design point is highly constrained which makes it very difficult to get the required performance. Hence the parameters are altered so that an optimum matching plot is obtained for performance analysis.

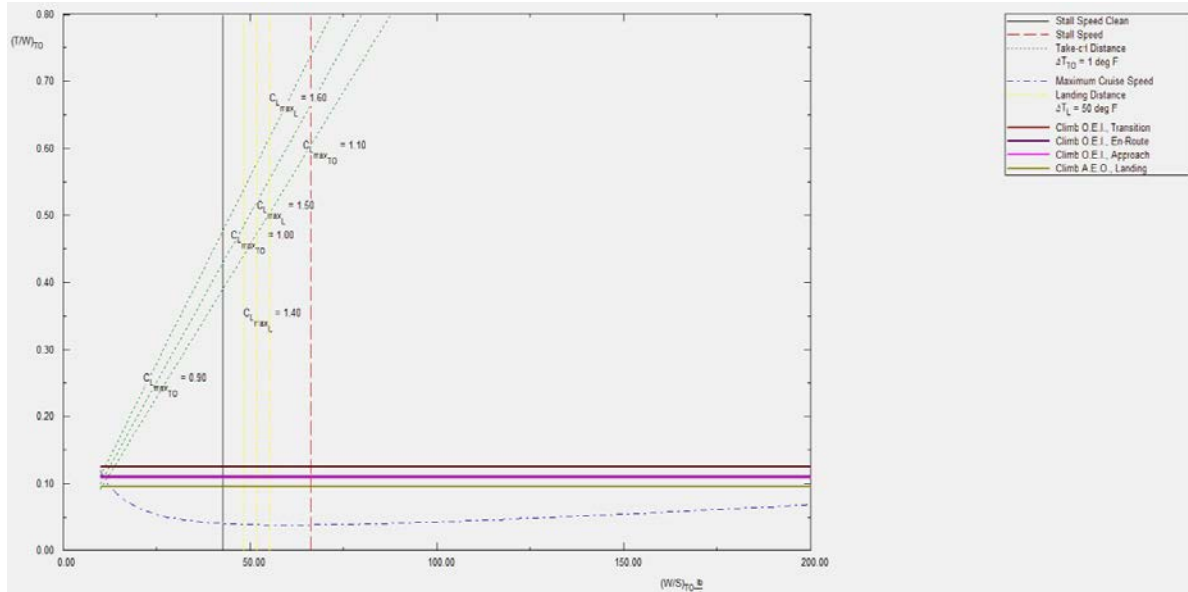


Figure 32 Optimum Design Point

9. Selection of Propulsion System

The propulsion system used in aircraft should be able to deliver power in accordance with the thrust to weight requirements calculated in above sections. The process involves following steps:

- Selecting appropriate type of propulsion system
- Determination of number of engines
- Integration of the engines into the configuration

a. Selecting Appropriate Type of Propulsion System

The selection of propulsion system is based on the following factors:

- Available installed power
- Thermal efficiency
- Reliability
- Cost
- Maintainability

A BWB aircraft has inherent aerodynamic efficiency which enables it to use less power in normal weather conditions. First idea would be to eliminate the emissions by using an all-electric propulsion system which can be powered by batteries as well as fuel cells but the major concern for this kind of system is the energy density available. With state of art technology available for batteries, it is not possible to meet the power requirements of huge airplanes. The only resort is

to use a more efficient engine which would not only decrease the estimation levels but would also bring down the operating cost of the airplane.

Another problem with the batteries is the cost affiliated with it. In a long run gasoline powered engine prove to be more cost efficient to battery operated motor. To meet the thrust requirement as well as to limit the noise levels targeted by the conceptual designs by Subsonic Ultra Green Aircraft Research, a new engine is being designed by a joint venture of NASA and General Electrics which is informally designated as “gfan+”.

The architectural concept is a 2-spool separate flow turbofan with an operating pressure ratio of 59 and a bypass ratio of 13. The engine features relatively low hot section temperatures. The low emission combustor, “NGEN + TAPS” provides effective improvements in NOx and particulate emission.

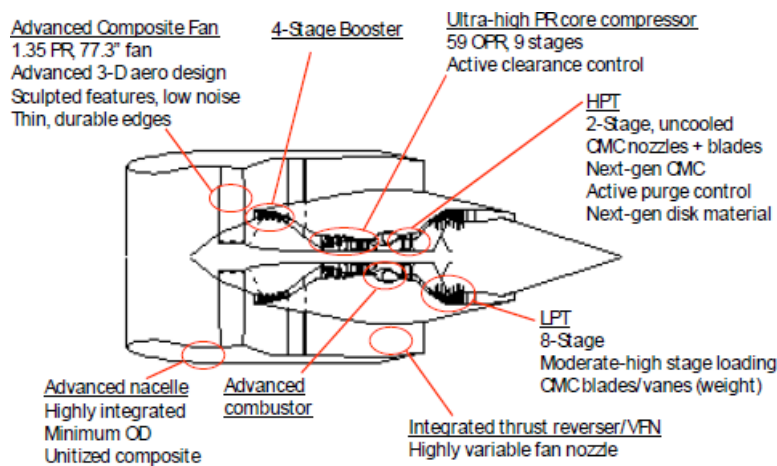


Figure 33 Conceptual “gfan+” engine.

Table 23 gfan+ Key Weight, Geometry, Performance.

Geometry		
Propulsion System Weight	7096 lbm	
Fan Diameter	77 in	
Length	122 in, spinner to TRF	
Performance Parameters		
	Thrust, lbf	SFC lbf/lbf-her
SLS	18800	0.211
Rolling take-off	13385	0.301
Top-of-climb	3145	0.475
Cruise	3028	0.470

b. Number of Engines and Integration into the Aircraft

The proposed BWB aircraft features 2 engines which are mounted aft of the aircraft over the top surface which reduces the interference with the flow of air hence creating less drag. Two engines provide an alternate during time of single engine failure. The engines are mounted aft of the CG which will make it a pusher configuration. Another advantage of the pusher engine would be the elimination of backwash due to engine over the aircraft, again reducing the drag and making aircraft more aerodynamically efficient.

10. Discussion

The manual calculations for various lift coefficients and speeds yielded wing loading ranging from 40.09 – 170.5 lb/ft². Due to BWB configuration, the maximum coefficients of lift during all the three phases of the aircraft are lower which reflects into the lower wing loading of the aircraft when compared to the traditional configuration. The AAA program yields a wing loading of 48 lb/ft². From the manual calculations, the thrust to weight ratio ranges from 0.11 to 0.63 which is in coherent with the thrust requirements from the AAA program.

The design point is selected based on the take-off and landing distance requirements with lowest possible W/S and T/W. With the possible lower W/S, the size of the wing is increases which results in higher drag. Its true vice versa but a small wing won't be able to generate sufficient lift for the aircraft. It requires high velocity which in turn would require higher values of T/W.

BWB configuration has very low C_{D0} for clean state hence the maximum cruise speed curve is very low. Any point above the cruise speed curve would satisfy the requirements. The point should be located on the left of the maximum stall speed line and should also meet the requirements of the for take-off and landing. The design point should be located well above the FAR 25 climb requirements.

The design point selected for the aircraft is $W/S = 48.5 \text{ lb/ft}^2$, $C_{L \text{ max TO}} = 0.9$, $C_{L \text{ max L}} = 1.4$ and $T/W = 0.44$. The point is located at the at the intersection of take-off and landing requirements which makes both the parameters critical.

11. Conclusion and Recommendation

a. Conclusion

The design point is so selected that it meets all the requirement for take-off, climb, cruise and landing. At $W/S = 48.5 \text{ lb/ft}^2$, $C_{L \text{ max TO}} = 0.9$, $C_{L \text{ max L}} = 1.4$ and $T/W = 0.44$, the lowest possible wing

loading and thrust requirements are obtained while meeting all the requirements. The new “gfan+” engine would be able to provide a thrust of 66352 lb as per the design point.

b. Recommendation

The design point can be varied depending upon the maximum lift coefficients at landing and take-off. The size of the wing depends on the wing loading and BWB is tends to have a lower wing loading which increases the wing span. It is recommended that an appropriate wing loading should be selected.

7. Fuselage Design

1. Introduction

This part of the report discusses about the preliminary design of fuselage and cockpit of the proposed BWB aircraft. It specifies the design parameters and dimensions of the fuselage and cockpit. Fuselage design depends upon following parameters:

- The maximum take-off weight of the aircraft
- Number of passengers
- Fuel Storage
- Location of engines
- Location of Landing gear
- Wing placement

Designing of the cockpit and fuselage is very critical due to human factor and it does not follow a specific method. Depending upon the purpose of the aircraft, when designing the cockpit and fuselage, the following things should be kept in mind:

- Number and weight of the cockpit crew member
- Number and weight of cabin crew member
- Number and weight of special duty crew member
- Number and weight of passengers
- Weight and volume of 'carry-on' baggage
- Weight and volume of 'check-in' baggage
- Weight and volume of cargo
- Number, weight and size of cargo container
- Weight and volume of special operational equipment
- Weight and volume of fuel
- Radar equipment
- Auxiliary power unit

Pilot visibility and reachability of the equipment and essential controls drives the cockpit design. The design of the fuselage is driven by comfort of passenger and crew members, space for lavatory, galleys and crew resting area.

The fuselage should be able to withstand the forces as well the moments due to numerous factors. The thickness of the fuselage shell depends on the overall purpose of the aircraft.

2. Layout design of the cockpit

The design of the cockpit should be such that it should meet the following requirements:

- The pilot and cockpit crew members should be positioned in such a way that they can reach the controls with minimum effort from the designated position.

- Essential instruments should be visible without any due effort.
- Communication between pilot and other members in the cockpit, by means of voice and sound, should be possible without any use of communicating devices.
- The visibility from the cockpit must meet the minimum required standards.

While designing cockpit, the weight and dimensions of the crew member should be kept in consideration as it is important that the design ensures the leg and arms movement needed to carry out the control either with sticks or button or pedals.

The following picture depicts the dimensions of an average pilot or crew member. For female crew member, the dimensions are to be multiplied by a factor of 0.85.

The dimensions of the crew member are given in the picture below.

A	B	C	D	E	F	G	H	I	K	L
1,600	870	230	300	620	350	435	850	140	760	300
1,750	920	255	335	685	390	475	950	150	805	330
1,900	990	280	370	750	430	515	1,050	160	875	360

A	M	N	O	P	Q	R	S	T	U
1,600	300	50	200	190	260	80	25	20	20
1,750	325	60	220	200	270	90	30	30	20
1,900	350	70	240	210	280	100	30	30	20

Figure 34 Dimension table.

The definitions of the dimensions mentioned above are given in the picture below.

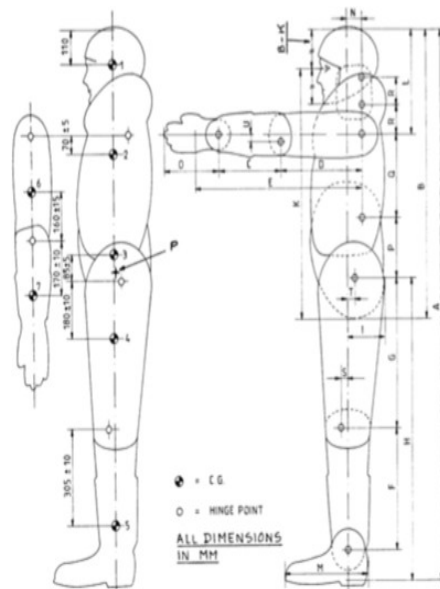


Figure 35 Dimensions of standing male crew member

Area for cockpit is very limited and is driven by the factor of unrestricted visibility for the pilot and copilot.

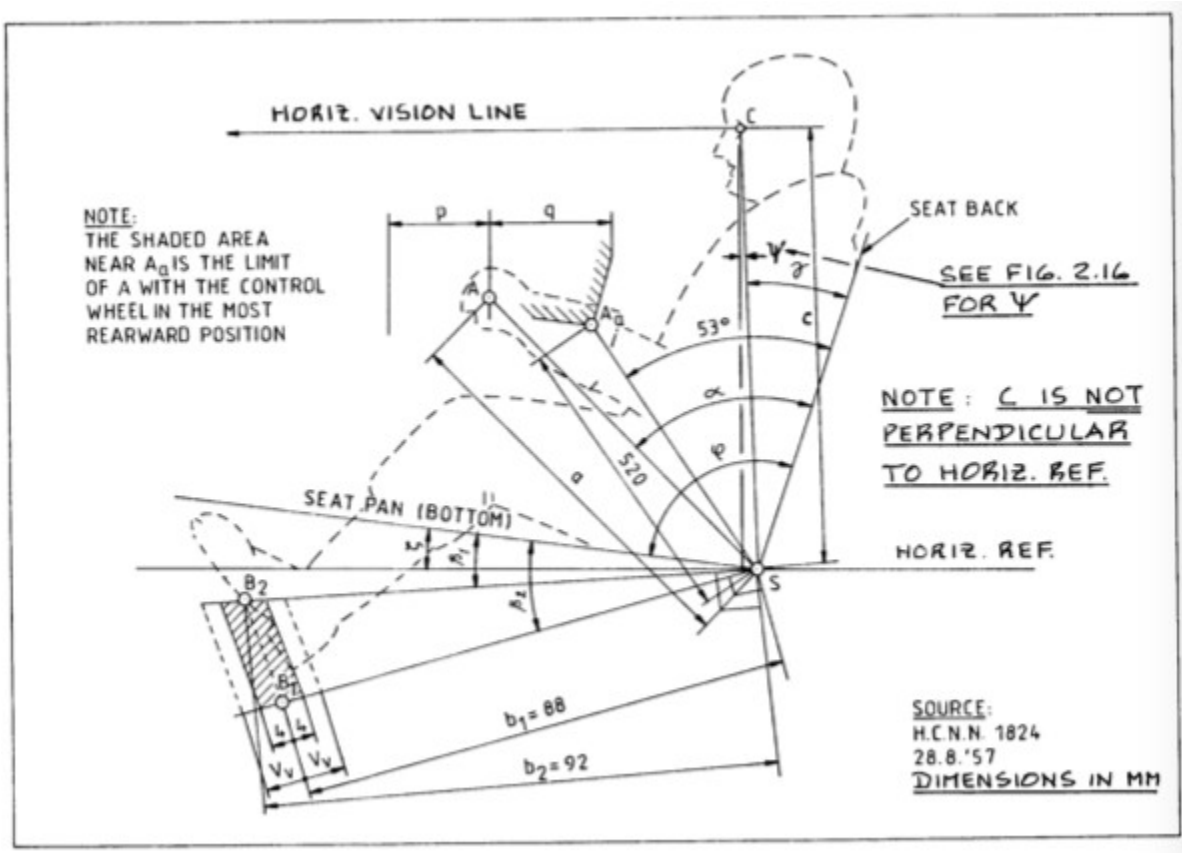


Figure 36 Cockpit design parameters.

Due to limited space, its design becomes critical as the design should accommodate the variation in the human size as well as the space for control panel. It can be obtained by arranging the seat position in adjustment and rudder paddle adjustments.

The proposed aircraft is assumed to have wheel type controller and the dimensions for such cockpit is given in the figure below:

For Wheel Type Controllers:

A	B	C	D	E	F	G	H	I	J	K
37	30.25	5	21	101	29.75	10.00	16.63	19	6	9
39	30.75	5	19	101	30.25	9.75	15.75	19	6	9
41	31.50	5	16	101	31.00	9.75	15.13	19	6	9
43	31.75	5	16	101	31.25	10.00	15.13	19	6	9

A	L	M	N	O	P	Q	R
37	10.00	36.0	5	9.25	15	7	25
39	10.50	35.0	5	9.25	15	7	25
41	10.75	34.5	5	9.25	15	7	25
43	11.00	34.5	5	9.25	15	7	25

Figure 37 Wheel type controller-based dimensions

The figure below shows the convenient access of controls with the areas that are marked for good as well as bad accessibility for a pilot.

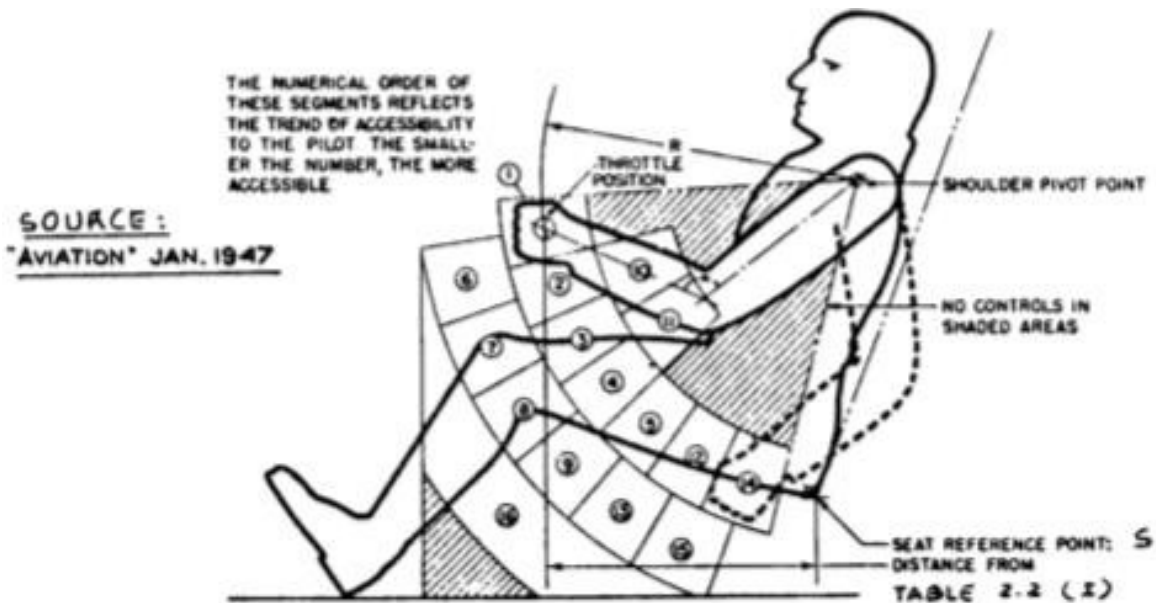


Figure 38 Quality of accessibility areas

There is no defined method for deducing the relationship between pilot seat and controls as human body varies to great extent for any method to implement. A range with limits in the figure are as follow:

- Variation in arm length (C+D+O): +/- 15 cm
- Variation in leg length (H): +/- 20 cm
- Variation in seat eye distance (C): +/- 12 cm

The no systematic relationship between each of these points implies that a considerable amount of room for adjustment should be available.

The following points should be kept in mind as they are directly concerned with work of the cockpit members:

Flight essential crew members and their primary controls should not be located within the 5 degrees of arcs.

According to FAR 23.771 and FAR.771 these requirements must be met for propeller driven airplanes only.

Following are the dimensions for civil transport cockpit with adjustments for wheel as well as stick type control.

Symbol	Wheel Control	Stick Control
a	67 (+/- 4)	63 (+/- 4)
ξ	7° (+/- 2°)	7° (+/- 2°)
p = Forward motion of point A:	18 (+/- 2)	16 (+/- 2)
q = Rearward motion of point A:	22 (+/- 2)	20 (+/- 2)
r = Sidewise motion of point A from center*:	-----	15 (+/- 2)
d = Distance between handgrips of wheel*:	38 (+/- 5)	-----
e = Wheel rotation from center*:	85° (max.)	-----
v = Distance between rudder pedal center lines*:	38 (+/- 12)	45 (+/- 5)
α	64° (+/- 3°)	70° (+/- 3°)
β_1	22°	same
β_2	10°	same
c	77 (+/- 2)	same
γ	21° (+/- 1°)	same
φ	102° (+/- 2°)	same
V _v = Adjustment range of pedals from center position B:	7 (+/- 2)	same
U _v = Forward and aft pedal motion from center position B*:	10 (+/- 2)	same
S _h = Horizontal adjustment range of S from center position*:	< 10	same
S _v = Vertical adjustment range of S from center position*:	8 (+/- 1)	same

Figure 39 Dimensions and Adjustments for cockpit design

Determination of Visibility from the cockpit:

For the following reasons, it is necessary to have a proper visibility:

- During take-off and operations, a pilot must have a good view of its immediate surroundings.
- During en-route operations, the pilot must be able to observe conflicting traffic.
- During combat, the outcome of the fight depends directly on the visibility of the pilot.

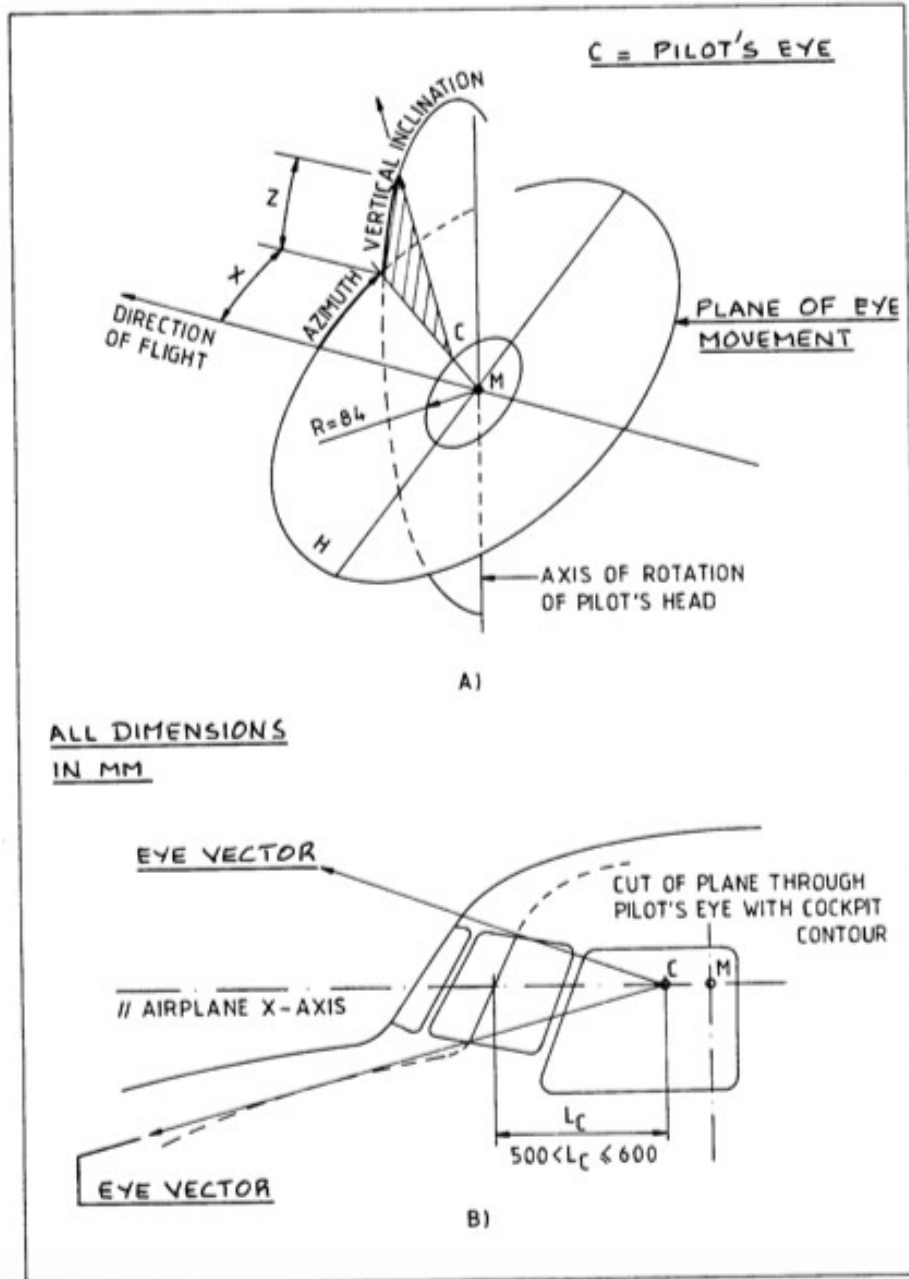


Figure 40 Definition of radial eye vector

The minimum visibility rules were put down for civil and military airplanes. There are different visibility requirements for different aircraft and its purpose depending upon the customer requirements. The required cockpit visibility is defined as the angular area that is obtained after intersecting the cockpit with the radial vectors emanating from the eyes of the pilot which are assumed to be centered on the pilot's head. Point C is an imaginary point which is assumed to be the center of the vision and is used to construct the visibility pattern. The point C should be located as precisely as possible as the seat position of pilot is determined according to it. The seat itself is relative to the controls and floor.

The flow of the cockpit design steps is as follows:

- Locate point C on the horizontal axis of vision.
- The distance should be within the indicated range.
- Draw angle $\Psi = 8.75$ degrees.
- Locate point as with the maximum distance 'c' of 80 cm.
- Design the pilot seat.
- Draw the cockpit control and seat motion.
- Check for visibility.

Airplanes with side by side arrangement for pilot and co-pilot, the area within the 30 degrees of starboard and 20 degrees of the port should be free from window frames and in the area from 20 degrees port to 60 degrees port, window frames should not be wider than 2.5 inches.

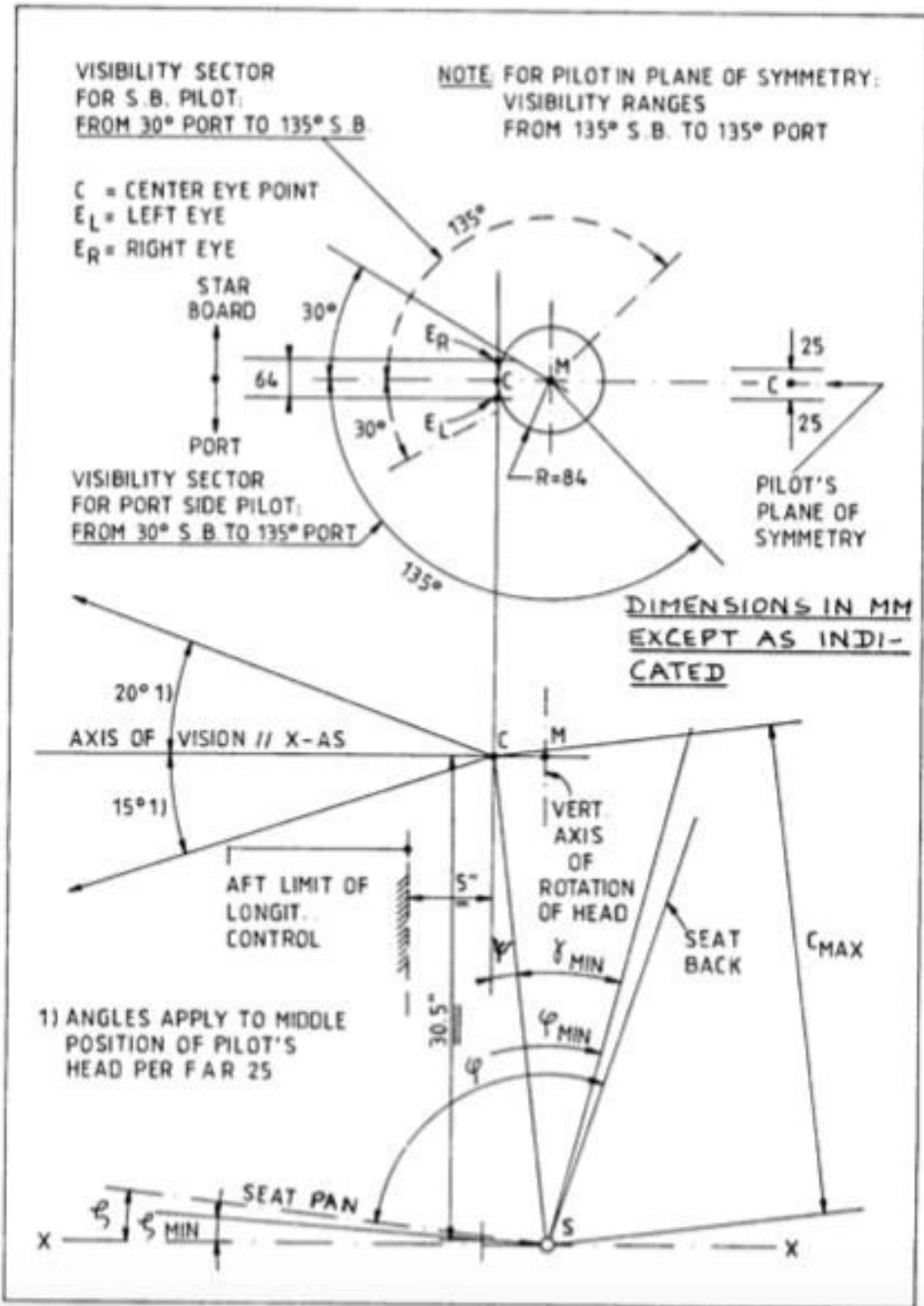


Figure 41 Visibility requirements

For safety reasons, the windows should meet the requirements of the bird strike test. Hence large windows would account for bulky frames, increasing the weight of the aircraft. Windows are also source for drag. Flat windows produce more drag when compared to curved windows but the later distort the image.

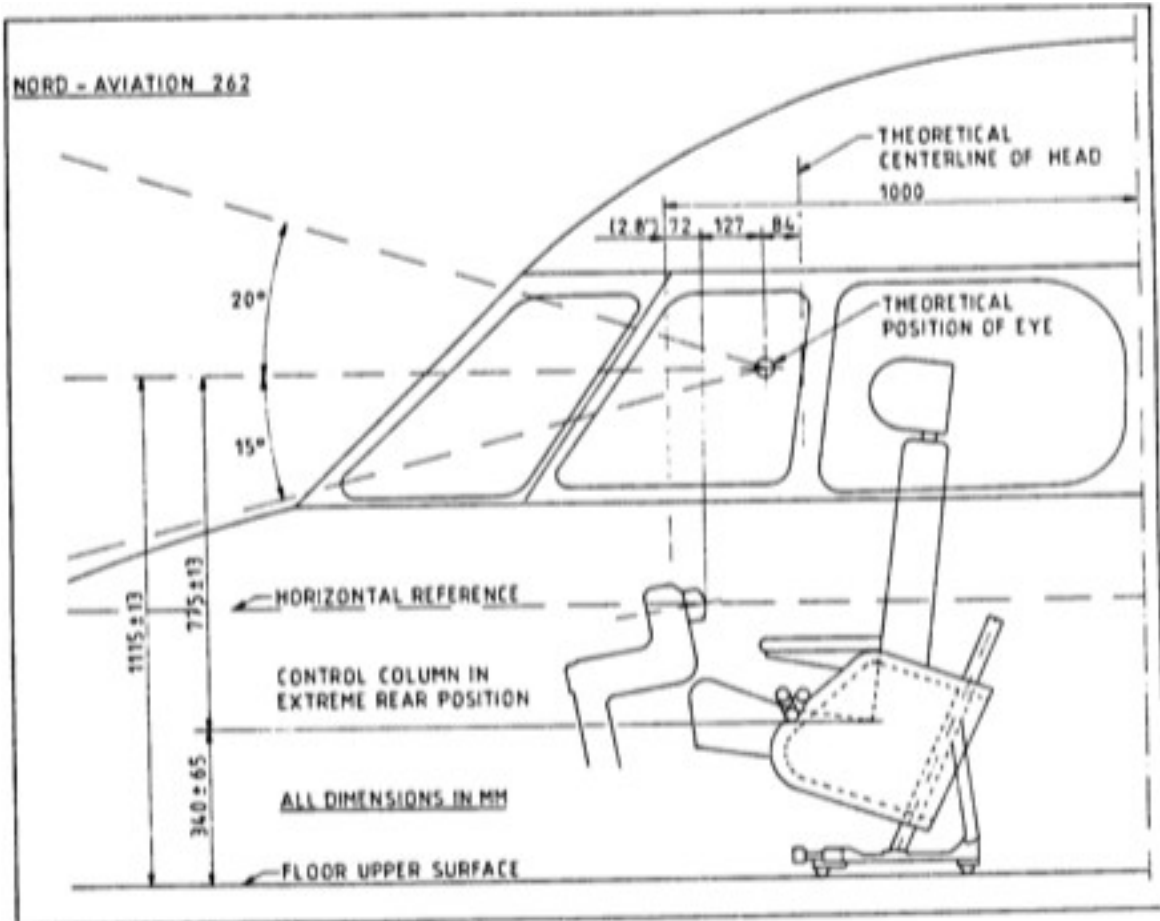


Figure 42 Cockpit layout

Layout Design of the fuselage

Following are the factors to keep in mind while designing a fuselage for a BWB aircraft:

- Number of persons.
- Division of seating i.e. first class, business class and economy class.
- Cabin provisions.
- Seating arrangement for crew members.

Most of the conventional aircrafts have a circular fuselage which has inherent property of uniform pressure distribution but with the irregular shape of a BWB fuselage, pressure distribution is a major problem. The most recent studies show that an elliptical cross section of the fuselage would provide a better pressure distribution. With elliptical cross section, passengers are seated in a horizontal fashion rather than vertical which allows same number of passengers in a relatively short cabin. The cabin width is also constrained by the shape of the airfoil used to reduce overall drag of the aircraft.

The uneven pressure distribution was a major concern while designing the fuselage for structural loads. To solve the problem, unique ideas were proposed some of which are:

Multi-bubble cabin concept

This concept separates the structure that carries the pressurization loads from the aerodynamic shell. The pressure shell is connected to outer skin via thick sandwich structure. The main drawback of the such configuration is, the outer shell should be able to carry the pressurization load in case the inner shell fails which leads to thicker outer shell hence, increasing the weight of the aircraft.

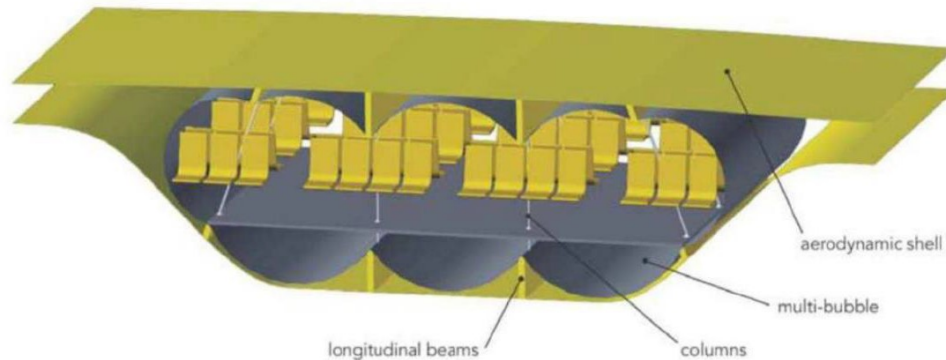


Figure 43 Multi-bubble configuration

Integrated skin and shell concept

This concept proposes to integrate the structure that takes pressurization load with the structure that bears the aerodynamic loads. This leads to rectangular cabins which again have the problem of pressure distribution.

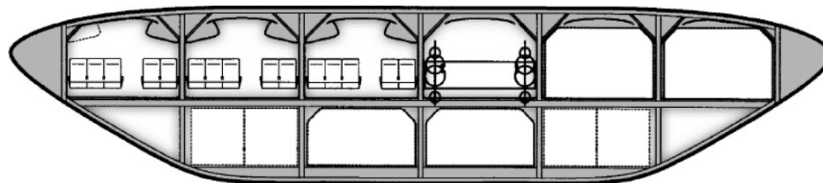


Figure 44 Integrated skin and shell Concept

Oval fuselage

It uses tangentially connected arcs and an aerodynamic shell to form an oval pressure vessel. The pressurization loads are taken via in-plane loading by means of four tangentially intersecting arcs.

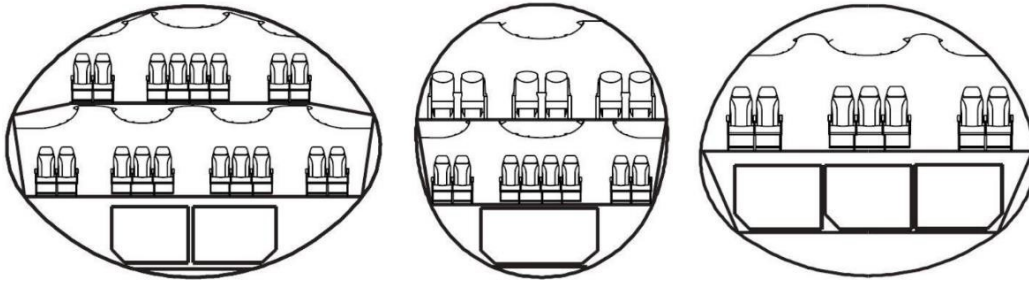


Figure 45 Oval fuselage

The fineness ratio of a BWB aircraft is low which is good for subsonic jet transports as it would suggest low probability of sudden variation in the cross section of the aircraft. The very low fineness ratio would result in large base inducing more drag while if the fineness ratio is too high, penalty is paid in terms of friction drag.

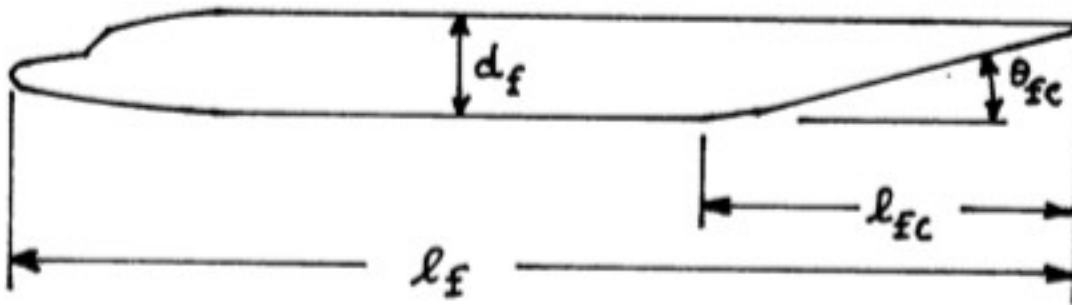


Figure 46 Definition of fineness ratio

The figure below provides the general value of the fineness ratio of various built aircraft.

Airplane Type	l_f/d_f	l_{fc}/d_f	θ_{fc} (deg)
Homebuilts	4 - 8	3*	2 - 9
Single Engine	5 - 8	3 - 4	3 - 9
Twins	3.6** - 8	2.6 - 4	6 - 13
Agricultural	5 - 8	3 - 4	1 - 7
Business Jets	7 - 9.5	2.5 - 5	6 - 11
Regionals	5.6 - 10	2 - 4	15 - 19***
Jet Transports	6.8 - 11.5	2.6 - 4	11 - 16
Mil. Trainers	5.4 - 7.5	3*	up to 14
Fighters	7 - 11	3 - 5*	0 - 8
Mil. Transports, Bombers and Patrol Airplanes	6 - 13	2.5 - 6	7 - 25****
Flying Boats	6 - 11	3 - 6	8 - 14
Supersonics	12 - 25	6 - 8	2 - 9

Figure 47 Fuselage parameters

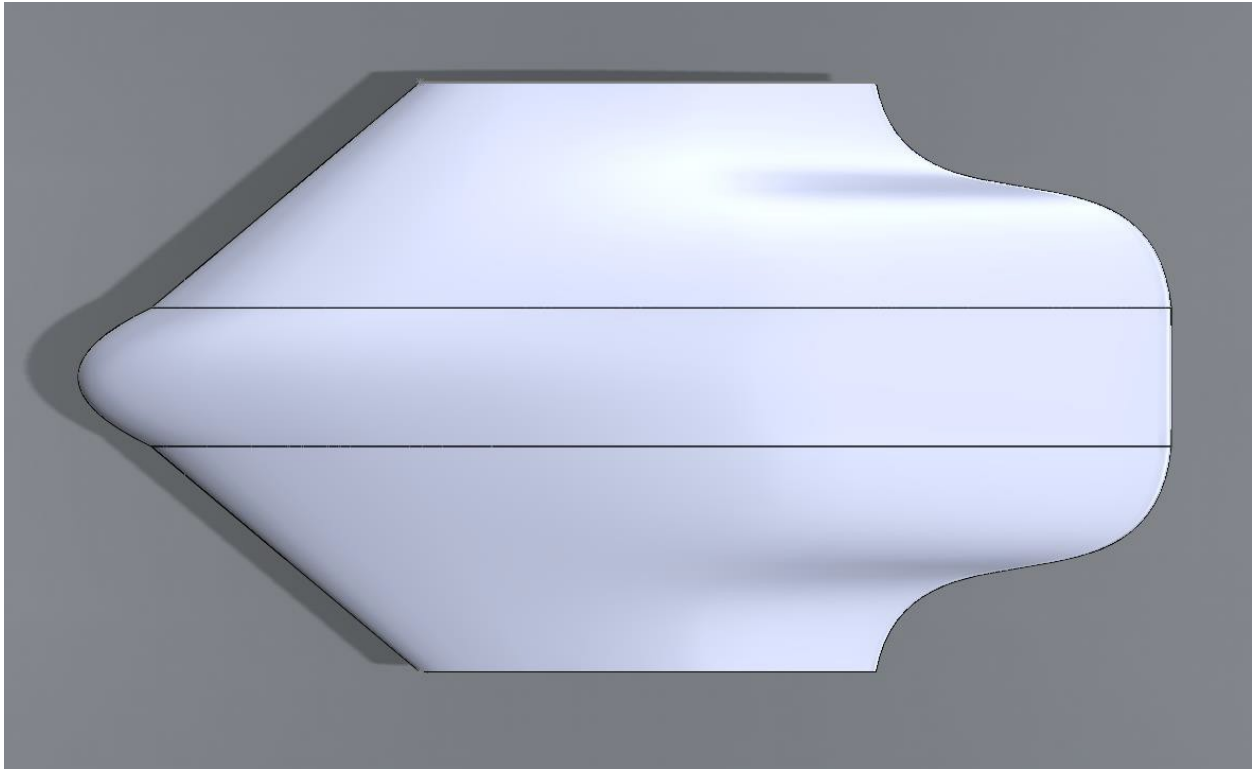


Figure 48 Top view of fuselage

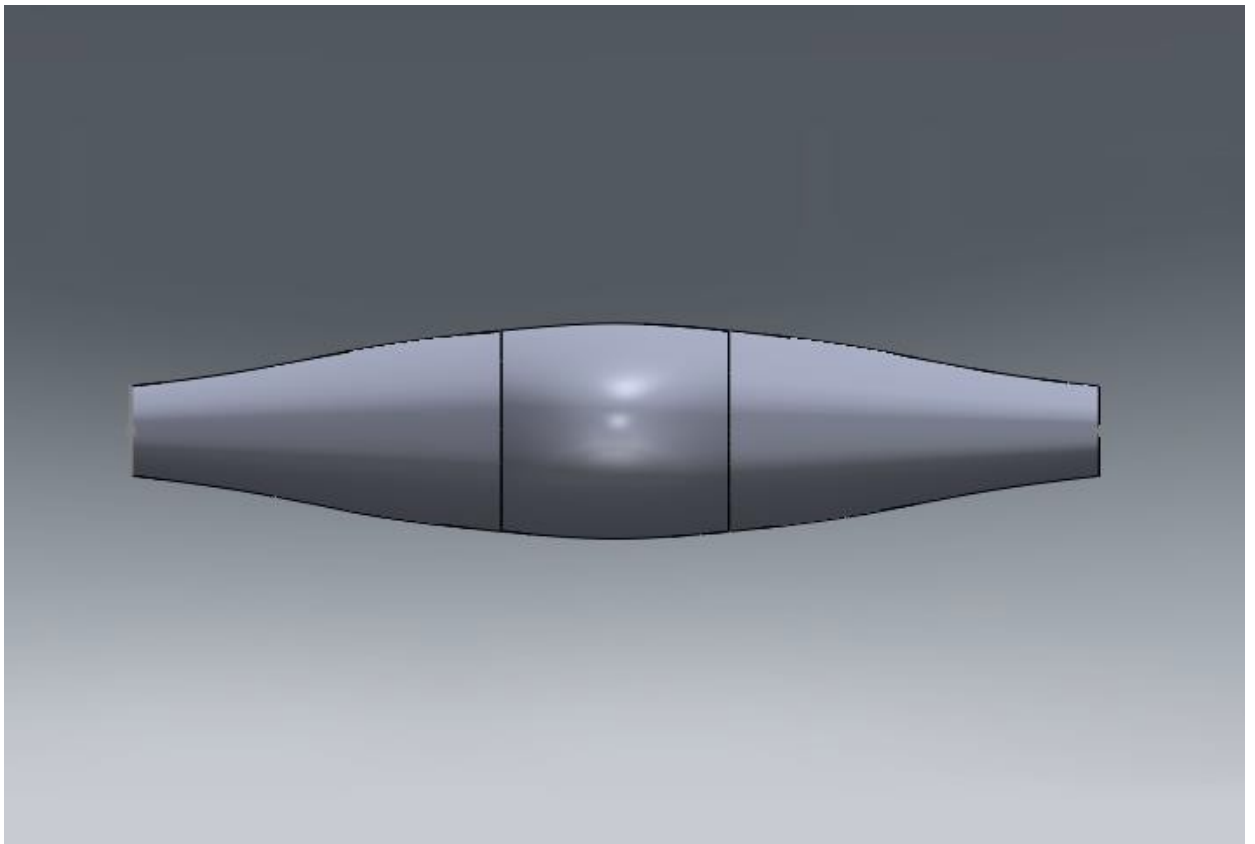


Figure 49 Front view of fuselage

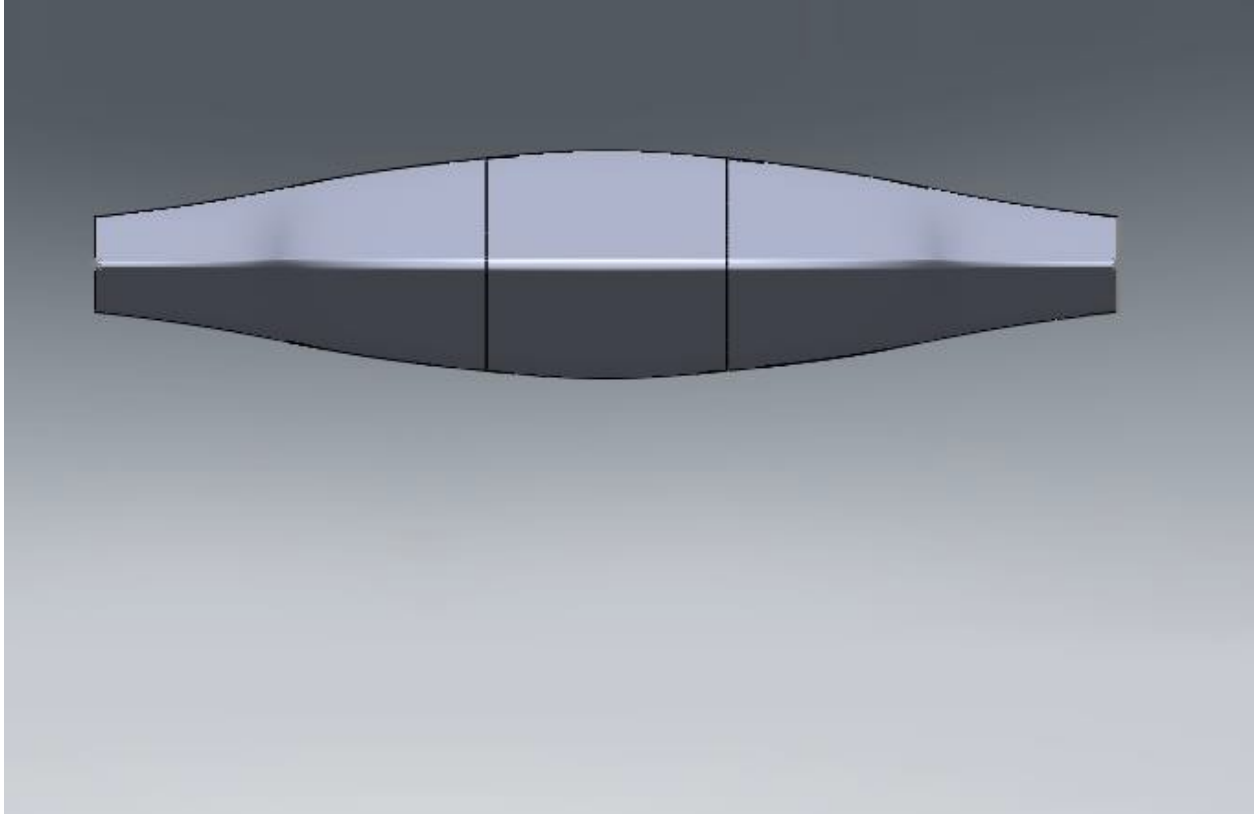


Figure 50 Rear view of the fuselage

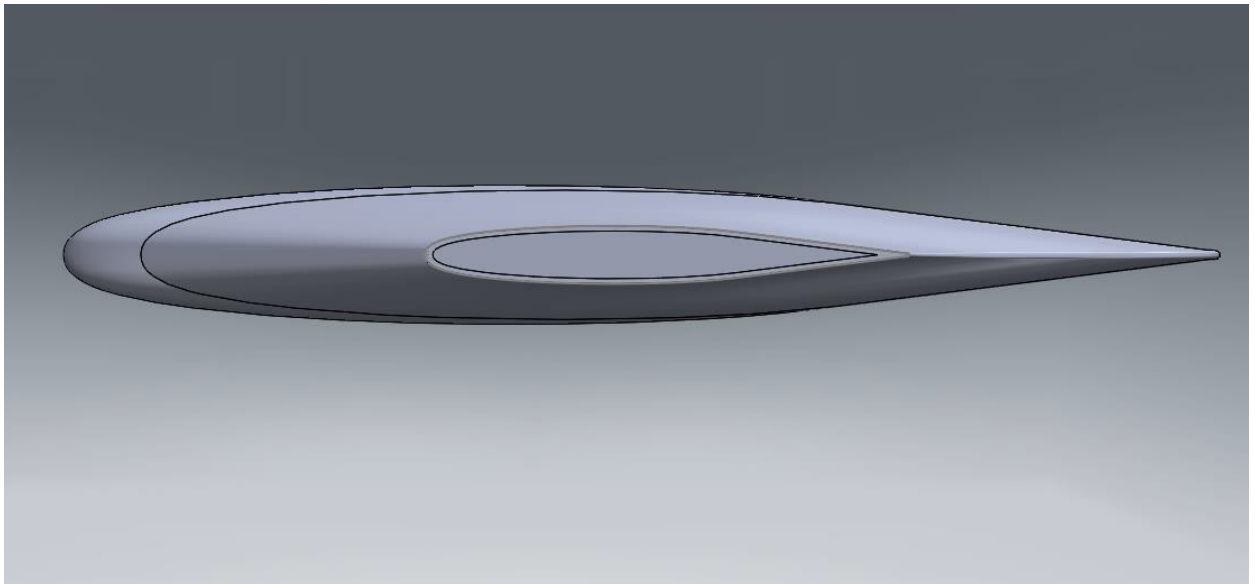


Figure 51 Side view of the fuselage

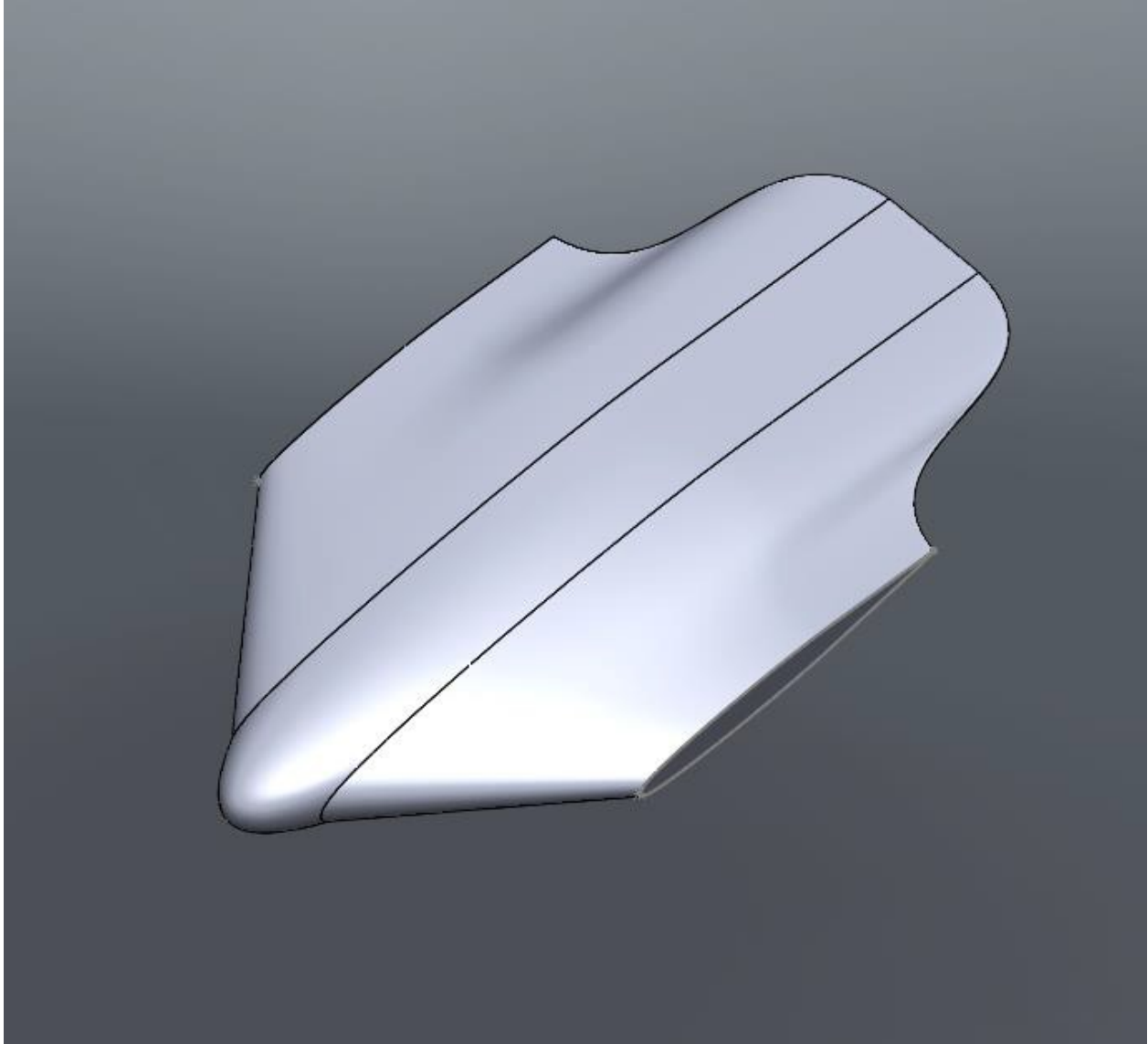


Figure 52 3D view of the fuselage

3. Aerodynamic Drag Condition

Fuselage is the major contributor to the overall drag produced by the aircraft. A conventional aircraft fuselage produces around 20 percent of the total drag. The concept of BWB aircraft is to reduce this drag by eliminating a separate fuselage and integrating it with wings. The gradual change in cross section area is also reduces drag produce by airplane. The following type drags are produced by fuselage:

- Friction drag
- Base Drag
- Compressibility drag
- Profile drag

Induced drag

The overall wetted area for a BWB aircraft is less than that of conventional aircraft. This would directly reduce the friction drag. The supercritical airfoil used for the fuselage allows laminar flow for a longer range of Mach number hence reducing the drag.

The fineness ratio of the fuselage increases with increasing the Mach number for cruise. While blunt bodies have an increased profile drag and promote flow separation. Such shapes can be result of poor cockpit design. The ideal shape streamline of the fuselage is obtained by integrating the windshields with in the body.

Interior Layout of Design of the Fuselage

The interior of the fuselage is a compromise between the comfort of passengers and weights and size of the installations in the cabin. The design should also promote easy loading and unloading of cargo as well as ease of maintenance.

The cabin of the aircraft houses the following:

- Layout pf the cross section
- Seating layout
- Layout for emergency exit doors
- Galley, lavatory and wardrobe layout
- Cargo bay layout
- Maintenance and servicing consideration

Due to its unconventional design, the main difference between the cabins of conventional aircraft and BWB is the planform shape. The cabin shape consists of a combination of rectangle and trapezium. This trapezium is also known as isosceles trapezium as it has equal base angle and one pair of opposite sides that are parallel.

There two different proposed cabin layouts of a BWB aircraft. One occupying the center body space completely for cabin while latter leave space for fuel tank or cargo bay. The figure below depicts the two kinds of proposed layouts.

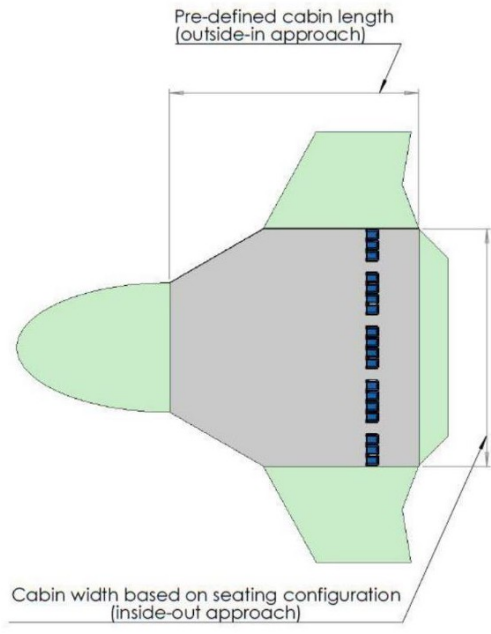


Figure 53 Cabin layout 1

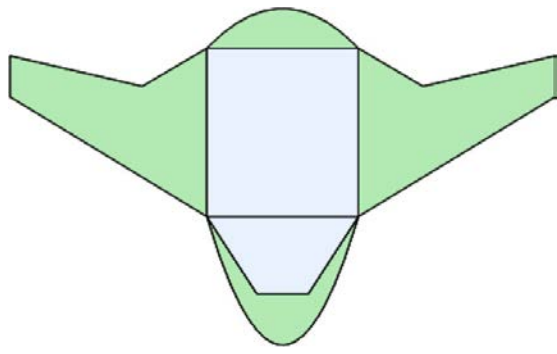


Figure 54 Cabin layout 2

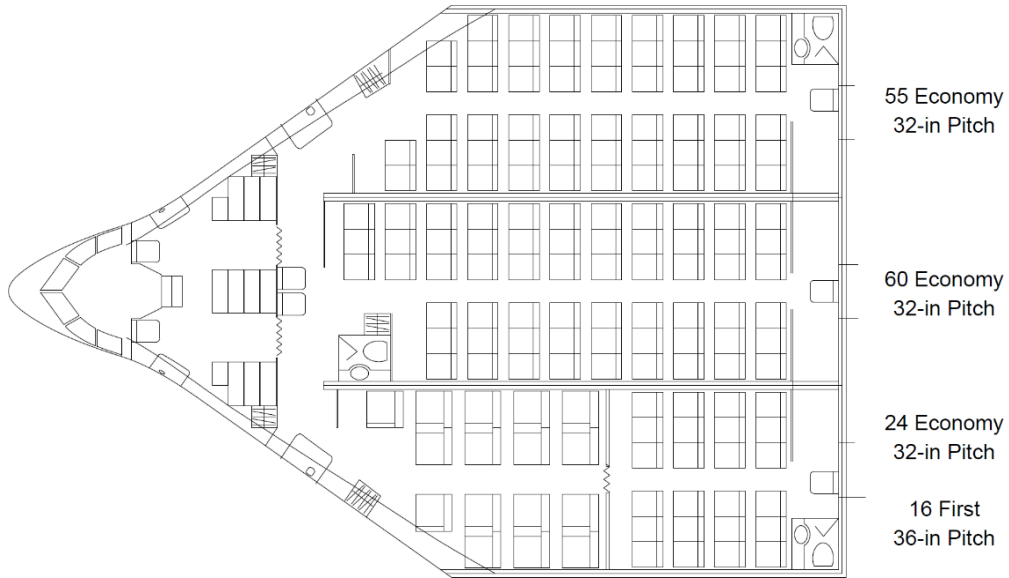


Figure 55 Seating layout of NASA SUGAR Ray

Using the conventional dimensions for seats, aisles, galley and other installations of the cabin, layout was made. The figure below shows the dimensions of the seats and aisles.

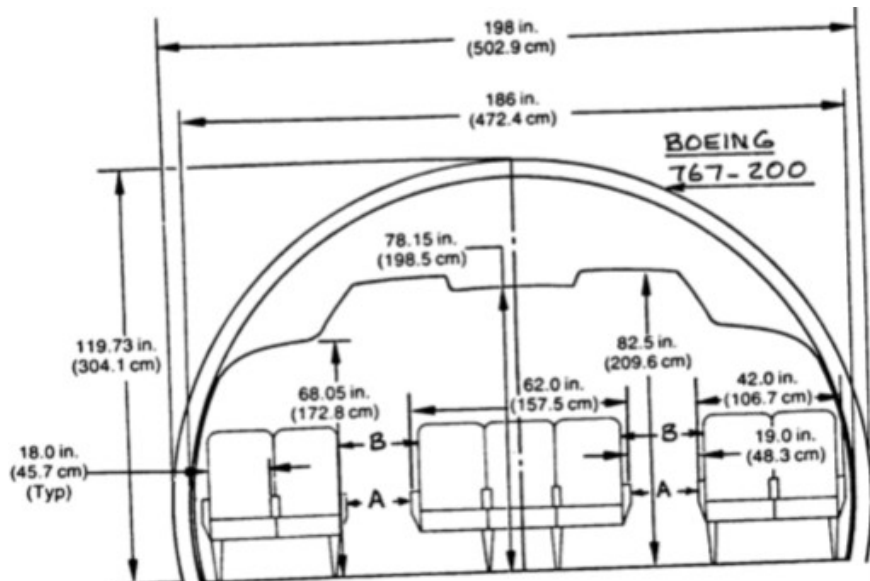


Figure 56 Minimum aisle requirements

Symbol	Unit	De Luxe	Normal	Economy
a	in.	20(18.5-21)	17(16.5-17.5)	16.5(16-17)
b	in.	47(46-48.5)	40(39-41)	39(38-40)
b	in.	---	60(59-63)	57
l	in.	2.75	2.25	2.0
h	in.	42(41-44)	42(41-44)	39(36-41)
k	in.	17	17.75	17.75
m	in.	7.75	8.5	8.5
n	in.	32(24-34)	32(24-34)	32(24-34)
p/p_{max}	in./in.	28/40	27/37.5	26/35.5
α/α_{max}	deg/deg	15/45	15/38	15/38

Figure 57 Dimensions of seat for different class

Frame Depths:

For small commercial airplanes: 1.5 inches.
 For fighters and trainers: 2.0 inches.
 For large transports: $0.02d_f + 1.0$ inches.

Frame Spacings:

For small commercial airplanes: 24 ~ 30 inches.
 For fighters and trainers: 15 ~ 20 inches.
 For large transports: 18 ~ 22 inches.

Longeron Spacings:

For small commercial airplanes: 10 ~ 15 inches.
 For fighters and trainers: 8 ~ 12 inches.
 For large transports: 6 ~ 12 inches.

Figure 58 Frame depth, spacing and longeron spacing

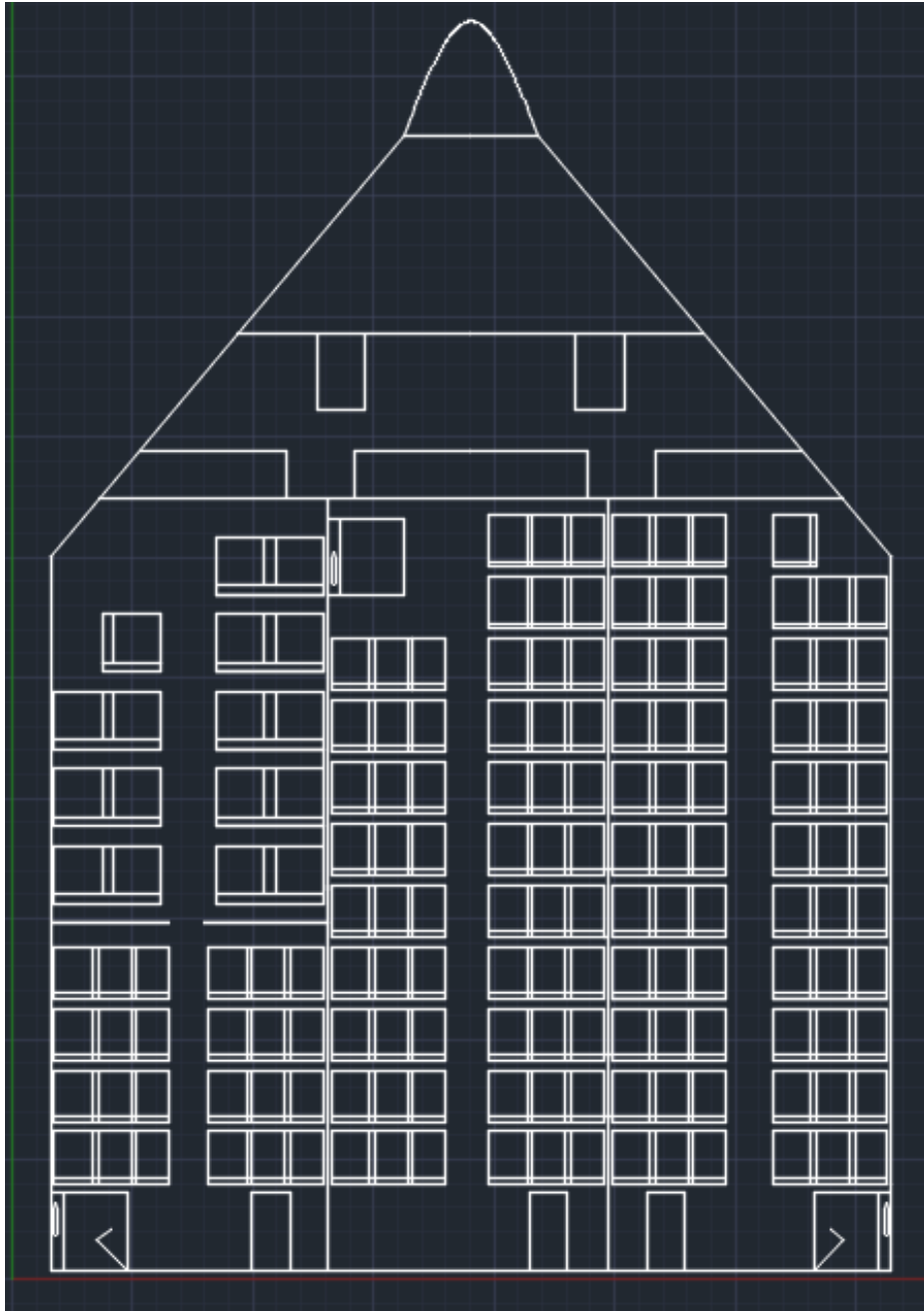


Figure 59 Cabin planform and seating layout of the proposed aircraft

4. Discussion

This report consists of the fuselage design of a BWB aircraft. There is no method to calculate the length of the aircraft. With the help of different dimensions of seats, galley, lavatory, cockpit, crew seating area and other lengths, the overall interior length of the cabin is calculated. The cockpit is designed like a conventional aircraft while a hybrid method is used for the sizing of cabin. The cockpit needs to meet FAR 25 visibility requirements.

8. Wing, High Lift System & Lateral Control Design

1. Introduction

This report contains the discussion of design of wing plan. Wing plan is a collective term used for different geometrical constraints of the wing with lateral control surfaces. It includes:

- Wing Area, S
- Aspect Ratio, A
- Sweep Angle, λ
- Thickness Ratio, t/c
- Airfoils
- Incidence angle, i_w and twist angle
- Dihedral angle, Γ_w
- Lateral control surface size and layout

The vehicle aerodynamics are affected significantly with the choice of wing plan as well as it also provides basic shape of the aircraft. A wing planform is such selected that it provides a high lift coefficient and sufficient volume for wing fuel tank and offering a minimum zero lift drag. The condition stated above is very ideal and cannot be achieved due to conflicting conditions. Thus, selection and design of the wing plan is a tradeoff between the desired properties and inherent properties established by mission requirements.

Certain values for the calculations are assumed based on the data from similar aircraft and or an educated guess is made. The various parameters, such as taper ratio, dihedral angle, thickness ratio, are calculated and based on which airfoil selection is made which satisfy the required clean C_{Lmax} . The results from manual calculations are verified with the help of AAA program.

The lateral control surfaces are designed to meet the requirements of the aircraft according to the obtained dimensions. The report also specifies the type and design parameters of the lateral control surfaces and high lift devices.

The wing is designed based on the calculations of the following parameter:

- Span
- Root chord
- Tip chord
- MAC (Mean Aerodynamic Chord)
- MGC (Mean Geometric Chord)
- Leading Edge Sweep angle
- Trailing Edge Sweep Angle
- Coordinates of aerodynamic center

2. Wing Planform Design

A BWB aircraft is a configuration which integrates fuselage and wings into a unibody which gradually transits into a wing. Hence there is no demarcation between fuselage and wing, the complete aircraft is considered as a wing. In the BWB configuration, the aircraft can be considered as a two-part wing:

- Inbound Wing
- Outbound Wing

The inbound wing can be considered as fuselage. This report discusses the designing of the outbound wing which houses the control surfaces. Size of the outbound wing would affect the following characteristic of the aircraft:

- Take-off/ Landing field length
- Cruise performance
- Weight
- Size and placement of fuel tanks

The important parameters on which the wing planform depend are the following:

- Gross Area
- Aspect Ratio
- Taper Ratio
- Dihedral Angle
- Sweep Angle

The gross area and aspect ratio is already calculated while sizing the airplane for performance (Report 4).

The gross wing area depends on the wing loading of the aircraft. From the matching graph, the design point gives a wing loading of 48 lb/ft and with the take-off weight is 150,800 lb.

$$S = \frac{W_{TO}}{\frac{W}{S}}$$
$$S = \frac{150800}{48} = 3142 \text{ sq. ft}$$

The aspect ratio is fixed while preliminary weight sizing to 7.8. The taper ratio of the aircraft is the ratio of chord of tip to the chord of root. It is fixed in accordance to the similar aircraft. For this aircraft the taper ratio is 0.25. The database for a BWB is not enough so, other traditional aircrafts with similar capacity are compared, major being the SUGAR Ray program.

Type	Dihedral Angle, Γ_w'	Incidence Angle, i_w'	Aspect Ratio, A	Sweep Angle, $\Lambda_{c/4}'$	Taper Ratio, λ_w	Max. Speed, V_{max}'	Wing Type
	deg.	root/tip deg.		deg.		kts	
BOEING							
727-200	3	2	7.1	32	0.30	549(22K)	ctl/low
737-200	6	1	8.8	25	0.34	462(33K)	ctl/low
737-300	6	1	8.0	25	0.28	462(33K)	ctl/low
747-200B	7	2	7.0	37.5	0.25	523(30K)	ctl/low
747SP	7	2	7.0	37.5	0.25	529(30K)	ctl/low
757-200	5	3.2	7.9	25	0.26		ctl/low
767-200	6	4.3	7.9	31.5	0.27		ctl/low
MCDONNELL DOUGLAS							
DC-9 Super 80	3	1.3	9.6	24.5	0.16	500	ctl/low
DC-9-30	1.5	NA	8.7	24	0.18	537	ctl/low
DC-10-30	5.3/3	+/-	7.5	35	0.25	530(25K)	ctl/low
AIRBUS							
A300-B4	5	NA	7.7	28	0.35	492(25K)	ctl/low
A310	11.1/4.1	5.3	8.8	28	0.26	483(30K)	ctl/low
Lockh. 1011-500	7.5/5.5	NA	7.0	35	0.30	525(30K)	ctl/low
Fkr F28-4000	2.5	NA	8.0	16	0.31	390	ctl/low
Rombac 111-495	2	2.5	8.5	20	0.32	470(21K)	ctl/low
BAe 146-200	-3	3.1/0	9.0	15	0.36	420(26K)	ctl/high
Tupolev Tu154	0	NA	7.0	35	0.27	526(31K)	ctl/low

ctl = cantilever (30K) = 30,000 ft altitude

Figure 60 Database for Wing

Manufacturer	AIRBUS											
Type	A300-	A310-	A319-	A320-	A321-	A330-	A330-	A340-	A340-	A340-	A340-	A3XX-
Model	600R	300	100	200	200	200	300	200	300	500	600	100
DIMENSIONS												
<i>Fuselage:</i>												
Length (m)	53.30	45.13	33.84	37.57	44.51	57.77	62.47	58.21	62.47	65.60	69.57	67.46
Height (m)	5.64	5.64	4.14	4.14	4.14	5.64	5.64	5.64	5.64	5.64	5.64	8.50
Width (m)	5.64	5.64	3.95	3.95	3.95	5.64	5.64	5.64	5.64	5.64	5.64	7.02
Finess Ratio	9.45	8.00	8.57	9.51	11.27	10.24	11.08	10.32	11.08	11.63	12.34	9.61
<i>Wing:</i>												
Area (m ²)	260.00	219.00	122.40	122.40	122.40	363.10	363.10	363.10	363.10	437.30	437.30	817.00
Span (m)	44.84	43.89	33.91	33.91	33.91	58.00	58.00	58.00	58.00	61.20	61.20	79.80
M.A.C.(m)	6.44	5.89	4.29	4.29	4.29	7.26	7.26	7.26	7.26	8.35	8.35	12.02
Aspect Ratio	7.73	8.80	9.39	9.39	9.39	9.26	9.26	9.26	9.26	8.56	8.56	7.79
Taper Ratio	0.300	0.283	0.240	0.240	0.240	0.251	0.251	0.251	0.251	0.220	0.220	0.213
Average (t/c) %	10.50	11.80										
1/4 Chord Sweep (°)	28.00	28.00	25.00	25.00	25.00	29.70	29.70	29.70	29.70	31.10	31.10	30.00

Figure 61 Wing Geometric Data for Conventional Aircraft

	WING	V-TAIL		
Area (gross)	4,136.0	90.8		
Aspect Ratio (gross)	6.865	1.705		
Taper Ratio (trap)	0.228	0.366		
MAC Inches (gross)	489.7	101.3		
Dihedral (Deg.)	3.0	62.0	Configuration	765-097
1/4 Chord Sweep (Deg.)	27.7	39.2	SWEEP (DEG)	27.7
Root Chord (Inches) (trap)	322.6	129.23	T/C-AVE	0.1312
Tip Chord (Inches) (trap)	73.6	44.90	AIRFOIL TYPE	CONVENTIONAL
Span (W/O Winglet)	1,936.8			

Figure 62 SUGAR RAY Geometric Data

The sweep angle can be obtained from the data of similar aircraft and can be verified using the graph of maximum mach number vs. leading edge sweep angle. The value of leading edge sweep angle can be calculated using the following equation:

$$\tan(\Lambda_{LE}) = \tan(\Lambda_c) + \frac{1 - \lambda}{A(1 + \lambda)}$$

$$\tan(\Lambda_{LE}) = \tan(27.7) + \frac{1 - 0.3}{7.8 * (1 + 0.3)}$$

$$\Lambda_{LE} = 30^\circ$$

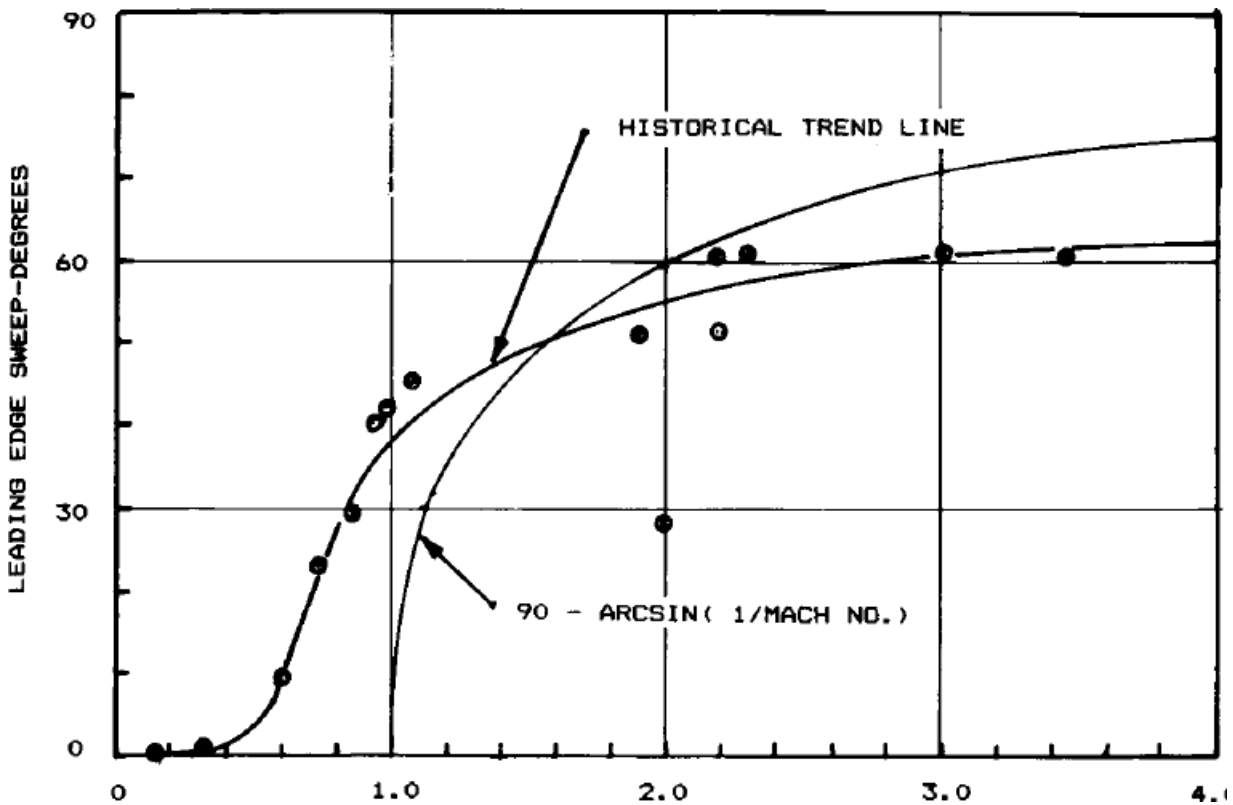


Figure 63 Mach Number vs Leading Edge Sweep

It can be observed from the graph that the sweep angle for leading edge is 28 degrees as the calculated value is within the limit. Hence the sweep angle assumed for the aircraft is acceptable. It is general practice that for every 10 degrees of sweep angle provides about 1 degree of effective dihedral. The sweep angle of 27.7 degrees can be approximate to 30 degree which would provide a dihedral of 3 degrees.

The thickness ratio of the airfoil used in the wing has a major impact on the stall behaviour and flow of air over the wing. An airfoil with high thickness ratio will encounter separated flow easily and would stall while a very thin airfoil would not be able to provide the required coefficient of lift as well as the volume for wing fuel tanks.

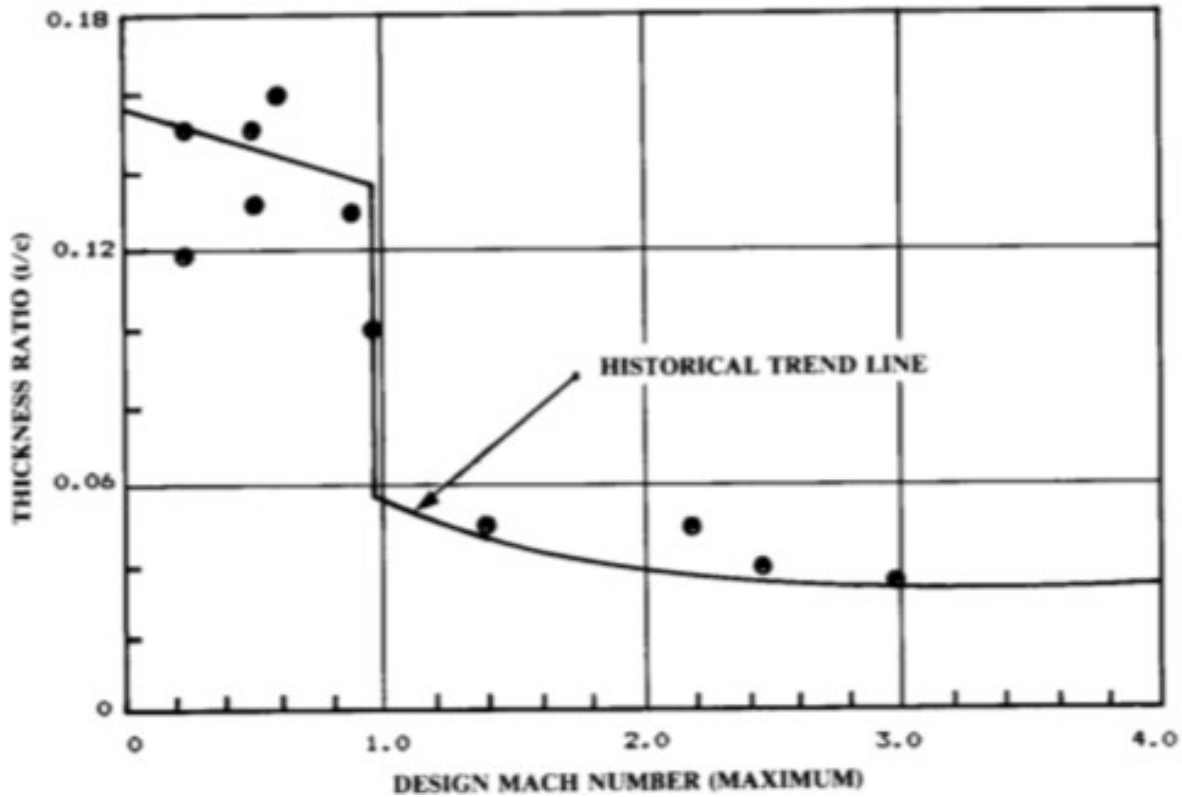


Figure 64 Design Mach Number vs Thickness Ratio

From the graph it is depicted that a thickness ratio of 0.13 is used for a speed of 0.77 mach.

3. Airfoil Selection

The selected airfoils should be able to provide the clean state $C_{L \max}$. As it is a BWB configuration, it is necessary the center body airfoil should be thick enough to accommodate cockpit, passengers, cargo as well all the equipment that are placed in the fuselage of a conventional aircraft configuration. While selecting the airfoil, it is should be kept in mind that the following calculations are satisfied by it.

$$C_l = \frac{L}{\frac{1}{2} \rho V^2 c(1)}$$

$$C_d = \frac{D}{\frac{1}{2} \rho V^2 c(1)}$$

$$C_m = \frac{M}{\frac{1}{2} \rho V^2 c(1)}$$

The thickness ratio obtained from the graph is 0.13. The center body features NASA(2)-0010 airfoil with 17% thickness while the inboard wing has NASA(2)-0714 and the outboard wing has the cross-sectional airfoil NASA(2)-041.

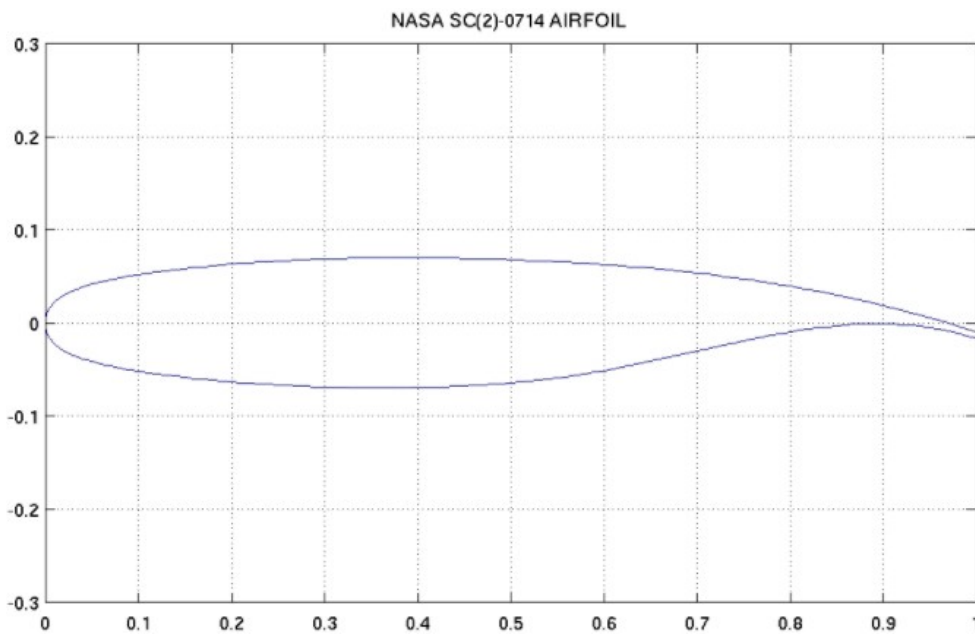


Figure 65 NASA (2)-0714

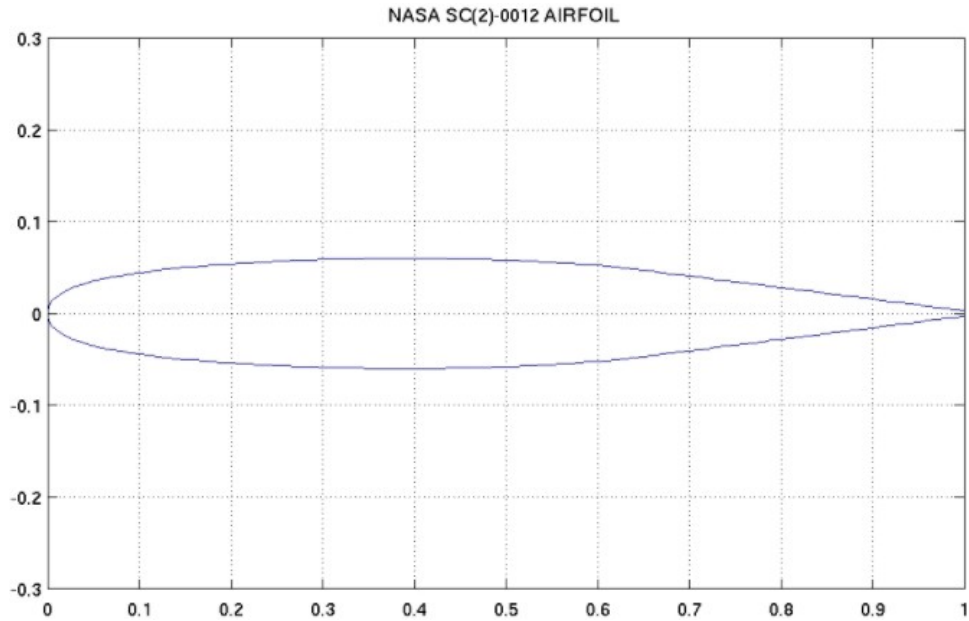


Figure 66 NASA(2)- 0012

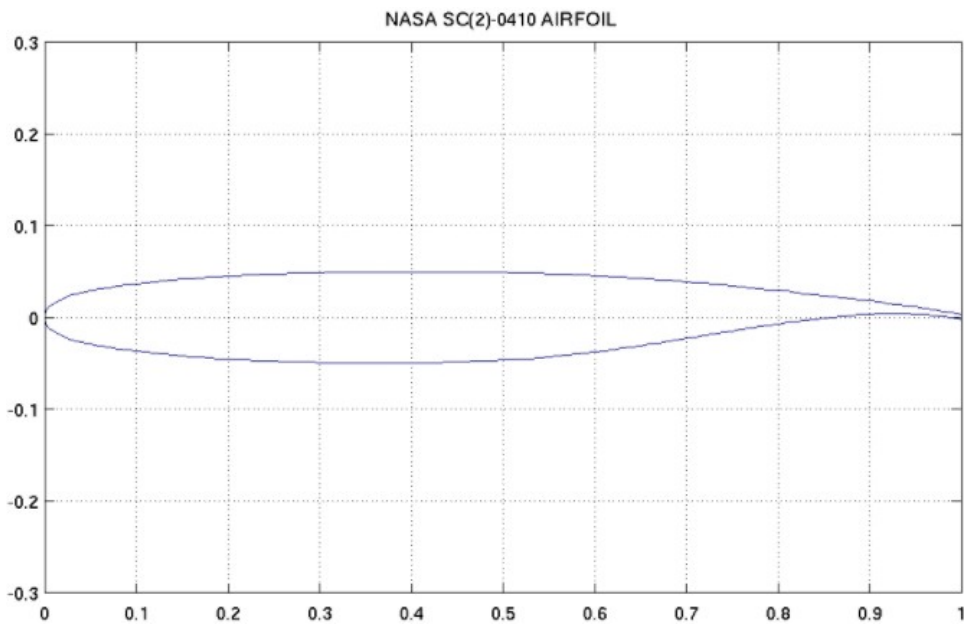


Figure 67 NASA (2)-0412

The incidence angle for similar BWB aircraft is not available but from conventional aircraft, it is observed that an inclination of 1 degree is provided to the wing. When compared to other parameters of the wing design, the incidence angle has little effect on the lift produced by the wing.

Twist is provided to the wing to change the stall behavior. There are two types of twist:

- Aerodynamic twist which is the angle between the zero-lift angle of the root and tip airfoil.

- Geometric twist is the change in angle of incidence of the root and tip airfoil.

A washout prevents the tip stall to a higher angle of attack so that the ailerons are effective even when the flow over the root of the wing is separated. Twist is eminent in small aircraft with large taper ratio and small sweep angles. Jet transports try to avoid or have a very small washout as the wings of the jet aircraft is characterized by small taper ratio and large sweep angles. Wing with such configuration would not like the root of the stall nor can afford to stall the tip. The root provides a major portion of the wing area to generate lift so, if the root stalls, the lift generated by the wing would decrease significantly.

Table 24 Wing Parameters Summary

Aircraft Configuration	Blended Wing Body
Type of the wing	Cantilever wing
Position of the wing	Mid wing
$C_{L_{cr}}$	0.2
Sweep Angle	27.7
Thickness ratio	0.13
Airfoils	NASA (2)- 0012 NASA (2)-0714 NASA (2)-0410
Taper Ratio	0.22
Wing Area	3412 sq. ft
Aspect Ratio	7.8
Span	163 ft

4. Wing CAD Model



Figure 68 3-D View of the Wing

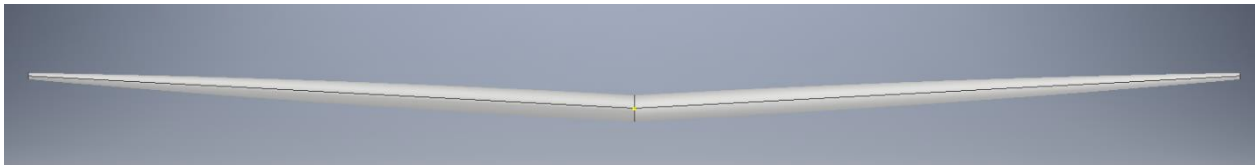


Figure 69 Front View of the Wing.

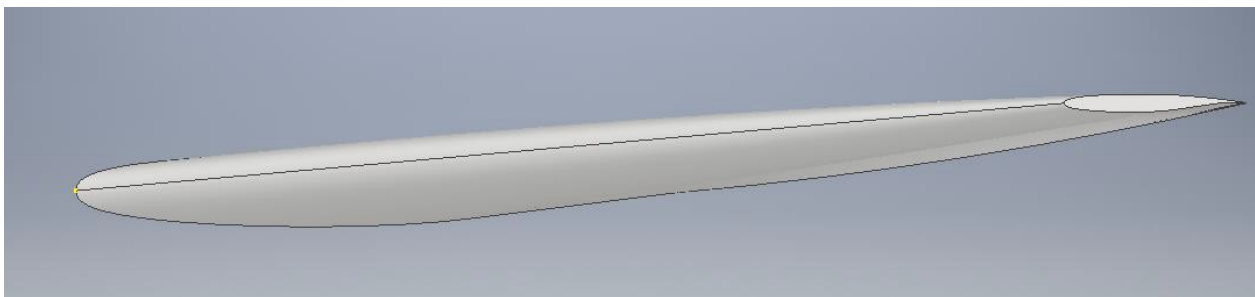


Figure 70 Side View of the Wing.

5. Wing Design Evaluation

AAA Program is used for the verification of the aircraft wing design.

Input Parameters											
b_w	163.00 ft	$c_{r,w}$	29.30 ft	$c_{t,w}$	8.00 ft	$\Lambda_{cst,w}$	27.7 deg	$x_{apex,w}$	0.00 ft	$y_{offset,w}$	0.00 ft

Figure 71 Wing planform data

Output Parameters							
S_w	3105.15 ft ²	i_w	0.30	$y_{mgc,w}$	33.44 ft	$\Lambda_{LE,w}$	30.5 deg
AR_w	8.56	\bar{c}_w	20.89 ft	$x_{mgc,w}$	19.66 ft	$\Lambda_{TE,w}$	18.6 deg

Figure 72 Wing planform output

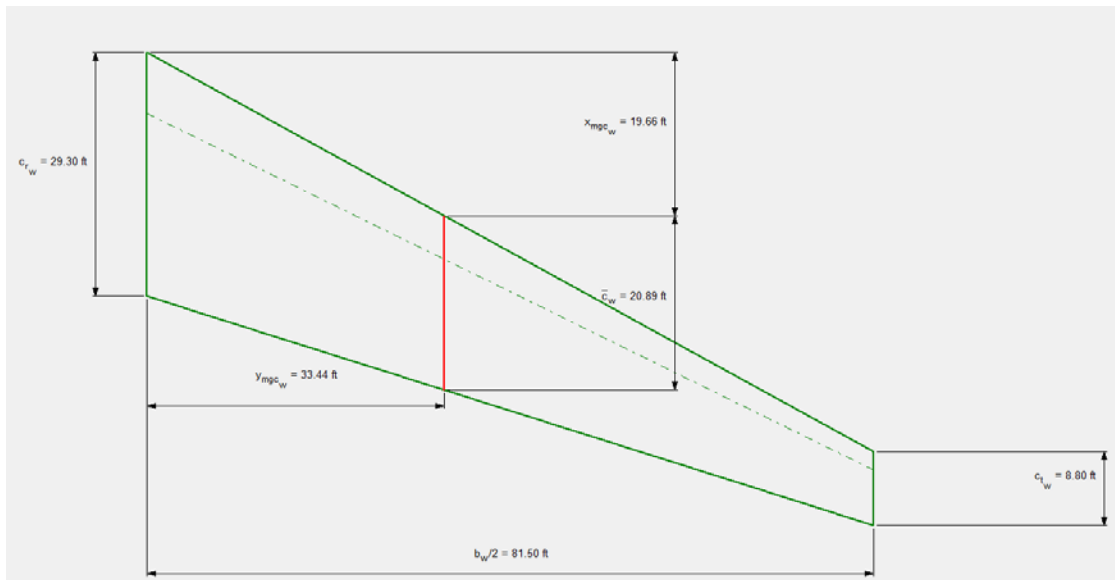


Figure 73 Wing planform

Input Parameters													
AR_w	8.56	i_w	0.30	c_{el}/c_{wl}	10.0 %	$(x_w/c)_{el}$	30.00 %	η_{el}	10.0 %	η_{et}	10.0 %	c_{et}/c_{el}	10.00 %
S_w	3105.15 ft ²	$\Lambda_{cst,w}$	27.7 deg	(c_{el}/c_{wb})	20.0 %	$(x_w/c)_{el}$	30.00 %	η_{el}	90.0 %	η_{et}	90.0 %	$(c_f/c)_{et}$	20.0 %

Elevon Airfoils		
Panel	Root Airfoil	Tip Airfoil
1	sc20714.dat	sc20410.dat

Figure 74 Elevons input data

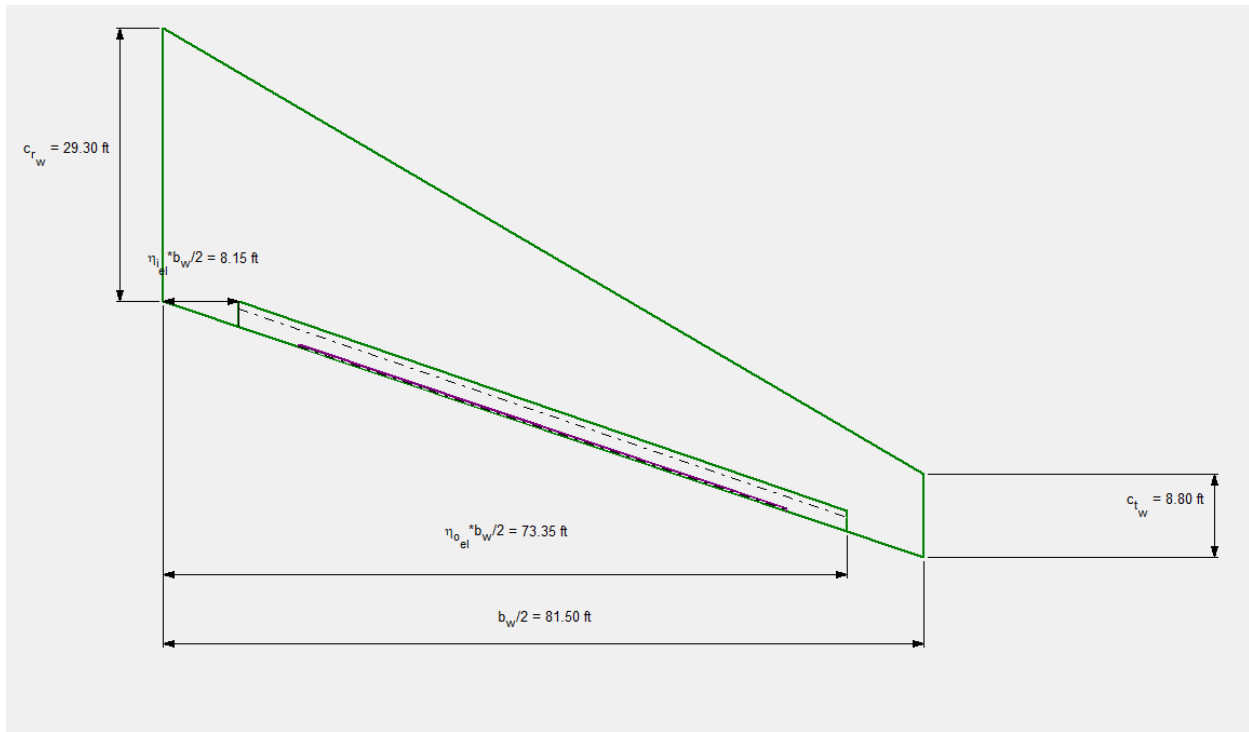


Figure 75 Wing planform with elevons

Output Parameters										
$c_{r_{el}}$	2.73 ft	$c_{b_{el}}$	0.82 ft	$c_{t_{el}}$	1.91 ft	c_{el}/c_w	8.9 %	c_{el}	2.46 ft	
$c_{l_{el}}$	2.17 ft	$c_{b_{o_{el}}}$	0.65 ft	$c_{r_{o_{el}}}$	1.52 ft	S_{el}	319.15 ft ²	Balance _{el}	0.43	

Figure 76 Elevons output data

Input Parameters										
AR_w	8.56	λ_w	0.30	$\eta_{i_{el}}$	10.0 %	$(c_{el}/c_w)_i$	10.0 %			
S_w	3105.15 ft ²	$\Lambda_{c^4_w}$	27.7 deg	$\eta_{o_{el}}$	90.0 %	$(c_{el}/c_w)_o$	20.0 %			

Figure 77 Slats input data

High Lift Devices Table

#	High Lift Device	η_i %	η_o %	$(c/c_w)_i$ %	$(c/c_w)_o$ %	$(x_{hl}/c)_i$ %	$(x_{hl}/c)_o$ %	Root Airfoil	Tip Airfoil	c_r ft	c_t ft	c_{b_i} ft	c_{f_i} ft	c_{b_o} ft	c_{f_o} ft	\bar{c} ft
		Input	Input	Input	Input	Input	Input	Input	Input	Output	Output	Output	Output	Output	Output	Output
1	Leading Edge Slat	10.0	45.0	15.0	15.0	10.00	10.00	sc20714.dat	sc20410.dat	4.09	3.01	0.41	3.68	0.30	2.71	3.58
2	Triple Slotted Flap	0.0	0.0	10.0	10.0	10.00	10.00	sc20714.dat	sc20410.dat	2.93	2.93	0.29	2.64	0.29	2.64	2.93
3	Leading Edge Slat	50.0	90.0	15.0	15.0	10.00	10.00	sc20714.dat	sc20410.dat	2.86	1.63	0.29	2.57	0.16	1.46	2.30

Figure 78 Slats output

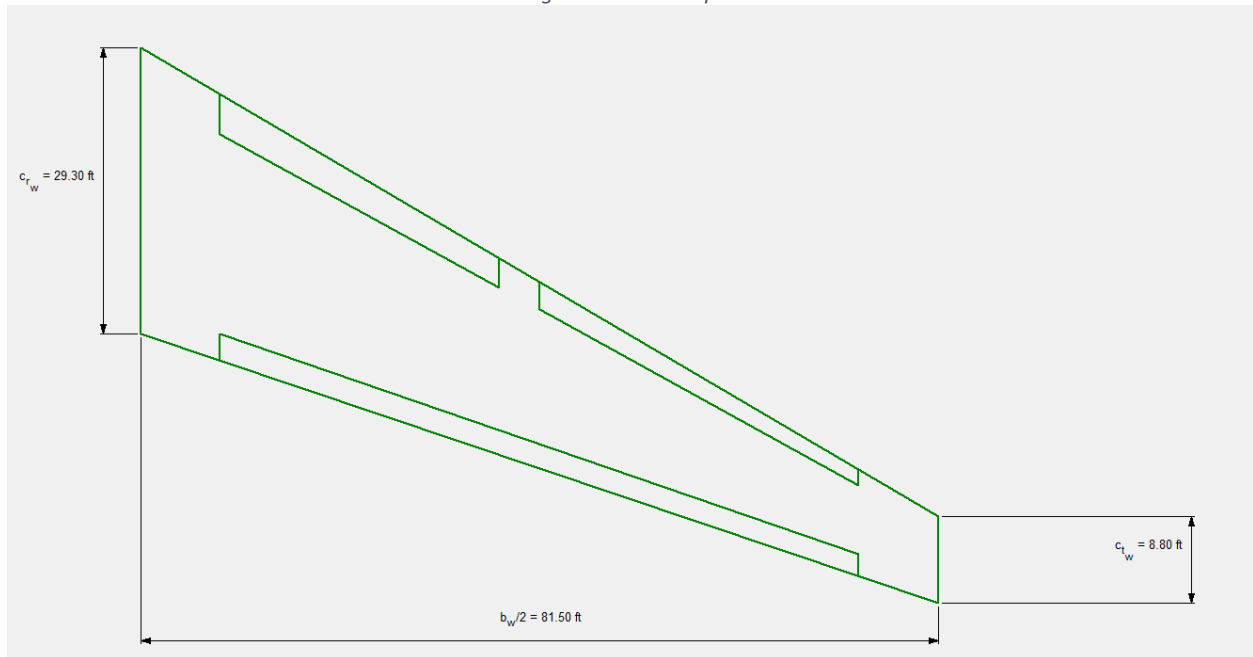


Figure 79 wing planform with slats and elevons

6. Design of High Lift Devices

The high dives are used to assist the aircraft to achieve the high lift requirements during take-off and landing. There are two types of high lift devices on wing:

- Leading Edge devices: Slats, leading edge Flaps
- Trailing Edge devices: Flaps

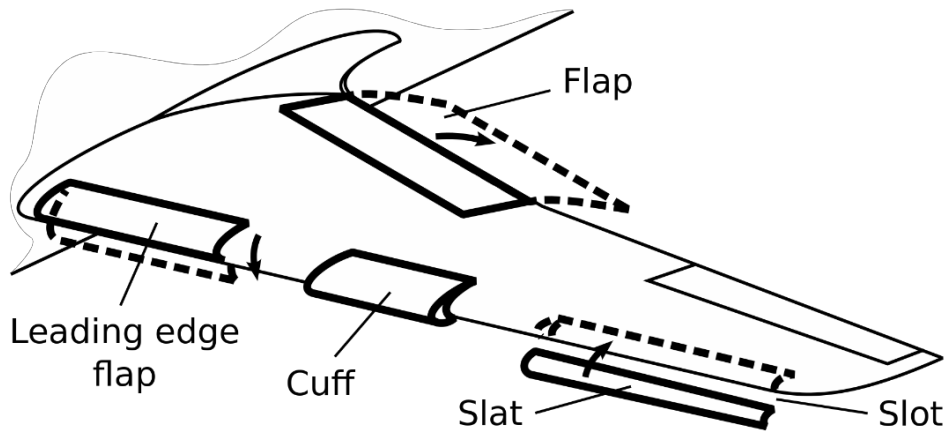


Figure 80 High Lift Devices

From the previous the previous reports, the aircraft design point was obtained using the following information:

Table 25 Data of the Proposed Aircraft

$C_{L \max}$	$C_{L \max TO}$	$C_{L \max L}$
1.2	1.3	1.4

The type of high-lift devices needed depends upon $C_{L_{maxTO}}$ and $C_{L_{maxL}}$ which depend upon the reynold's number.

$$R_{n_t} = \frac{\rho V C_t}{\mu} = \frac{0.2874 * 227.15 * 1.8}{0.000014322} = 8204806.4$$

$$R_{n_r} = \frac{\rho V C_r}{\mu} = \frac{0.2874 * 227.15 * 8.23}{0.000014322} = 37514198.4$$

$$C_{L_{unswept}} = \frac{0.95 (C_{L_{centerbdy}} + C_{L_{inbound}} + C_{L_{outbound}})}{3}$$

$$C_{L_{unswept}} = \frac{0.95(0.9 + 1.6 + 1.015)}{3} = 1.11$$

$$C_{L_{swept}} = C_{L_{unswept}} \cos(\Lambda)$$

$$C_{L_{swept}} = 1.11 * \cos(27.7) = 0.98$$

$$C_{L_{max}} = 0.91$$

The unswept wing $C_{L_{max}}$ is within the 5% margin of the assumed $C_{L_{max}}$ so it is acceptable to use the value. The wing should be able to produce the above calculated lift.

$$\Delta C_{L_{maxTO}} = 1.05 (C_{L_{maxTO}} - C_{L_{max}}) = 1.05 (1.3 - 0.91) = 0.41$$

$$\Delta C_{L_{maxL}} = 1.05 (C_{L_{maxL}} - C_{L_{max}}) = 1.05 (2.0 - 0.91) = 1.14$$

From the calculations, it is evident that high lift devices are needed to meet the requirements during take-off and landing.

The required incremental sectional lift can be calculated using

$$\Delta C_{L_{max}} = \Delta C_{L_{max}} \left(\frac{S}{S_{wf}} \right) K_{\Lambda}$$

Where K_{Λ} is a factor that accounts for the effect of sweep angle in the flaps down setting. The factor is calculated as

$$K_{\Lambda} = (1 - 0.08 \cos^2 \Lambda_c) \cos^4 \Lambda_c = 0.9427$$

The flaps cannot be used for the BWB configuration as it would give a strong nose down moment which is countered by a horizontal tail. As the configuration does have a horizontal tail, the leading-edge slats are used to get the required lift.

The slats would pose a problem of higher angle of attack. The data from Roskam does not provide any theoretical calculations for slat design but can be approximated using the following formula:

$$C_{l_{max_{with\ slats}}} = C_{l_{max_{without\ slats}}} (C''/C)$$

With $(C''/C) = 1.5$

$$C_{l_{max_{with\ slats}}} = 1.47$$

For calculating the flaps parameters, the location of the spar is required.

$$\begin{aligned} \text{Leading Edge Spar} &= 0.2C_r \\ \text{Trailing Edge Spar} &= 0.695C_t \end{aligned}$$

Table 26 Spar Calculation

	Tip	Root
LE	1.2	5.4
TE	4.17	18.76

$$\frac{C_f}{C} = (C_r - 18.76)/C_r = 0.3$$

The calculations show that the leading-edge slats would provide the required lift but would increase the angle of attack.

7. Design of Control Surfaces

The absence of horizontal tail from the BWB configuration calls for the integration of longitudinal and lateral control surfaces. The elevons are designed with the conventional method of designing the ailerons but the difference that the control surfaces would run through the entire trailing edge of the wing. The configuration would provide enough moment arm for the elevon for longitudinal control.

The elevons would stay at the trailing edge spar and would continue to the trailing edge. The run of the elevons is from the 0.1 fraction of the wing to the 0.9 fraction of the half span of the outboard wing.

The elevons would start at 7 ft from the root of the outboard wing to the 55 ft of the outboard wing. The entire length of the elevons is required for the pitch control of the aircraft.

8. Drawing

i) Span

$$b = (AS)^{\frac{1}{2}} = (7.8 * 3412)^{\frac{1}{2}} = 163 \text{ ft}$$

ii) Root Chord

$$C_r = \frac{2S}{b(1 + \lambda)} = 29.3 \text{ ft}$$

iii) Tip Chord

$$C_t = \lambda * C_r = 0.3 * 29.3 = 8.8 \text{ ft}$$

iv) Mean Aerodynamic Chord

$$C = \frac{2}{3} * C_r * \frac{1 + \Lambda + \Lambda^2}{1 + \Lambda}$$
$$C = \frac{2}{3} * 29.6 * \frac{1 + 0.3 + 0.09}{(1 + 0.3)} = 21.12$$

v) Mean Geometric Chord

$$MGC = \frac{S}{b} = \frac{4132}{163} = 20.93$$

vi) Leading Edge Sweep Angle

$$\tan(\Lambda_{LE}) = \tan(\Lambda_c) + \frac{1 - \lambda}{A(1 + \lambda)}$$
$$\tan(\Lambda_{LE}) = \tan(27.7) + \frac{1 - 0.3}{7.8 * (1 + 0.3)}$$
$$\Lambda_{LE} = 30^\circ$$

vii) Position of Aerodynamic Center

$$A. C = 0.25 \text{ of } MAC$$
$$0.25 * 21.12 = 5.28 \text{ ft}$$

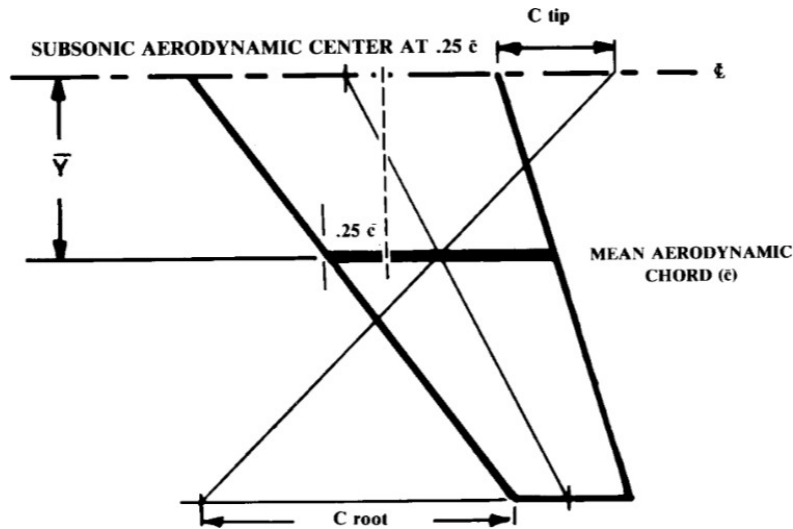


Figure 81 Graphical Representation of the MAC

$$X = 0.25 * C$$

$$X = 0.25 * 21.12 = 5.28$$

$$Y = \frac{b}{6} * (1 + 2\Lambda) * (1 + \Lambda)$$

$$Y = \frac{29.6}{6} * (1 + (2 * 0.3)) * (1 + 0.3) = 56.55$$

9. Discussion

The wing of the proposed BWB is considered to start from the center body of the aircraft. The root chord is at the center which is an imaginary extension of the wing. The coefficient of lift is calculated based on the imaginary chord even though it does not have any actual airflow over the root. The data is compared with NASA SUGAR Ray conceptual design and are acceptable. SC(2)-0012 airfoil is used to design the center body hence the root airfoil of the wing is the same. The section of wing which has airflow over it has two different airfoils, SC(2)-0714 and SC(2)-0410. The supercritical airfoils are used to as it has higher critical Mach number and a flat top and bottom provides an added advantage for enough thickness to for cabin placement.

The configuration does not allow the use of flaps but slats or the leading-edge flaps can be used to get the required lift. Again, the leading-edge flaps would also decrease the lift by a greater extend and results is higher complexities. The slats are used compromising the angle of attack to gain the required coefficient of lift for take-off and landing.

The other solution to the problem is to design rear flaps that could counteract the nose down movement while using the flaps but not much data is available for such configuration and designs and hence is not a subject of discussion in the report.

The AAA analysis of the maximum coefficient of lift is not included in the report as the software has limitation of using only two airfoils for analysis while the wing design of the proposed aircraft uses three different airfoils of supercritical series 2.

10. Conclusion

The wing design of BWB aircraft has a small design space due to the geometric configuration of the aircraft. The wing is designed from the center line of the body but the actual flow over the wing is experienced by the root of the outboard wing. This method is necessary as the whole aircraft body would contribute in generating lift hence, the configuration can be assumed as a flying wing.

The use of high lift devices on the wing is very much constrained to slats as there is no horizontal tail to counteract the strong nose down moment due to the use of flaps. The use of slats would increase the angle of attack of the aircraft to achieve the required lift. It would also make the passengers uncomfortable. This problem can be eliminated by using the rear flaps to provide a nose up pitching moment while using the flaps but the method to design such a flap is not yet established and is subjected to experimentation.

The longitudinal and lateral control surfaces are integrated and run through the entire trailing edge of the outboard wing. It is necessary to provide such a large span as it would also act as an elevator providing necessary control surface to assist the V-tail configuration of the empennage.

9. Design of Empennage & Longitudinal & Directional Control

1. Introduction

This report discusses about the preliminary design of blended wing body. The detail discussion of the vertical and horizontal stabilizer with longitudinal control surface is the primary focus of the report.

The conventional empennage design would depend upon the following parameters:

- Wing area
- Aspect ratio
- Taper ratio
- Thickness ratio
- Dihedral angle
- Airfoils
- Incidence angle
- Sweep angle
- Control Surface sizing

The unconventional configuration of the BWB does not allow the design of the of horizontal stabilizing surface in the conventional way. The longitudinal control surface must be integrated with later control surface for the required control authority and stability of the aircraft. The inherent design of the BWB aircraft makes it difficult to control with marginal stability. A V-tail configuration is selected for the aircraft and full span trailing edge elevon which can act like aileron as well as elevators.

2. Overall Empennage Design

The empennage would consist of a V-tail which would not require a separate horizontal tail. The BWB configuration does not allow the use of traditional horizontal surface which necessitates the integration of longitudinal and lateral control surfaces. The full span elevons are used with stabilator for more longitudinal control authority. The rudders are sized in the conventional way and a dihedral angle is calculated based on the area calculated for vertical and horizontal surface. To trim the aircraft for a forward center of gravity than aerodynamic center, stabilator is used in the proposed aircraft.

Determine the location of the Empennage

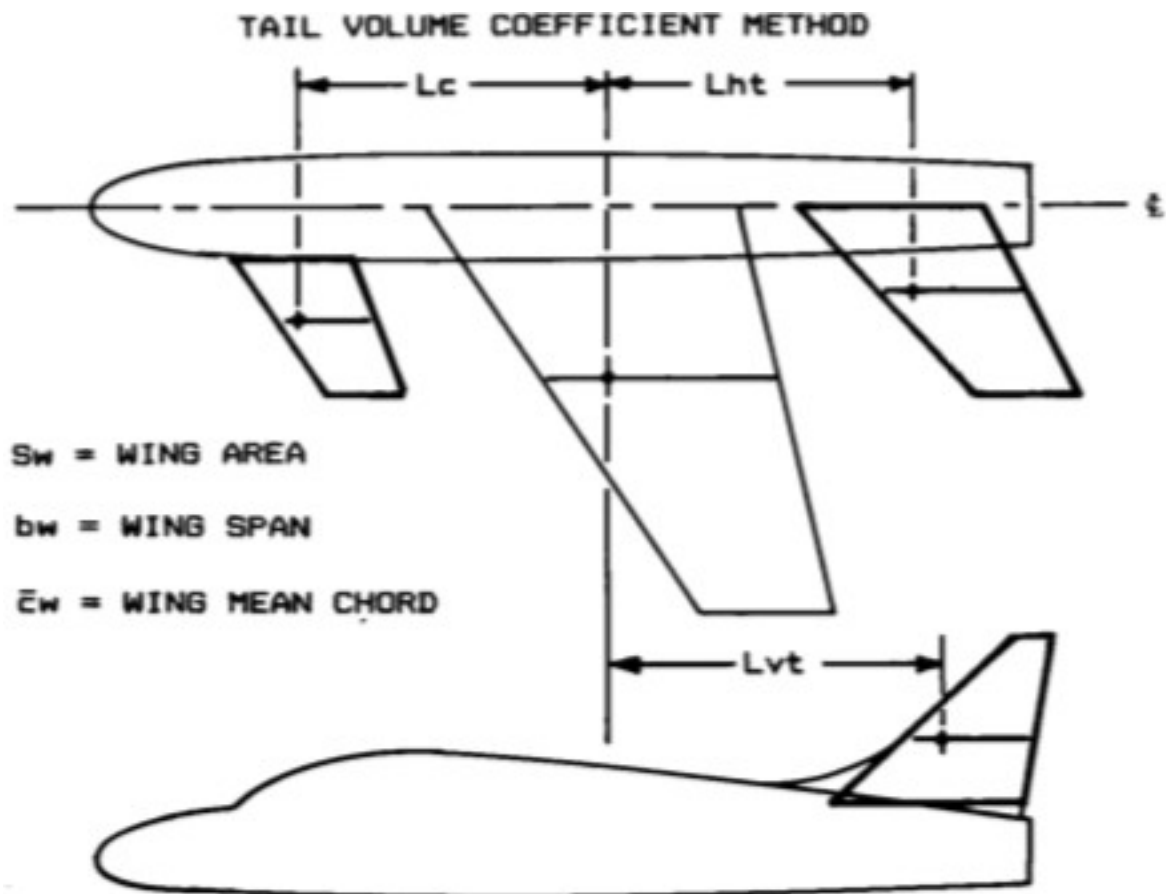


Figure 82 Definition of moment arms

- L_h : location of the horizontal stabilizer with respect to that quarter chord of the wing
- L_v : location of vertical stabilizer with respect to the quarter chord of the wing
- L_c : location of the canard with respect to the quarter chord of the wing

The L_c and L_h is not applicable to the proposed aircraft as it doesn't have a canard or a horizontal stabilizer.

For a V-tail configuration, the moment arms for the vertical and horizontal stabilizers are assumed to be equal. Generally, the moment arm for the jet transport is 45% to 50% of the fuselage length. Hence the location of the vertical and horizontal stabilizer is 50% of the fuselage length. The length of the fuselage is equal to the chord length of the airfoil used for center body of the aircraft.

$$L_{VT} = L_{HT} = 50\% \text{ of fuselage length} = 75 \text{ ft}$$

There is no much data available for the design of empennage for BWB aircraft. The minimal data available for BWB does not account for the vertical stabilizer as they have a flying wing configuration. So, the conventional method and data has been assumed for the design of BWB empennage. The data has been borrowed from the book by Raymer D. "Aircraft Design: A Conceptual Approach". The two vertical stabilizers are located at the extremes of the fuselage.

3. Design of Horizontal and Vertical Stabilizer

Design of Vertical Stabilizer

The BWB configuration call for a V-Tail empennage because of its inherent design. As a V-Tail configuration is selected, the parameters for horizontal and vertical stabilizer are calculated under the same section as the horizontal area is calculated for reference and dihedral angle.

For design of V-Tail, the horizontal and vertical stabilizers are calculated in a conventional way. The areas calculated for both is taken as the reference for V-Tail and butterfly angle is calculated.

Hence the area for the vertical stabilizer can be calculated with the following equation:

$$c_{VT} = \frac{L_{VT} * S_{VT}}{b_w * S_w}$$

The equation is rearranged to provide the area of the vertical tail.

$$S_{VT} = \frac{c_{VT} * b_w * S_w}{L_{VT}}$$

The volume coefficient of the vertical stabilizer is assumed from the experimental data for aircrafts with similar purpose.

For a V-tail, moment arm for horizontal and vertical stabilizers is assumed to be equal. The moment arm for a jet transport is usually 50% of the fuselage length.

$$S_{VT} = \frac{c_{VT} * b_w * S_w}{L_{VT}} = 225.34 \text{ ft}^2$$

In the analogous way, the area of horizontal stabilizer is calculated

$$S_{HT} = \frac{c_{HT} * C_w * S_w}{L_{HT}} = 583.95 \text{ ft}^2$$

The area of the V-Tail is calculated using the projection vertical on the horizontal tail. This can be calculated using the following equation:

$$S_{vee} = \sqrt{S_H^2 + S_V^2} = 626 \text{ ft}^2$$

The root chord of the vertical tail can be calculated as:

$$c_{r_{VT}} = \frac{2 * S}{b(1 + \lambda)} = 11.53 ft$$

Tip chord of the vertical stabilizer:

$$c_{t_{VT}} = \lambda * c_{r_{VT}} = 0.4 * 25 = 5.42 ft$$

The butterfly angle can be given as

$$\Gamma_H = \arctan(\sqrt{S_{VT}/S_{HT}}) = 40 \text{ degrees}$$

The butterfly (Γ_H) angle calculated should be near 45°. The obtained angle is 40° which is acceptable.

Type	Dihedral Angle, Γ_v deg.	Incidence Angle, i_v deg.	Aspect Ratio, Λ_v	Sweep Angle, $\Delta_c/4_v$ deg.	Taper Ratio, λ_v
Homebuilts	90	0	0.4 - 1.4	0 - 47	0.26 - 0.71
Single Engine Prop. Driven	90	0	0.9 - 2.2	12 - 42	0.32 - 0.58
Twin Engine Prop Driven	90	0	0.7 - 1.8	18 - 45	0.33 - 0.74
Agricultural	90	0	0.6 - 1.4	0 - 32	0.43 - 0.74
Business Jets	90	0	0.8 - 1.6	28 - 55	0.30 - 0.74
Regional Turbo-Props.	90	0	0.8 - 1.7	0 - 45	0.32 - 1.0
Jet Transports	90	0	0.7 - 2.0	33 - 53	0.26 - 0.73
Military Trainers	90	0	1.0 - 2.9	0 - 45	0.32 - 0.74
Fighters	75 - 90	0	0.4 - 2.0	9 - 60	0.19 - 0.57
Mil. Patrol, Bomb and Transports	90	0	0.9 - 1.9	0 - 37	0.28 - 1.0

Figure 83 Data of geometric constraints for empennage

	WING	V-TAIL	H-TAIL
Area (gross)	4,136.0	90.8	N/A
Aspect Ratio (gross)	6.865	1.705	
Taper Ratio (trap)	0.228	0.366	
MAC Inches (gross)	489.7	101.3	
Dihedral (Deg.)	3.0	62.0	
1/4 Chord Sweep (Deg.)	27.7	39.2	
Root Chord (Inches) (trap)	322.6	129.23	
Tip Chord (Inches) (trap)	73.6	44.90	
Span (W/O Winglet)	1,936.8		

Figure 84 SUAGR RAY Data

As there is no feasible data available except for the NASA SUGAR Ray, the data has been borrowed from the same design. The data for SUGAR Ray is analogous with the data table in the book by Roskam.

Table 27 Geometric data for proposed tail

	Vertical Tail
Aspect Ratio	1.705
Sweep Angle	39.2
Taper Ratio	0.4
Thickness Ratio	0.28
Incidence Angle	0
Airfoil	NACA- 0012

The leading-Edge sweep angle can be calculated in the same way as of the wing

$$\tan \Lambda_{VT} = \tan \Lambda_{c_{4VT}} + \left[\frac{1 - \lambda_{VT}}{A(1 + \lambda_{VT})} \right] = 0.9407$$

$$\Lambda_{VT} = 43.25^\circ$$

Span is calculated for the half of the area:

$$b_{VT} = \sqrt{\frac{S_{VT}}{A \left(\frac{1}{2} \right)}} = 30 \text{ ft}$$

The span of the V-Tail halved for one vertical tail. So, the span come out to be 15 ft for each.

Mean Aerodynamic chord of the V-Tail can be calculated as:

$$c_{\bar{v}} = \frac{2}{3} * c_{rV} * \left(\frac{1 + \lambda_V + \lambda_V^2}{1 + \lambda_V} \right) = 5.2 \text{ ft}$$

The distance of mean aerodynamic chord from the root of the vertical stabilizer is:

$$Y_V = \frac{b}{6} \left(\frac{1 + 2\lambda_V}{1 + \lambda_V} \right) = 4.98 \text{ ft}$$

4. Empennage Design Evaluation

Input Parameters											
b_v	15.00 ft	i_v	0.0 deg	Z_{apex_v}	0.00 ft	$Y_{c_{t/4}_v}$	14.36 ft	Method	Tip Based	N_{panel_v}	1
Vertical Tail Geometry Table											
Panel	c_r ft	c_t ft	X_r ft	X_t ft	Z_r ft	Γ deg	ϵ_t deg	Root Airfoil	Tip Airfoil	Y_r ft	$Y_{c_{t/4}}$ ft
Panel	Input	Input	Input	Input	Input	Input	Input	Input	Input	Output	Output
1	11.5300	5.4200	0.0000	13.7612	0.0000	50.0000	0.0000	n0012.dat	n0012.dat	1.7715	1.7715

Figure 85 Vertical Tail inputs

Output Parameters											
c_{r_v}	11.53 ft	$S_{v_{net}}$	127.13 ft ²	C_{D_v}	8.84 ft	α_{D_v}	39.2 deg	X_{apex_v}	0.00 ft	Y_{t_v}	14.36 ft
c_{t_v}	5.42 ft	AR_v	1.77	Z_{mgc_v}	6.60 ft	α_{E_v}	42.5 deg	$Y_{c_{t/4}_v}$	1.77 ft	Γ_v	50.0 deg
S_v	127.13 ft ²	i_v	0.47	X_{mgc_v}	6.05 ft	α_{TE_v}	27.0 deg	Y_{apex_v}	1.77 ft	ϵ_{q_v}	0.0 deg

Figure 86 Tail geometric outputs

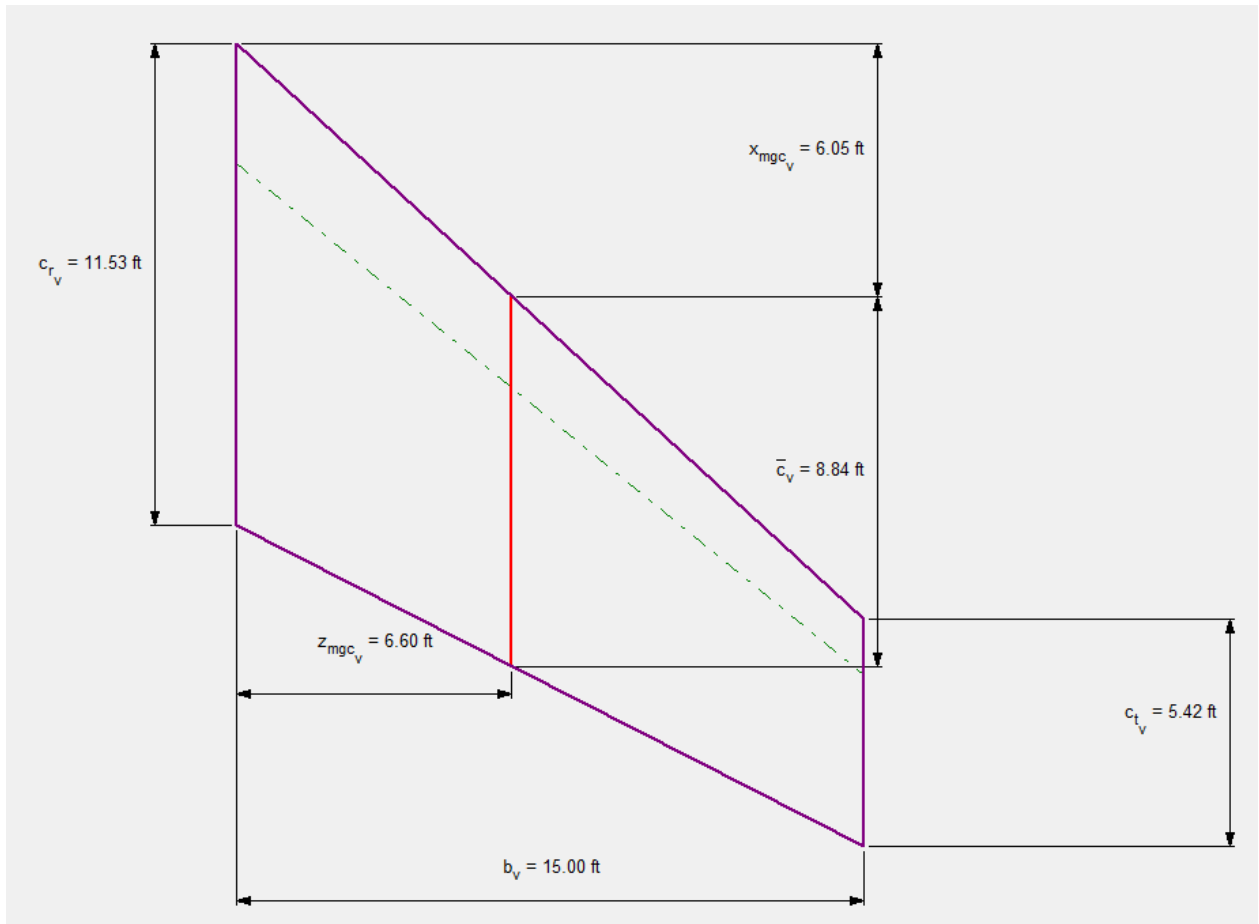


Figure 87 Tail geometry

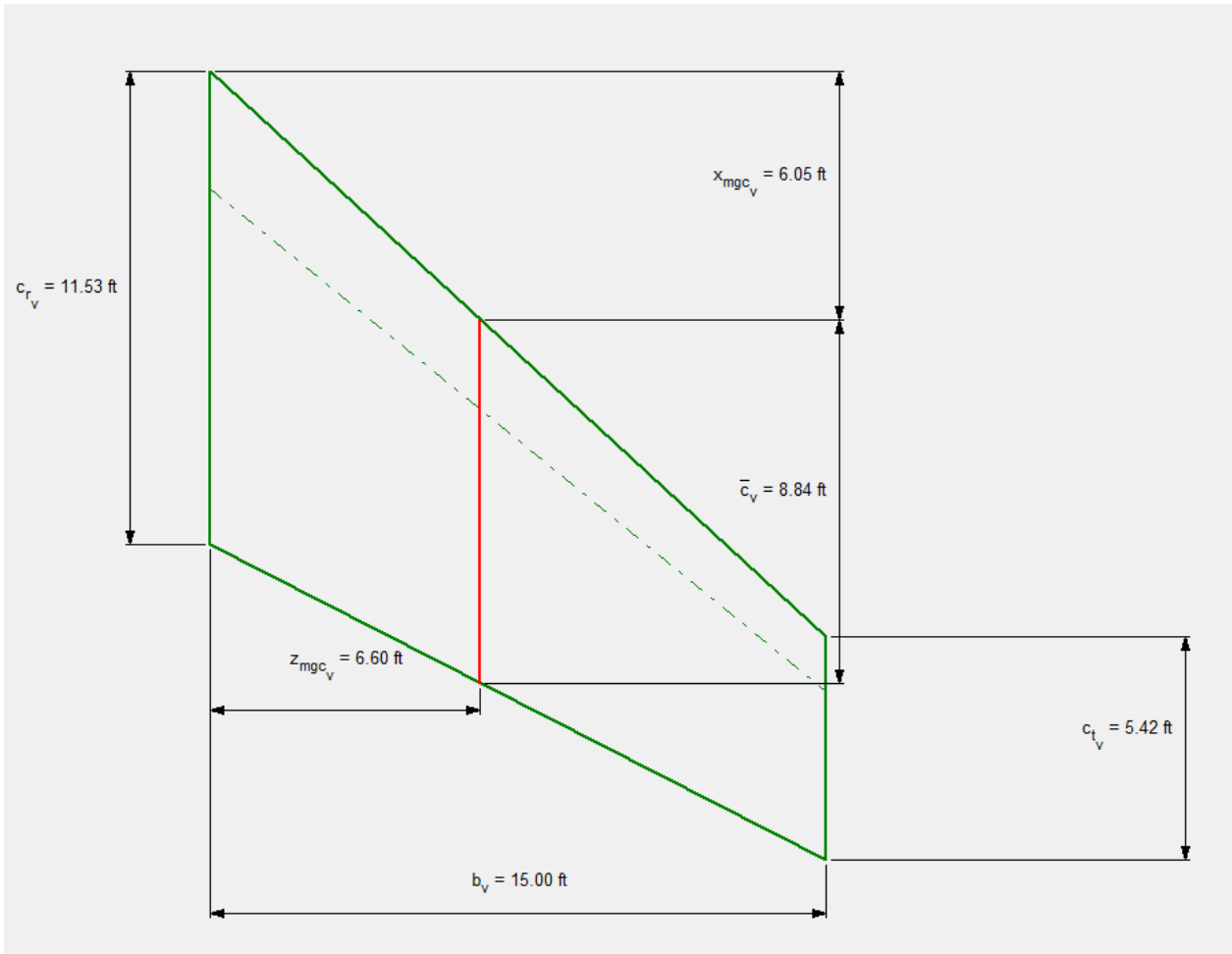


Figure 88 Vertical tail planform

Input Parameters										
AR_V	1.77	λ_V	0.47	$(c/c_v)_i$	30.0 %	$(x_{in}/c)_i$	10.00 %	η_i	10.0 %	
S_V	127.13 ft ²	Δ_{α}^i	39.2 deg	$(c/c_v)_o$	30.0 %	$(x_{in}/c)_o$	10.00 %	η_o	90.0 %	

Rudder Airfoils		
Panel	Root Airfoil	Tip Airfoil
1	n0012.dat	n0012.dat

Figure 89 Rudder inputs

Output Parameters										
C_{r_r}	3.28 ft	C_{b_r}	0.33 ft	C_{f_r}	2.95 ft	c/c_V	27.0 %	C_r	2.61 ft	
C_{t_r}	1.81 ft	$C_{b_o_r}$	0.18 ft	$C_{f_o_r}$	1.63 ft	S_r	30.51 ft ²	Balance _r	0.11	

Figure 90 Rudder output

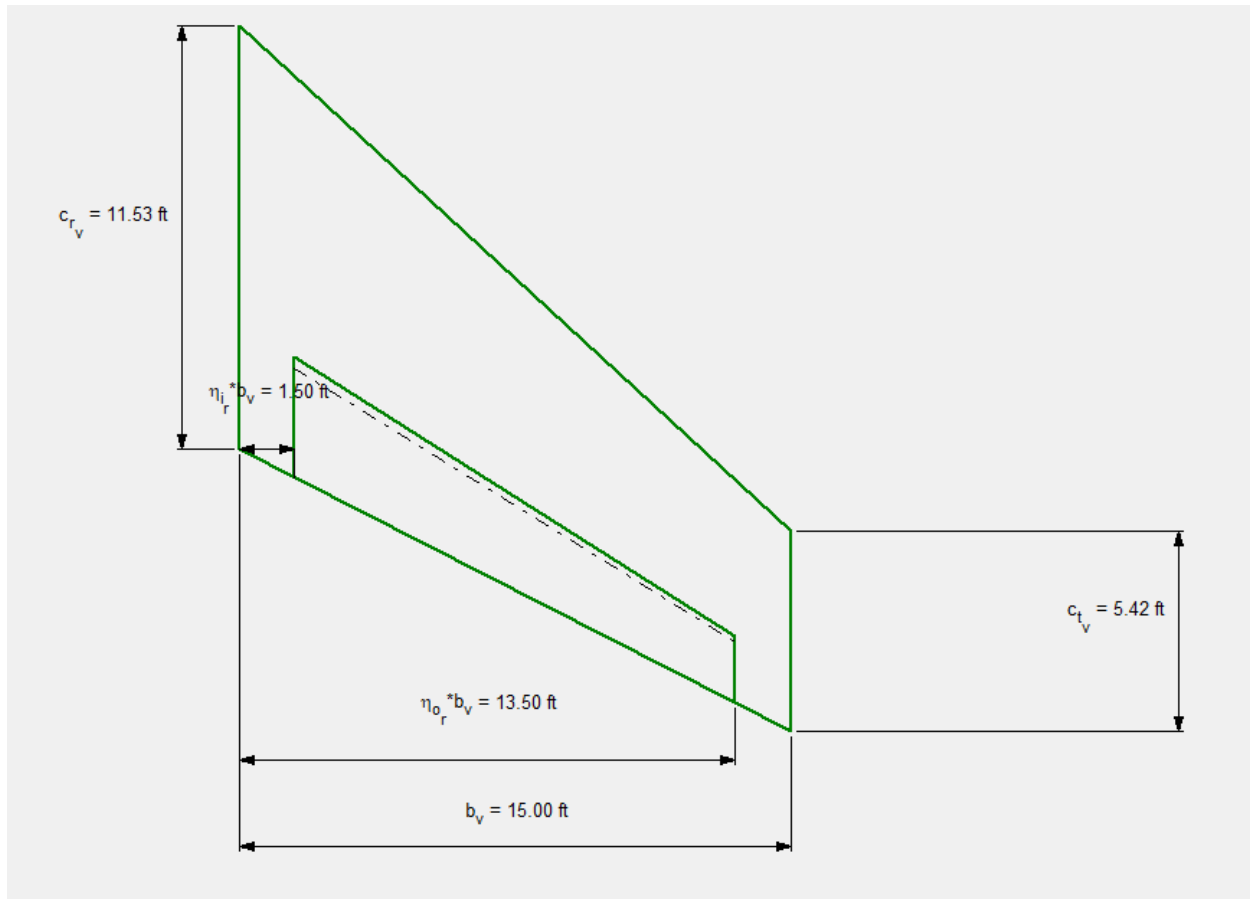


Figure 91 Vertical tail with rudder

5. Design of Longitudinal and Directional Control

The longitudinal and directional control surfaces comprise of elevator and rudder respectively. Multipurpose surface is like elevons and ruddervator are used to control the longitudinal and lateral control. Typically, the ruddervator size is 25-50% of the chord length of the vertical stabilizer and stabilator to be designed would be of the same size as of ruddervator. The ruddervator would run from fuselage to 90% of the vertical stabilizer. The span of the ruddervator is 27 ft. The root chord is 3.5 ft at the root and 1.5 ft at the tip.

The rear flaps can be used to achieve the desired longitudinal stability, but the design methodology is still under research. The drawings of SUGAR Ray show the use of such flaps to attain the pitch control authority.

6. CAD Drawing

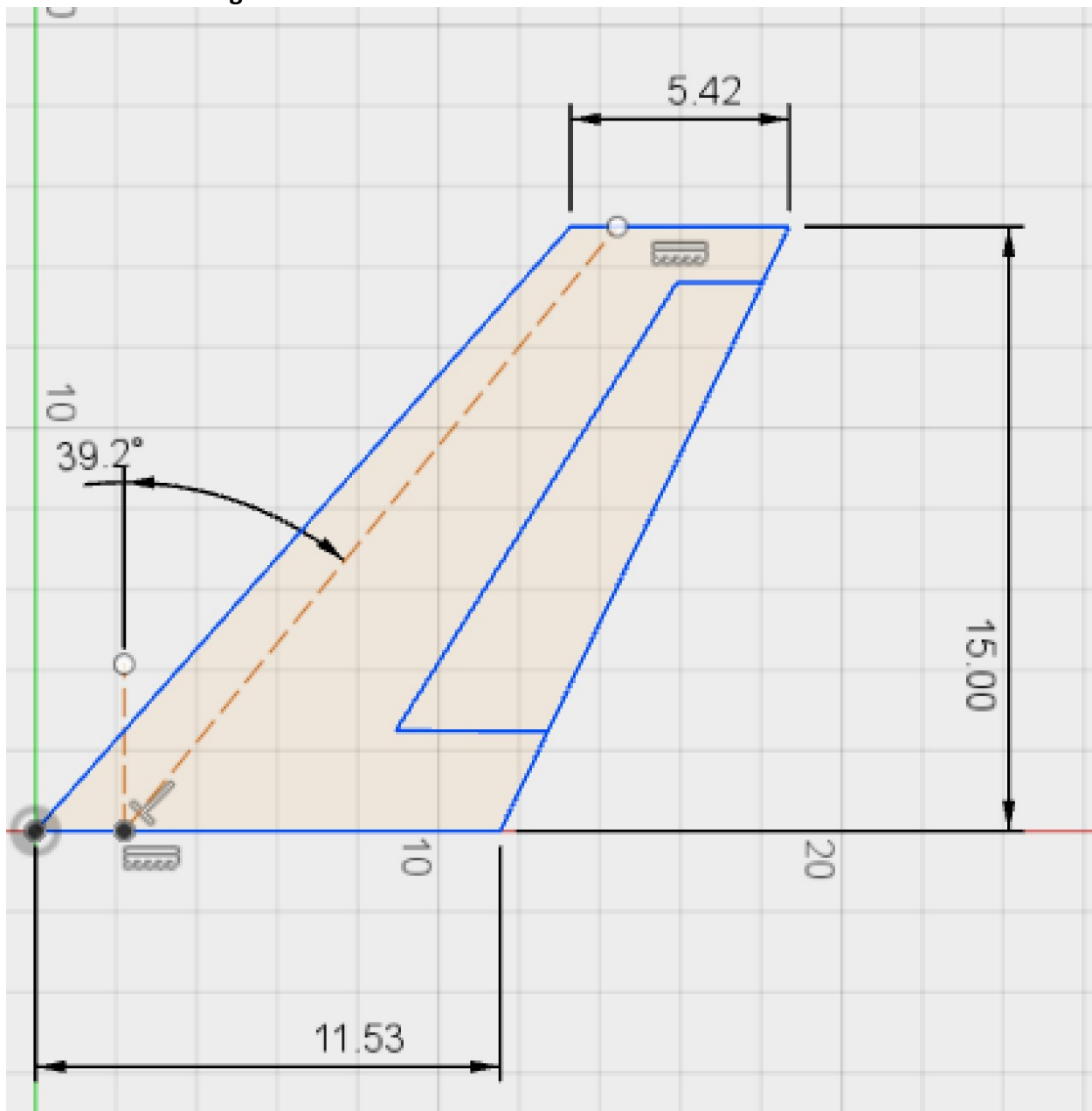


Figure 92 2D CAD for Vertical tail

7. Discussion

Low lateral and longitudinal stability and small natural yaw damping are the weak points of the flying wing since the beginning of the aviation. The primary reason for not introducing a BWB aircraft for civil aviation industry is the inherent instability. The aircraft has very small control authority. Research on different configuration has been going on to obtain a high-fidelity control model of the aircraft. Some configurations make the use of elevons which acts as the lateral as well as the longitudinal control surface. From the report of NASA, SUGAR Ray project uses a

vertical stabilizer to counteract the directional stability problem and to have a more directional control authority. The use of rear flaps is still under research which as it would have effect on the overall lift to weight ratio of the aircraft. With the use of new flex technology materials, it is possible to have a smooth transiting airfoil design which would have less effect on lift to drag ratio.

The V tail configuration is necessary to provide with integrated rudder and elevator. The multi-control surfaces largely improve the control authority compared to the mono-control baseline. The proposed aircraft uses ruddervator as well as elevons to counteract the high longitudinal instability and to have a required pitch control. It also uses the innovative technology of flex or structure which is still under research.

8. Conclusion

The aircraft has inherent stability problem which is the show stopper for the aircraft to enter the civil aviation. The report discusses the design of V-tail and proposed rear flaps for achieving the required stability and longitudinal and directional control authority. Still more research is need on the control area so that more efficient control surfaces are implemented and designed for an unconventional aircraft.

10. Landing Gear Design: Weight and Balance Analysis

1. Introduction

This report discusses about the preliminary design for landing gears for an aircraft. The report provides with a rapid and accurate method for weight bifurcation, CG position and placement and design of the landing gears. The design of landing gear depends on the following characteristics:

- Number, type and size of tires
- Length and diameter of strut
- Preliminary disposition
- Retraction feasibility

The method for designing the landing gears for unconventional configuration of BWB aircraft is analogous to the design methodology for tube and wing configuration aircrafts.

The number, type and size of tires as well as the length and diameter of the struts depends on the static load supported by nose and main landing gear. The preliminary disposition of the landing gear is dependent on the center of gravity (CG) location of the aircraft. The retraction feasibility depends on the space available after making an actual CAD drawing of the fuselage and retraction system.

2. Estimation of the Center of Gravity Location for the Airplane

The CG location of the aircraft depends on the weight distribution of different components of the aircraft. The CG tends to change during the flight due to the consumption of the fuel. The CG travel is necessary to control and constraint it within a safe limit else the aircraft can become unstable. The location of the CG provides the moment arm of the different components of the aircraft. The placement of these components is critical because it would result in the CG travel if the weight of the component tends to change during the flight.

The Class I method for estimation of take-off weight depends on the assumption that the weights of different components of the aircraft can be calculated using the weight ratios of the similar aircraft. But the data in Roskam is very conservative does not provide any information on BWB aircraft. Hence the data from the NASA SUGAR Ray report has been used with the modifications in the weight ratios to calculate the weight of component groups of the aircraft.

The preliminary sizing provides the following values for weights

$$W_{TO} = 152000 \text{ lb}, W_E = 67400 \text{ lb and } W_{PL} = 32980 \text{ lb}$$

The weight disintegration of the NASA SUGAR Ray main components is provided below.

GROUP	WEIGHT (LB)	% TOGW
WING	12,500	6.8
TAIL	904	0.5
BODY	41,137	22.5
LANDING GEAR	7,198	3.9
PROPULSION	15,918	8.7
ENGINE, NACELLE, PYLON	14,192	7.8
ENGINE SYSTEM	400	0.2
FUEL SYSTEM	1,326	0.7
FLIGHT CONTROLS	6,015	3.3
ELECTRICAL	3,346	1.8
INSTRUMENTS	1,079	0.6
AVIONICS & AUTOPILOT	3,225	1.8
FURNISHINGS & EQUIPMENT	9,080	5.0
PNEUMATICS, AIR CONDITIONING, APU	3,553	1.9
ANTI-ICING	186	0.1
MANUFACTURER'S EMPTY WEIGHT (MEW)	104,142	57.1
OPERATIONAL ITEMS	6,350	3.5
OPERATING EMPTY WEIGHT (OEW)	110,493	60.5
USEABLE FUEL	35,582	19.5
PAYLOAD	36,425	20.0
TAKEOFF GROSS WEIGHT (TOGW)	182,500	100.0

Figure 93 Weight distribution of SUGAR Ray

The weight of the different component groups of the calculated using the analytical method of weight ratios. Different weights of the components provided in the table below.

Table 28 Weight distribution of proposed aircraft

No.	Type of Components	W (lb)	X (in)	Y (in)	
1	Fuselage Group	23072.4	399.84	0	
2	Wing Group	10254.4	609.68	0	
3	Empennage Group	754	843.21	0	
4	Engine Group	12214.8	725.75	0	
5	Landing Gear Group	NG	603.2	95.39	0
		MG	5428.8	415.42	0
6	Miscellaneous	15080	150	0	
Empty Weigh					
7	Trapped Fuel and oil	460	698	0	
8	Crew	1230	324.25	0	
Operating Empty Weight					
9	Fuel	50020	721.23	0	

10	Passengers	28000	324.25	0
11	Baggage	4980	324.25	0

The moment arm of every group of the contributing to the weight of the aircraft is found using the empirical formula given in the book by Roskam.

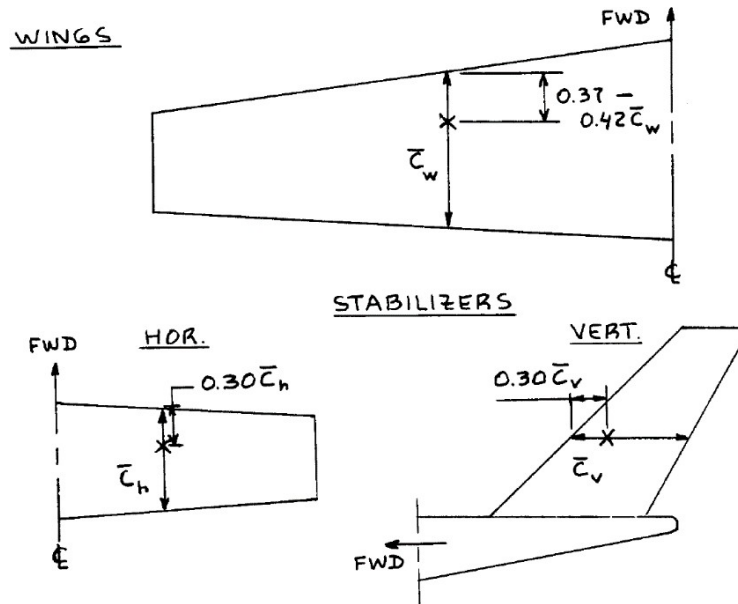


Figure 94 CG for Wing and Tail

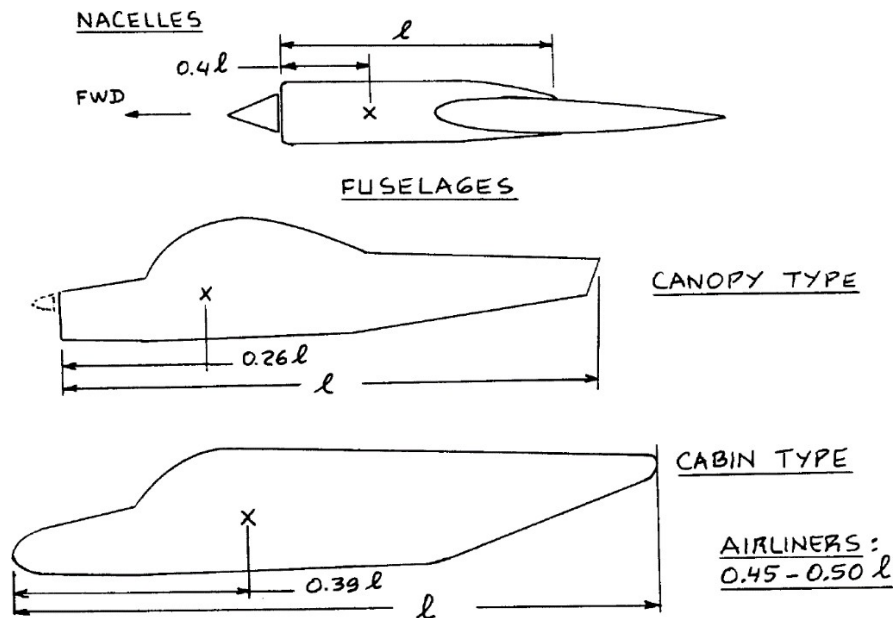


Figure 95 CG for nacelle and fuselage

The location of the CG is determined using the formulas in the figure (1) and figure (2). The distance of the CG is measured from the nose of the different components using a 2D CAD drawing of the aircraft and is tabulated below.

The moment arm of different components is calculated.

$$\text{Moment Arm} = \text{weight} * X$$

Table 29 Weights and moment arms of the proposed aircraft

No.	Type of Components	W	X	WX	Y	WY	
1	Fuselage Group	23072.4	399.84	9225268	0	0	
2	Wing Group	10254.4	609.68	6251903	0	0	
3	Empennage Group	754	843.21	635780.3	0	0	
4	Engine Group	12214.8	725.75	8864891	0	0	
5	Landing Gear Group						
		NG	603.2	95.39	57539.25	0	0
		MG	5428.8	415.42	2255232	0	0
6	Miscellaneous	15080	150	2262000	0	0	
Empty Weigh		67407.6					
7	Trapped Fuel and oil	460	698	321080	0	0	
8	Crew	1230	324.25	398827.5	0	0	
Operating Empty Weight		69097.6					
9	Fuel	50020	721.23	36075925	0	0	
10	Passengers	28000	324.25	9079000	0	0	
11	Baggage	4980	324.25	1614765	0	0	

The total moment arm is the summation of the moment arm of all the moment arm of every group. The total arm is the 770422211 lb.in and the total weight is 152097.6 lb.

The following figures show the approximate CG location of major components of the aircraft via 2D drawings of top view and side view. It also depicts the distance of CG form the nose.

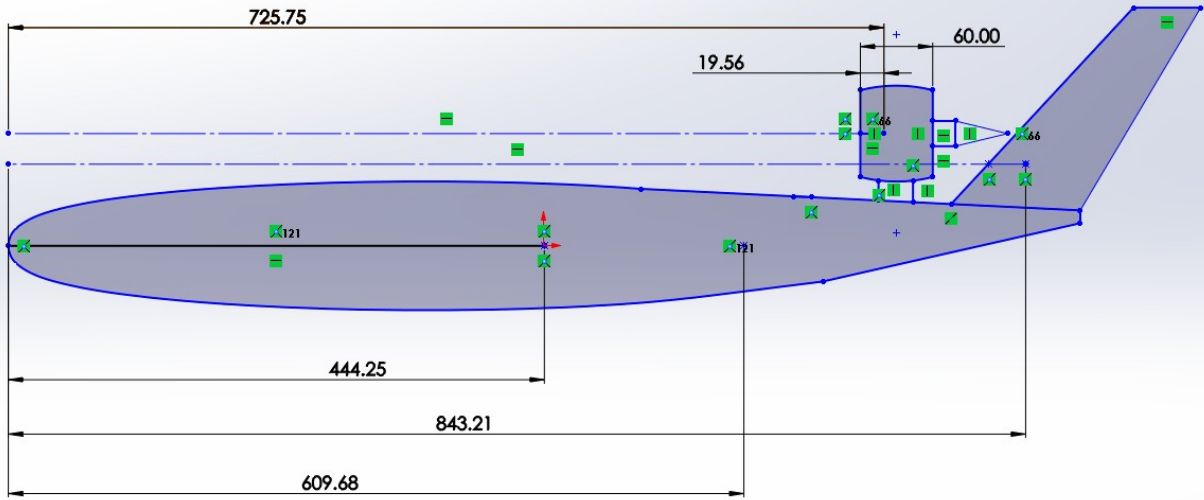


Figure 96 Side View with CG location

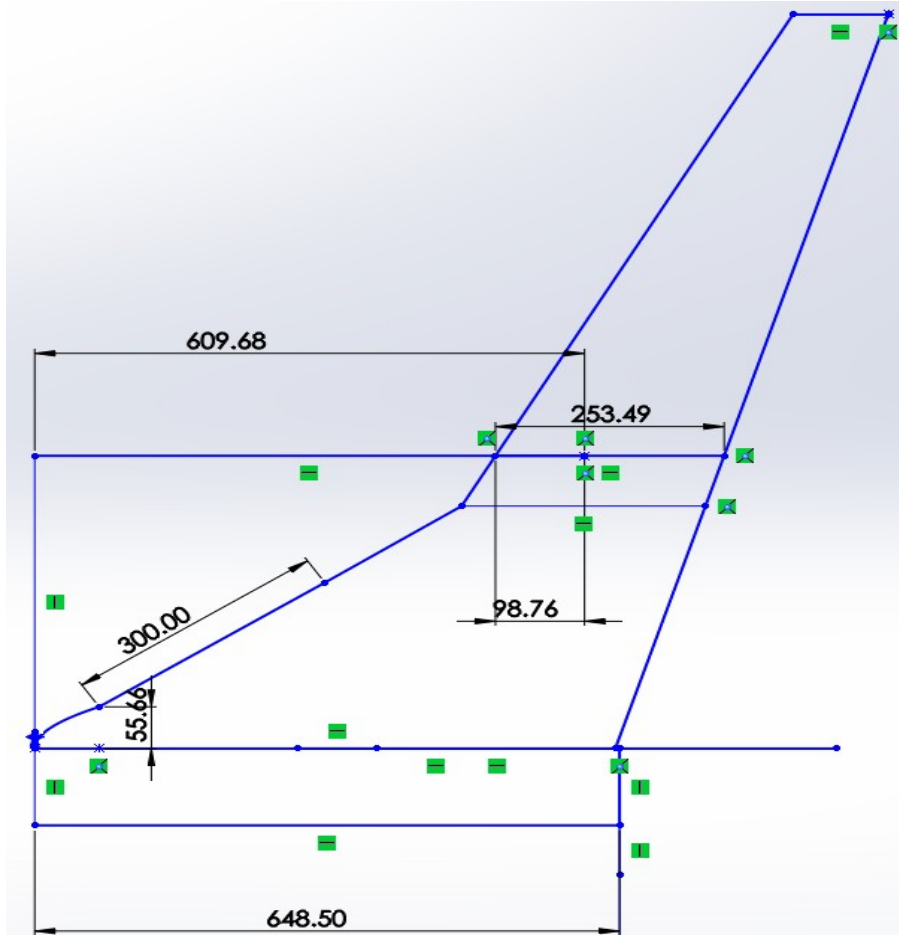


Figure 97 Top View with CG location

From the data calculated for different weight and CG location, a CG excursion diagram is obtained using different loading conditions.

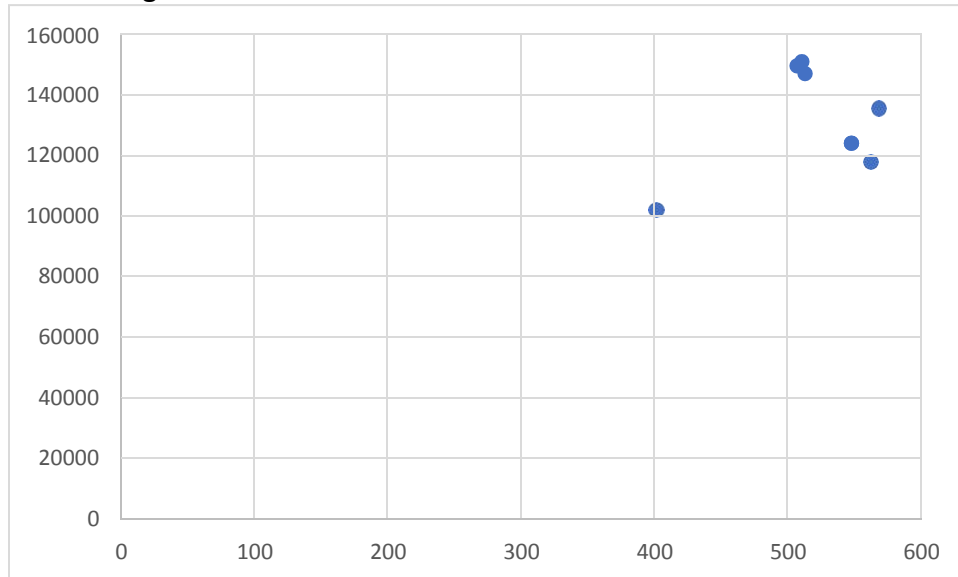


Figure 98 Proposed Aircraft: Weight excursion diagram of the proposed aircraft

By observing the figure above, it can be concluded:

- Most forward CG location occurs at 102077.6 lb of weight at 401.32 inches from nose.
- Most aft CG location occurs at 135607.6 lb of weight at 568.13 inches from nose.

The CG travel is around 190 inches which is not acceptable.

3. Landing Gear Design

The proposed aircraft has the application in civil aviation for passenger transport. The landing gear chosen for the airplane is retractable tricycle configuration as it provides good ground clearance with easy boarding of passengers and loading of cargo. It also provides a surface without inclination which is necessary for the comfort of passengers. The load is distributed among the nose gear and main gears which provides a support the weight of the aircraft. The main wheels are placed at some distance of the CG to satisfy the tip over condition for landing gear. The nose gear is usually small as it supports only 10% of the total weight while 90% of the weight is supported by main gears. The height of both the gears is same as the aircraft should be leveled but the main gears have heavier tires.

The nose gear is placed for the directional stability for take-off and landing. After calculating the weight and balance data, the next step is associated with the landing gear strut disposition. The landing gear strut should meet the following two geometric criteria:

- Tip over criteria: The main landing should be located aft to the CG and at 15 degrees of angle (longitudinal tip over criteria). The figure 7 and 8 depicts the longitudinal and lateral tip over criteria respectively.

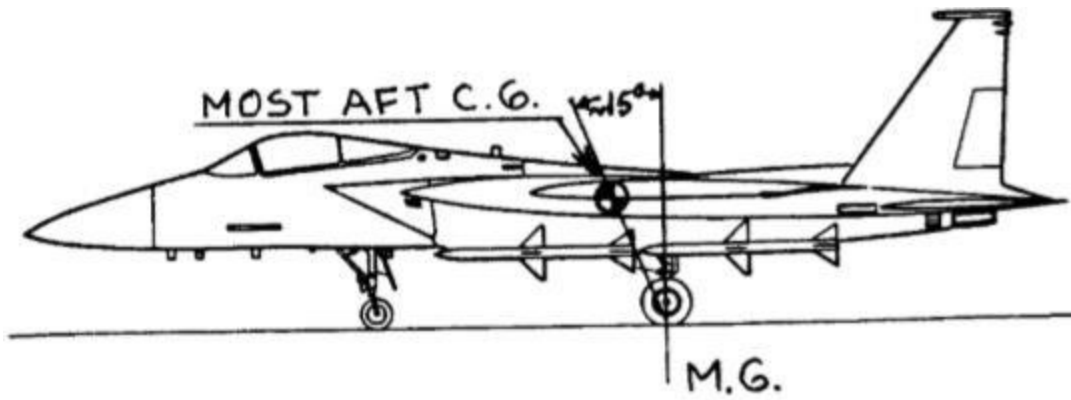


Figure 99 Longitudinal tip over criteria

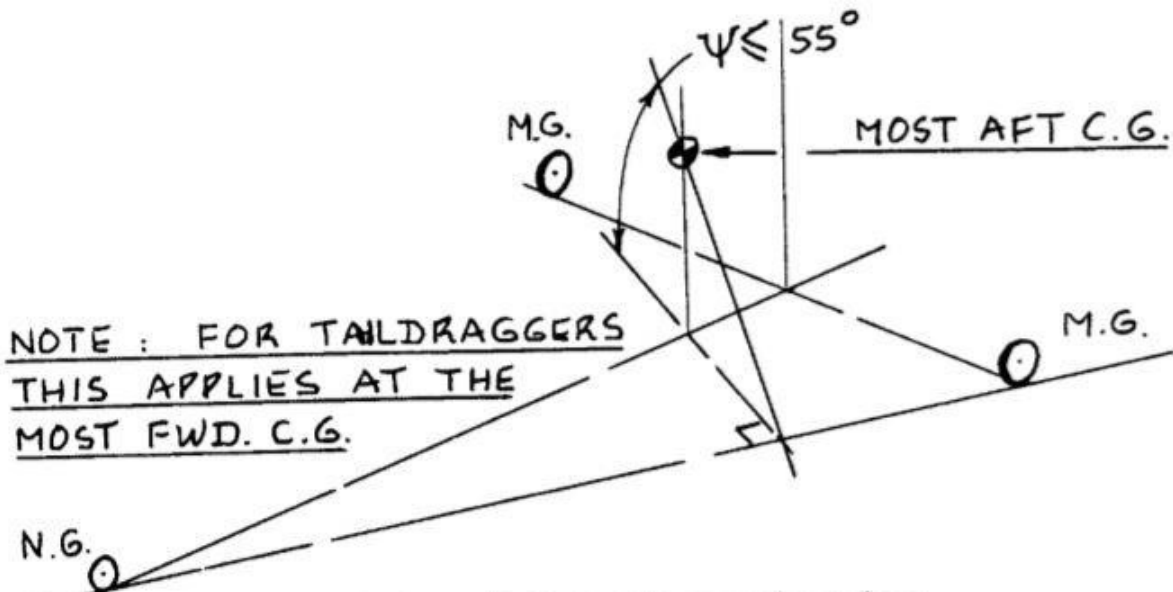
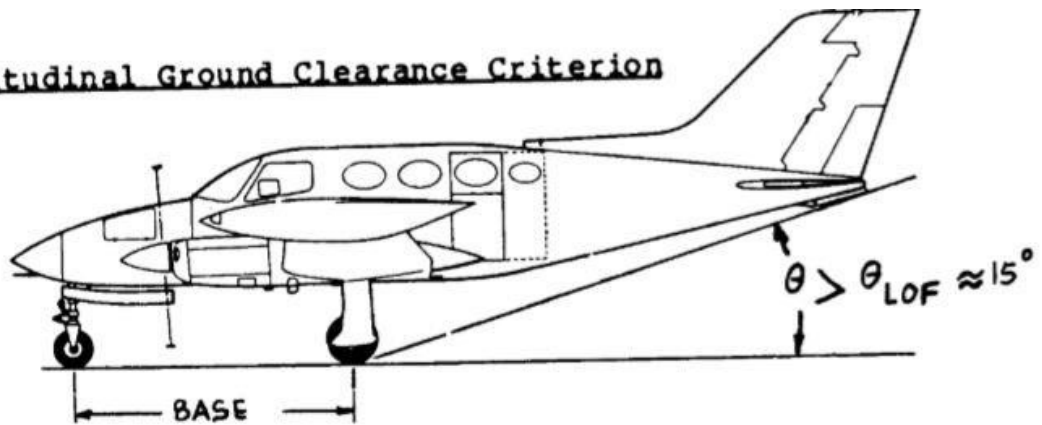


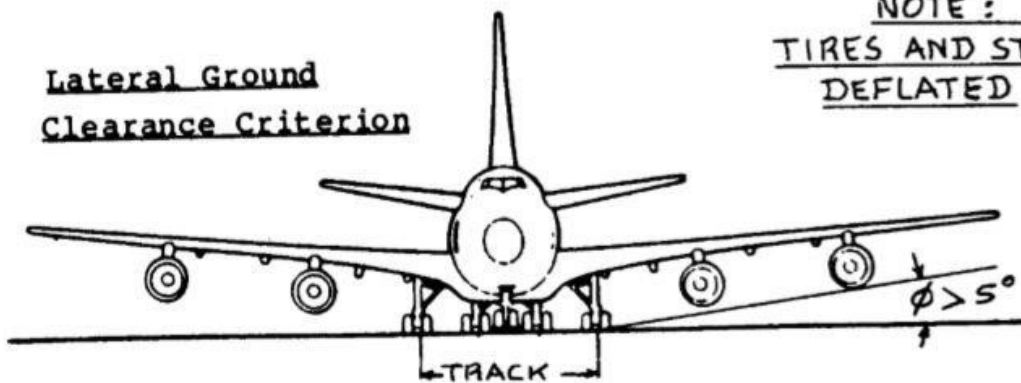
Figure 100 Lateral tip over criteria

- Ground Clearance criteria: Sufficient ground clearance is required for take-off and landing especially for low wingers.

Longitudinal Ground Clearance Criterion



Lateral Ground Clearance Criterion



NOTE :
TIRES AND STRUTS
DEFLATED

Figure 101 Ground clearance requirement

By considering all the criteria, the strut disposition is shown in the figure below.

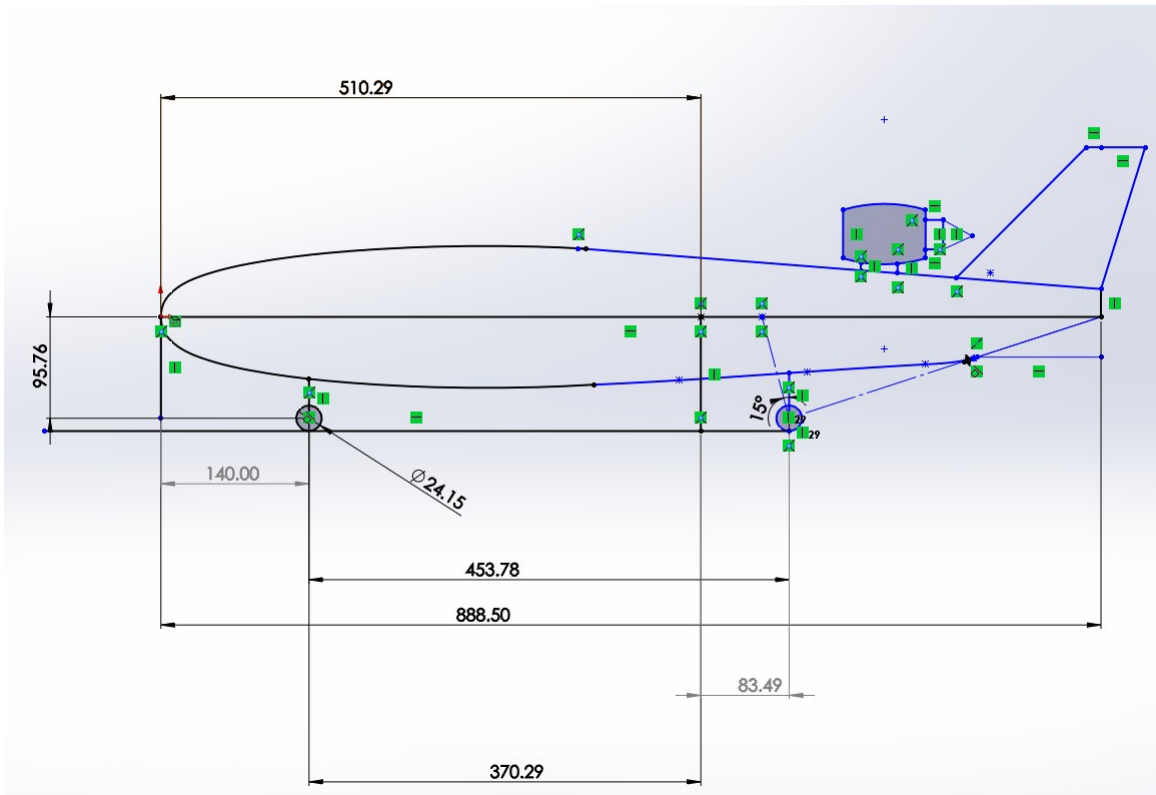


Figure 102 Landing gear disposition

After disposing the struts, the maximum static load per strut can be calculated:

Nose wheel strut:
$$P_n = \frac{W_{T0} \cdot l_m}{l_m + l_n} = 27984.1 \text{ lbs}$$

Main gear strut:
$$P_m = \frac{W_{T0} \cdot l_n}{\text{number of strut} \cdot (l_m + l_n)} = 62056.8 \text{ lbs}$$

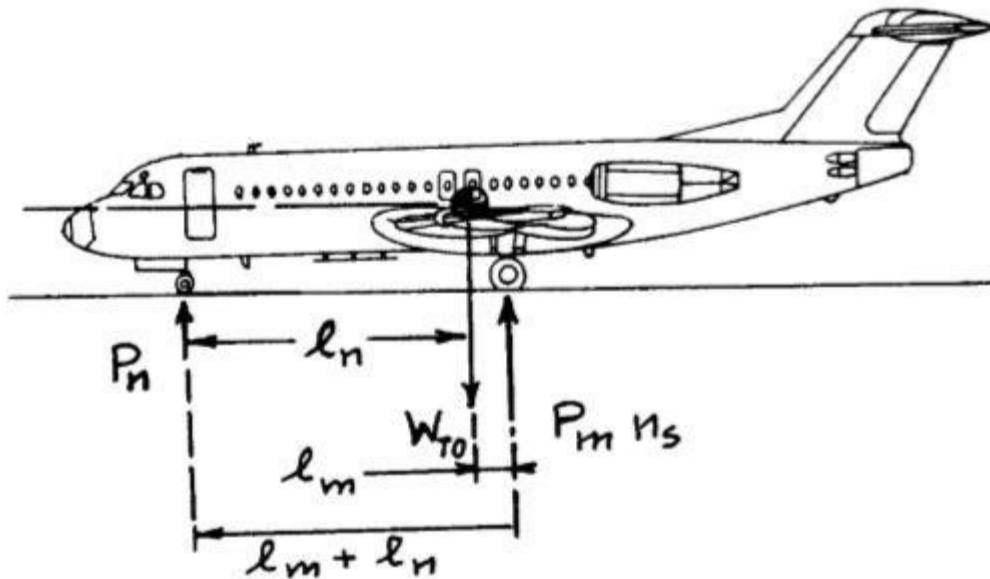


Figure 103 Geometric definitions for Static load calculation

The gear load ratios are found using $\frac{P_n}{W_{TO}} = 0.18, \frac{P_m}{W_{TO}} = 0.82$

From the similar weight aircrafts, it's quite safe to assume that two nose wheels would take the load while for every strut of the main landing gear would need four tires to support the load. The tire size from the chart available in Roskam is:

Table 30 Wheel dimensions for main landing gear

Main Wheel	
No of wheel	8
Maximum Diameter	29.4 in
Maximum Width	7.85 in
Rolling radius	12.7 in
Pressure	270 psi
Weight on Wheel	16965 lb
Main Wheel Strut loading	62056.75
Load ratio	0.82

Table 31 Wheel dimensions for nose landing gear

Nose Wheel	
No of wheel	2
Maximum Diameter	24.15 in
Maximum Width	5.5 in
Rolling radius	10.6 in
Pressure	355 psi
Weight on Wheel	7540 lb
Loading	2784.1
Load factor	0.18

The contact area of the tires depends on the weight and width of the tire and can be calculated by:

$$W_w = PA_p$$

$$A_p = 2.3\sqrt{wd} \left(\frac{d}{2} - R_r\right)$$

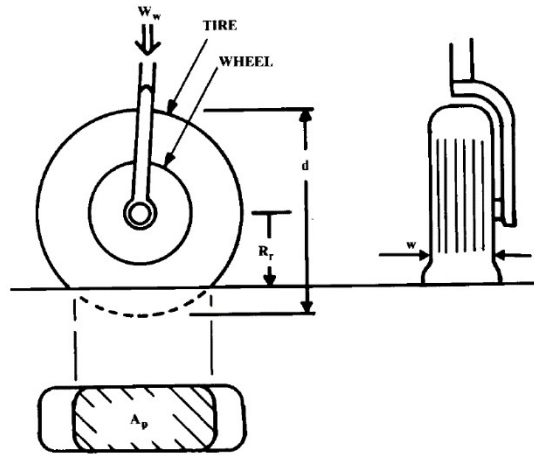


Figure 104 Contact Surface

Table 32 Contact area for nose and main landing gear

Contact Area of the Tire	
Main wheel	
Ap	69.88 in
P	242.76 psi
Nose Wheel	
Ap	39.10 sq. in
P	192.84 psi

4. Weight and Balance

Table 33 Revised moment arm of the proposed aircraft

No.	Type of Components	W (lb)	X (in)	WX	Y	WY
1	Fuselage Group	23072.4	399.84	9225268	0	0
2	Wing Group	10254.4	609.68	6251903	0	0
3	Empennage Group	754	843.21	635780.3	0	0

4	Engine Group		12214.8	725.75	8864891	0	0
5	Landing Gear Group	NG	603.2	140	84448	0	0
		MG	5428.8	593.78	3223513	0	0
6	Miscellaneous		15080	150	2262000	0	0
Empty Weigh			67407.6				
7	Trapped Fuel and oil		460	698	321080	0	0
8	Crew		1230	324.25	398827.5	0	0
Operating Empty Weight			69097.6				
9	Fuel		50020	721.23	36075925	0	0
10	Passengers		28000	324.25	9079000	0	0
	Baggage		4980	324.25	1614765	0	0

Table 34 Loading Conditions and CG of the proposed aircraft

Condition	CG (in)	Weight (lb)
Fully loaded	513.0745	152097.6
Half passengers + Full fuel	541.9895	135607.6
All Passenger+ half luggage	516.2172	149607.6
Zero passengers + full luggage	555.6788	124097.6
No PAX and Cargo	570.732	117995.2
Zero fuel	411.0743	102077.6
PAX only	519.4663	147117.6
Cargo Only	555.6788	124097.6

From the revised CG calculations, a new CG excursion diagram is created

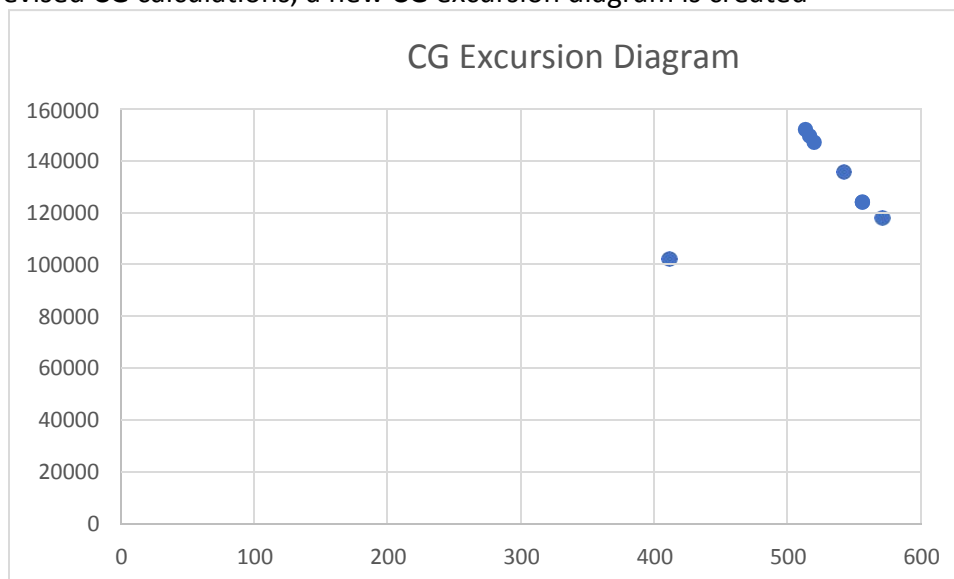


Figure 105 Revised CG excursion diagram of the proposed aircraft

From the figure above, it is observed:

- Most forward CG occurs at 102077.6 lb at 411.08 inches from nose
- Most aft CG occurs at 135607.6 lb at 541.98 inches from nose
- CG travel: 130 inches

5. Discussion and Conclusion

The landing gear for the proposed BWB is designed according to the conventional method. The CG. The BWB configuration has the problem of too much CG travel which is due to the placement of fuel tank just behind the cabin and the aft engines. The landing gears are placed 49.5 ft from the nose and the nose gear is placed with a base of 37.8 ft. Both the landing gears meet the tip over requirements. The fuselage sweep angle is 15 degrees and the proposed aircraft is a high wing aircraft, so the ground clearance requirements are also met.

The revised CG excursion diagram shows that there is 60 inches of less travel after the revision. The CG travel for this configuration is inevitable due to placement of different components, hence to arrest the travel, the components are to be placed accord to their effect on CG travel. The retractability of the landing gears has been checked using 2D drawings and empirical formulas as ample space below the passenger area is available for the retraction.

11. Stability and Control Analysis

1. Introduction

This report discusses about the class I stability and control analysis which is performed according to the steps provided by Roskam in airplane Design Part II. This report calculates and analyze the characteristics like static longitudinal stability and static directional stability. The static stability is the initial tendency of the vehicle to return to its equilibrium state once disturbed from it without any human or auto-pilot interference. While the dynamic stability deals with the time history of the vehicle's motion after its initial response to the static stability.

A dynamically stable aircraft is always statically stable. But the vice-versa is not true. The control deals with the change in the characteristics for desired outcome. The aircraft control deals with the deflection of the ailerons, elevator, rudder or other control surface to exert a force to that changes the behavior of the aircraft.

The x-plots for longitudinal and directional stability provides the minimum area of the horizontal tail and vertical tail for stability, respectively. The proposed aircraft is a BWB aircraft which does not have a horizontal tail hence the x plot for longitudinal stability is not plotted.

For unconventional configuration, it is difficult to achieve the static stability and may require more number of iterations. This report contains only one iteration.

2. Static Longitudinal Stability

For conventional aircraft, the static longitudinal stability is calculated by plotting the aerodynamic center and center of gravity change as a function of tail area. As the aircraft the is a BWB which does not have a horizontal tail, the static stability is calculated based on the position of center of gravity and aerodynamic center. It is not a function of horizontal tail area.

Static margin for the proposed aircraft can be calculated using the following equation:

$$m_s = -(C_{cg} - X_{AC})/MAC = -0.023$$

The static margin is negative hence the aircraft is longitudinally unstable.

3. Static Directional Stability

The directional stability is calculated using the conventional method as the configuration has a V-tail to make the aircraft directionally stable. The following equation shows the relationship between the vertical tail area and the side slip moment coefficient. The same equation is used to plot a x-plot for directional stability.

$$C_{n_\beta} = C_{n_{\beta wf}} + C_{L_{av}} \left(\frac{S_v}{S} \right) \left(\frac{x_v}{b} \right)$$

Where,

$$C_{n_{\beta wf}} = -57.3K_N \left(\frac{S_f l_f}{S b} \right)$$

The desired value for $C_{n_\beta} = 0.0010$.

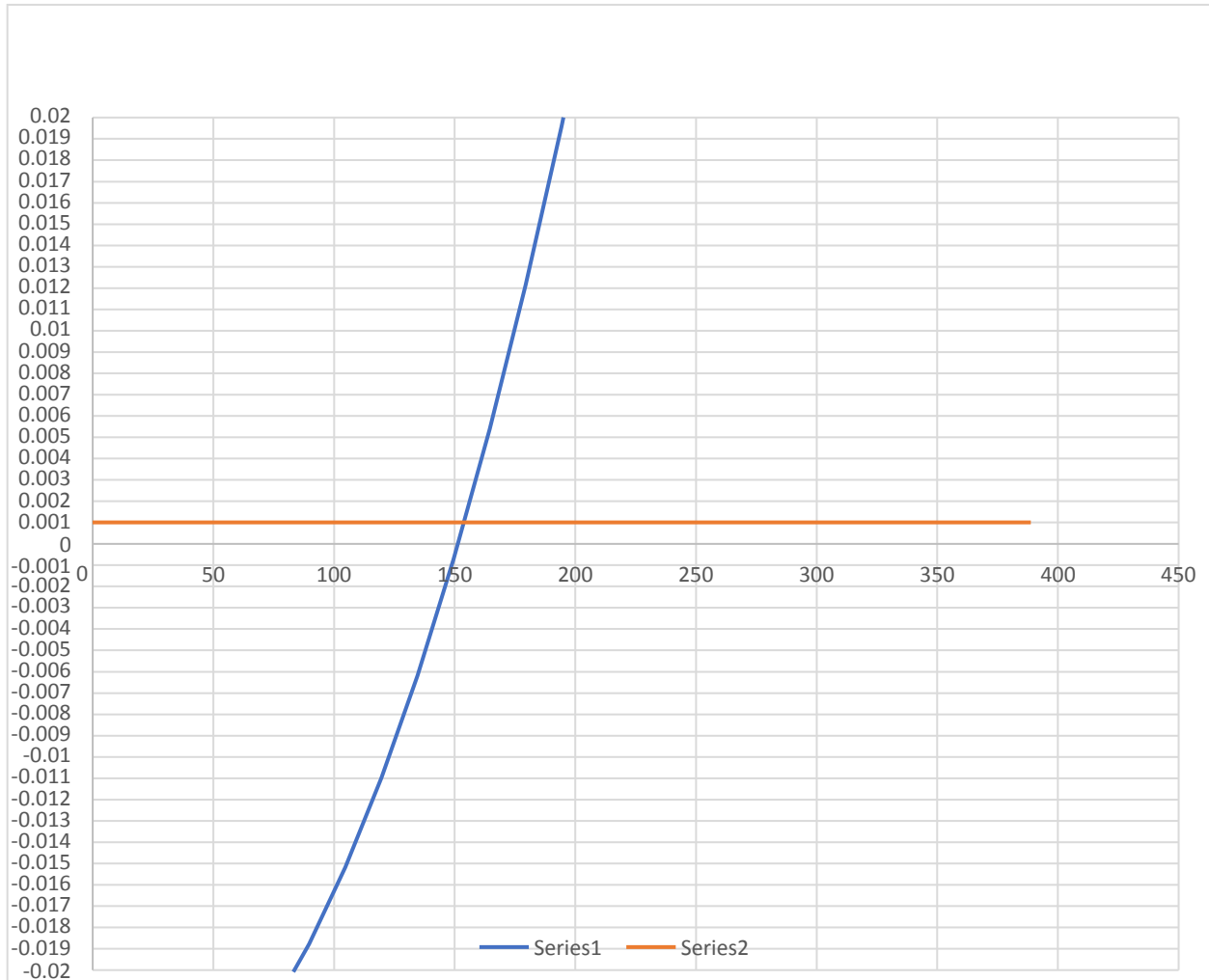


Figure 106 X-Plot for Directional Stability

From the X-plot it can be observed that there is a change in the vertical tail area. The area depicted by the plot is for each tail hence both the vertical tails need to be redesigned according to the area from the plot.

From the revised design, the deflection obtained for the vertical is:

$$k_{\beta} = - \frac{1.6436196}{-1.6426196} = 0.95 \text{ deg/deg}$$

The distance Y_t is from the center line of the fuselage to the thrust line of the engine which is 7.15 ft. The critical engine out yawing moment is $45240 \times 7.17 = 323640$ lb. ft. The total yawing moment for the proposed BWB aircraft is therefore $1.25 \times 323640 = 404550$ lb. Ft.

The one engine out landing stall speed for the proposed aircraft is $1.25 \times 170 = 212.5$ knots. For the vertical tail and rudder geometry the rudder control power derivative is calculated:

$$C_{n_{\delta_r}} = -4.5590 \text{ deg}^{-1}$$

The rudder deflection of 0.95 degree at required V_{mc} is yielded from the power coefficient, which is acceptable.

4. Empennage Design- Weight & Balance- Landing Gear Design- Longitudinal Static Stability & Control Check

The vertical stabilizer area changes for the required stability coefficient. The vertical stabilizer needs to be redesigned according to the area from the x-plot of the directional stability. The redesign of the stabilizer would be on the current assumptions hence, the actual design would be done in the class II sizing with the actual coefficients.

5. Discussion and Conclusion

The aircraft is longitudinally unstable and directionally stable with the change in the vertical tail area. The vertical tail area is lower than the proposed tail design in the empennage report. The longitudinal instability is due to the CG being aft to the aerodynamic center and there is no horizontal tail to balance it. It is assumed that the aircraft has de-facto longitudinal stability. During the calculations for the stability, many of the values were assumed as there is no validated methodology to conduct the stability analysis for a BWB aircraft. The directional stability data has some error due to assumption of the values for directional stability of the aircraft. The longitudinal stability can be improved by placing the wings in such a way that the aerodynamic center is forward to the CG. The iteration for the proposed aircraft will be explored further in Class II design process.

12. Drag Polar Estimation

1. Introduction

In the previous reports, detailed analysis of the design of wing, fuselage, empennage and landing gear have been conducted. The aircraft design and configuration are almost locked for the first iteration of the design process. During the weight sizing report, the values of the drag polars were assumed to estimate the weights of the aircraft. It is crucial to verify whether the proposed design would have similar lift to drag ratio as it was evident during sensitivities studies that the lift to drag ratio has a drastic effect on the weight of the aircraft as well as the range of the aircraft. The drag is calculated depending upon the wetted area of components over which the air flows. The drag due to different components of aircraft is calculated in the report.

2. Airplane Zero Lift Drag

The zero lift drag of aircraft is calculated from the total wetted area. A 3D view of the aircraft is needed to calculate the wetted area. The book by Roskam also provides empirical formulas to calculate. The wetted area of the aircraft is the integral over the perimeter versus the distance from the nose to tail. For the proposed aircraft, the wetted area would be less than the similar airplane with conventional configuration. The wetted area is further reduced due to the absence of horizontal tail.

The following components would contribute in the wetted area of the aircraft:

- Wing
- Vertical tail
- Fuselage
- Nacelles

The wetted area for the above-mentioned components using the following formulas:

a) Wing planform:

$$S_{wet_W} = 2 * S_{exp_W} * \left\{ 1 + 0.25 * \left(\frac{t}{c_r} \right) * \frac{1 + \tau\lambda}{1 + \lambda} \right\}$$

Where, $\tau = \frac{c_t}{c_r} = \frac{0.14}{0.10} = 1.4$ and $\lambda = \frac{c_t}{c_r} = 0.22$

b) Wetted Area for Vertical

The above equation can be used to find the wetted area of the vertical

$$S_{wet_{V.T.}} = 615 \text{ ft}^2$$

c) Wetted area of the fuselage

For streamlined fuselage without a cylindrical mid-section, the following equation is used:

$$S_{wet_{fus}} = \pi D_f L_f \left(0.5 + \frac{0.1351 L_n^2}{L_f} \right) \left(1.015 + \frac{0.3}{\lambda_f} \right) = 7245 \text{ sq ft}$$

The total wetted area for the proposed aircraft is 8843 sq. ft. The approximate of the wetted area in previous report is 8313 sq. ft. The fuselage is the body where other components of the aircraft are mounted and the area which intersects the fuselage needs to be subtracted from the calculated wetted area. The area to be subtracted from the total wetted area are the area base area covered by vertical tail, engine pylons and the wing area that is covered within the fuselage. The difference between the calculated wetted area and assumed wetted area is 7 percent which is acceptable.

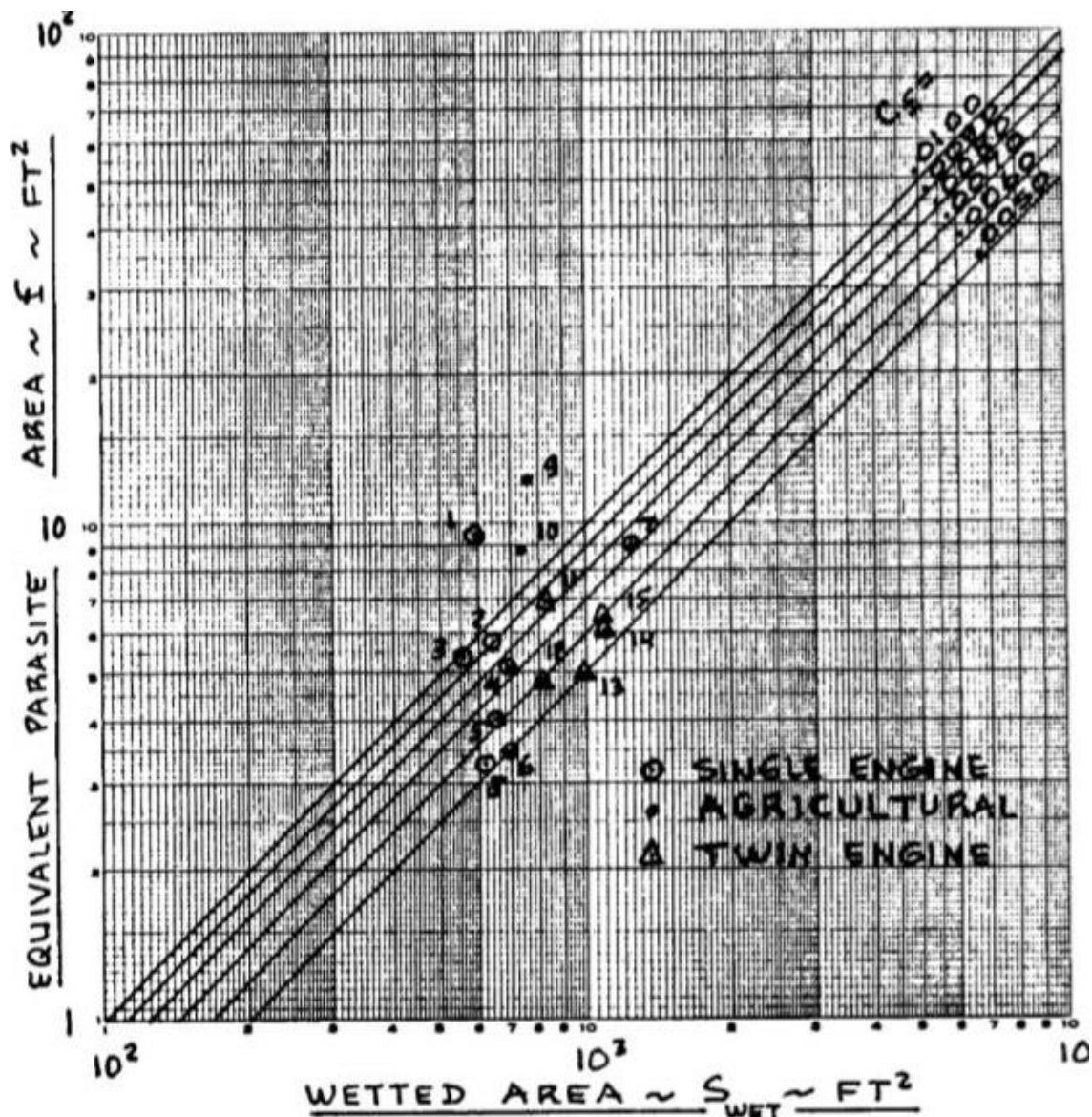


Figure 107 Wetted area vs equivalent parasite area

From the above figure, the equivalent parasitic area (f) can be found out using wetted area of the aircraft. The wetted area for 8843 sq. ft provides a parasitic area of 25 sq. ft.

The equivalent parasitic area is related to zero lift drag of the aircraft by the equation:

$$C_{D_0} = \frac{f}{S} = 0.007327$$

3. Low Speed Drag Increment

3.1 Flap Drag Increment

The drag is increased when the flaps are engaged during take-off and landing. The drag is further increment due to landing gears. The overall aircraft drag depends on the current configuration of the aircraft.

Table 35 Drag increment due to flaps

Configuration	ΔC_{D_0}	Aspect Ratio	E
Take-off flaps	0.005	7.8	0.85
Landing flaps	0.01	7.8	0.80

a. Landing Gear drag increment for Take-off and Landing

The landing gear drag increment:

Table 36 Drag increment due to landing gear

Configuration	ΔC_{D_0}	Aspect Raito	E
Landing gear	0.01	7.8	No effect

4. Compressibility Drag

The compressibility drag accounted for the Mach number 0.35 and above. The speed of the aircraft is high enough to account for compressibility drag which can be found out from the graph

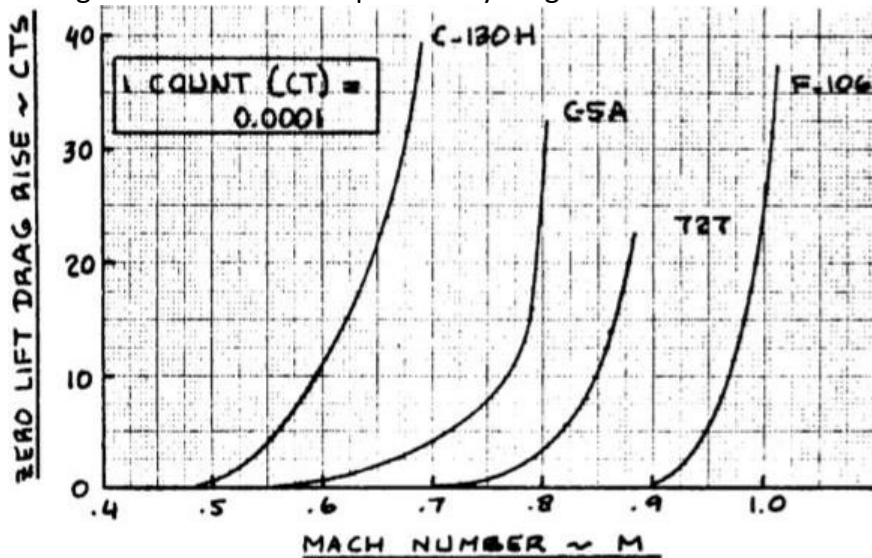


Figure 108 Mach number vs zero lift drag rise

From the graph, it is observed that the compressibility drag increment for 0.77 Mach number is 0.0005.

5. Airplane Drag polars:

From the above calculated data, the drag polars for different configuration of the aircraft can be calculated:

Table 37 Zero lift drag coefficient: Proposed aircraft

W_{TO}	$(W/S)_{TO}$	S	S_{wet}	F	C_{D_0}
152000 lbs.	48	3412	88432	25	0.0073

From the above data, the drag polars are calculated:

Table 38 Summary of Drag Polars

Configuration	Aspect Ratio	E	Drag Polar
Clean	7.8	0.9	0.0073 + 0.0453 C_L^2
Take-off flaps	7.8	0.85	0.0128 + 0.0480 C_L^2
Landing flaps	7.8	0.8	0.0128 + 0.0510 C_L^2
Landing gear	7.8	No effect	0.0223 + 0.0453 C_L^2

The L/D can be calculated from the drag polars

$$\frac{L}{D} = \sqrt{\pi A e / 4 C_{D_0}}$$

Table 39 Drag Polars

Configuration	L/D
Clean	26.54
Take-off flaps engaged, landing gear down	13.67
Take-off flaps engaged, landing gears up	20.73
Landing flaps engaged, landing gear down	12.21
Landing flaps engaged, landing gear up	17.58

6. Discussion and Conclusion

The above calculations are based on class I drag calculation method, which accounts only for major components of the aircraft. The calculation of drag is simplified using the assumptions. The drag increment due to flaps and landing gear is assumed and from a predefined range in book by Roskam. The values are very conservative as they are based on old technologies and material.

13. Environment/ Economic Trade-off; Safety/ Economic Trade-off

1. Drawing and Summary of Most Important Design Parameters

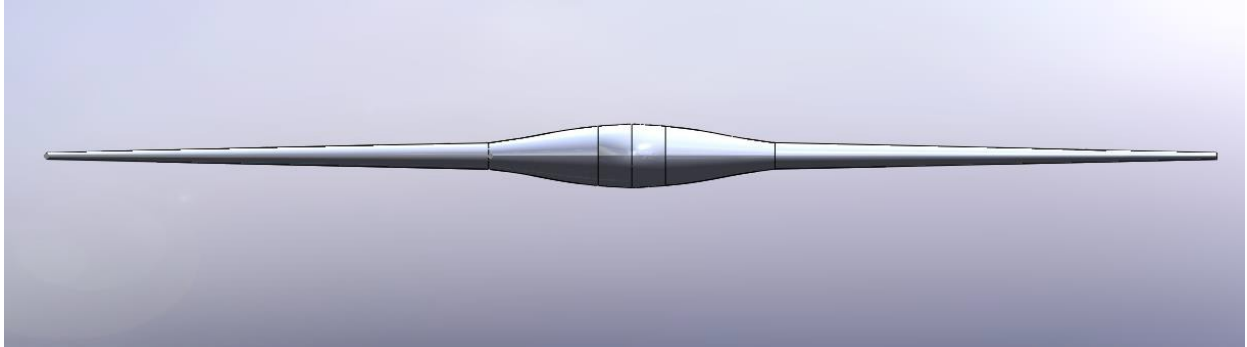


Figure 109 Front view of the aircraft

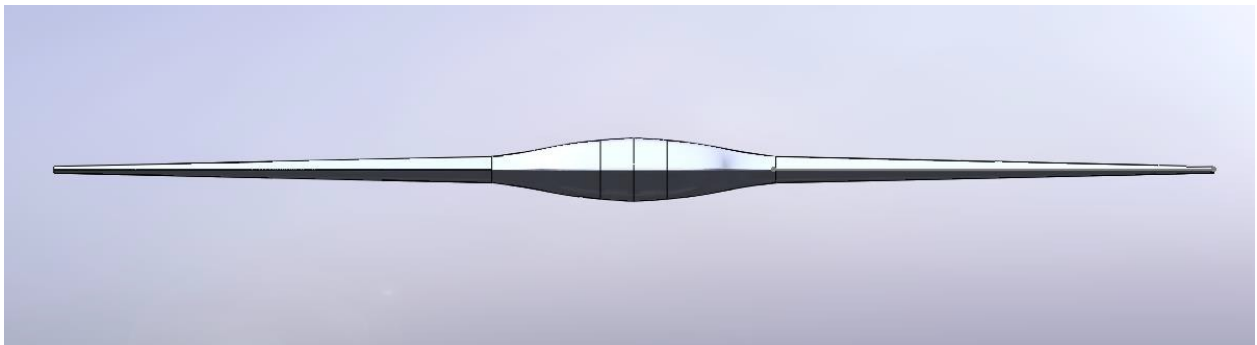


Figure 110 Rear view of the aircraft

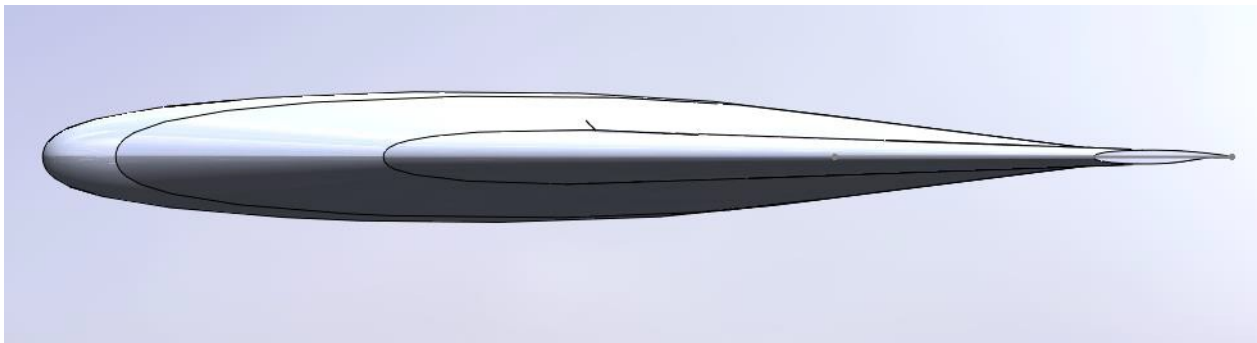


Figure 111 Side View of the aircraft

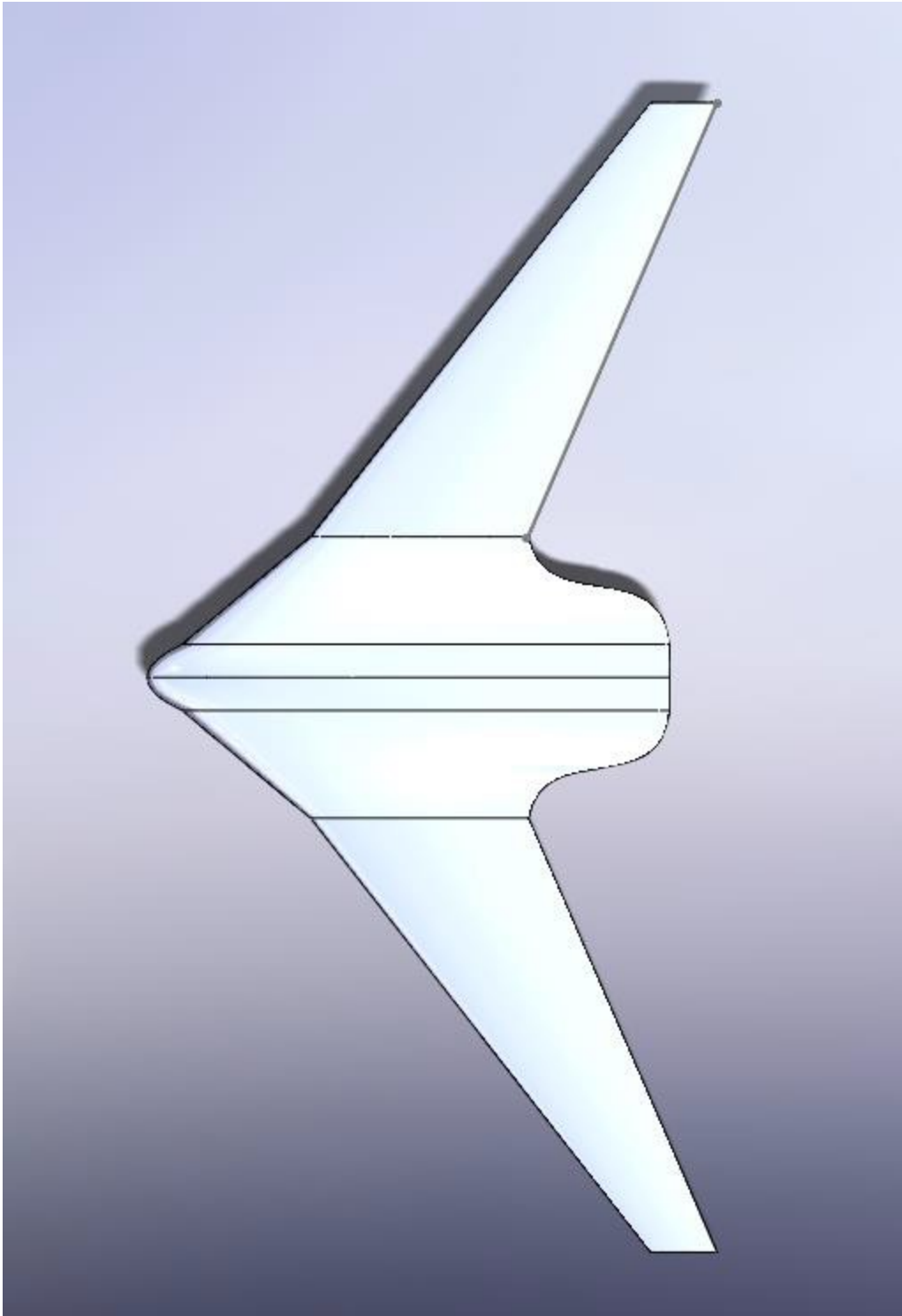


Figure 112 Top view of the aircraft

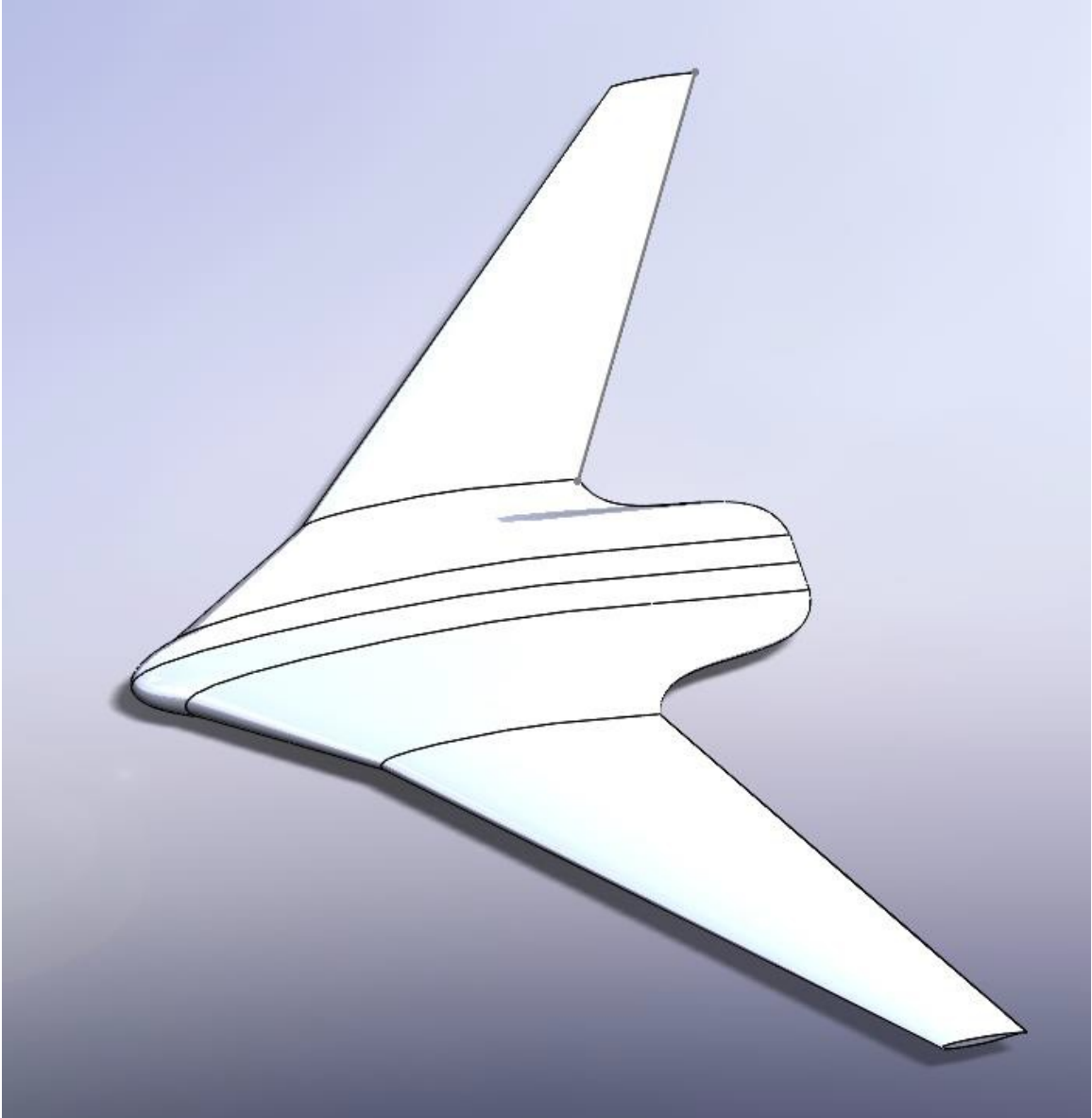


Figure 113 3D view of the aircraft

Table 40 Aircraft Details

	Wing	Vertical Stabilizer
Area	3412 ft ²	656 ft ²
Span	163 ft	23 ft
Mean Geometric Chord	20.93 ft	9.61 ft
Aspect Ratio	7.8	1.705
Sweep Angle	27.7 degrees	39.2degrees
Taper Ratio	0.22	0.4

Thickness Ratio		0.13	0.28
Airfoil	Center body	SC(2)-0012	NACA 0012
	Root	SC(2)-0714	
	Tip	SC(2)-0410	
Dihedral Angle		3 degrees	
Elevons Chord Ratio		0.30	NA
Elevons Span		0.1-0.9	NA
Slats chord Ratio		0.4	NA
Slats span		0.1-0.45 & 0.6-0.9	NA
		Fuselage	Cabin Interior
Length		74 ft	
Maximum height		12.5 ft	7.5 ft
Maximum Width		40 ft	37 ft

2. Recommendations

The proposed aircraft uses the conventional airfoils which have been designed for the conventional aircrafts. Using the method developed by NASA Langley Research Center, an airfoil can be designed for application in BWB fuselage. (Larkin & Coates, 2017)

The aircraft is longitudinally unstable, more iterations on the design and more experimentation with different configurations for static and dynamic stability data. The instability is due to the distance of aerodynamic center. The placement of AC can be changed by changing position of the wing on the aircraft. Research on the BWB stability shows that with slightly unstable aircraft it is possible to build an aircraft which can be used in civil aviation.

Control authority of the BWB is small but with the new technology of morphing wing, the tail of the inboard wing can have variable camber to provide the longitudinal stability a control authority. The directional control authority can be increased with the use of two vertical stabilizers with a dihedral angle which is supposed to provide more directional stability and control. More robust control laws are needed for a BWB aircraft autopilot control.

More iterations for the same design need to be performed to get accurate results. The conventional method for design of an aircraft cannot be used to design a BWB aircraft. Some modifications are needed in the methodology.

3. Environmental and economic trade-off

Depletion of fossil fuel reserves and increasing the carbon level on the air have been major driving force to find more efficient technology a design. Total 27% of USA greenhouse emissions is from transportation (Government). 12% of the GHG emissions are contributed by aviation industry and according to GAO report 2008, 1% of total air pollution of the world is due to aviation. The GHG emissions can be reduced using effective propulsion system with proper aircraft design.

The BWB aircraft design is one of the feasible solution to the solution to the above-mentioned problem. The proposed aircraft is based on the NASA Subsonic Ultra Green Aircrafts (SUGAR) Ray project. The program focuses on the reduction of the air pollution and noise produced by the aircrafts. With the major focus on these two issues, the BWB is the most advance configuration stated in the report.

The concept of a BWB aircraft is to decrease the fuel burn for the flight. With the use of this configuration, 27% decrease in fuel burn can be achieved. The proposed aircraft still uses gas engines which can be replaced by batteries or fuel cells which are more environmental friendly, but the energy density of batteries and fuel cell is not up to the mark and cannot be used for long range and high payload vehicles. The major issue with the battery is its disposal after its life. Batteries saves the air but pollutes the land.

The proposed aircraft uses innovative technologies which are under research phase and the technology has not been introduced for commercial use, hence the cost of the aircraft would be much higher when compared to the conventional counterpart which uses much matured technologies which have gone through rigorous experimentations and validation (M. Bradley, 2011).

In past, these problems were taken seriously until 1980 (Torenbeek, 2010). But with the rising environmental issues more work was put into increasing the efficiency of the aircraft, but the rate of success was slow and could not match with the rising demand for air transport. The proposed configuration of the aircraft is the answer to issues that the aviation industry is facing currently.

The cost involved in manufacturing the BWB aircraft is going to be high initially as the technology is not matured but once it is matured and validated, the cost will reduce significantly. The advance materials and engines used in the aircraft constitute most of the cost (C Goldber, 2017). The proposed aircraft is the answer to many of the environmental issues, but the use of gas turbine engines can be re-place by the engines which run on hydrogen. It would completely solve the problem of air pollution and would not affect other biosphere like batteries and fuel cells.

4. Safety and economic Trade-off

The main setback of the BWB aircraft is low stability and control authority. These issues were relevant in the past too. The first flying wing configuration aircraft meant for military use, YB-49, was never introduced to the US Airforce due the structural and stability issues. There has been rigorous research and experimentations for the similar configuration without any fruitful outcome. The most recent flying wing aircraft, B-2, uses an active flight stabilizing system to make the aircraft stable. But according to the regulations of FAR 25, the commercial airplane need to be inherently stable hence an active SAS system cannot be used (Siouris & Qin, 2007). Since the failure of YB-49 the interest of research was shifted to more conventional aircraft and to make them more efficient. (Torenbeek, 2010)

The configuration of the BWB aircraft does not have a horizontal tail due to which, the BWB aircraft have major longitudinal stability issues. Most of the configurations of BWB aircraft does not have an inherent longitudinal stability. The experiments have been conducted for static stability and the only feasible solution is to have a slightly unstable aircraft. (Denieul, 2017)

Recently NASA MADCAT (NASA, n.d.) project uses the morphing wing which can change the twist as well as the chamber of the airfoil to have the desired characteristic in real time. This technology can be used for BWB to address its problems for inherent stability. Another issue faced is the comfort of passengers during landing due to high angle of attacks which is necessary to obtain the high lift coefficients. This problem can be eliminated by making the passenger surface swivel but again it's an innovative solution and never been tested. It would also increase the weight of the aircraft due the swiveling system. The cost involved in implementing these solutions would be very high as the technology is not matured and tested.

The instable aircraft pose a safety issue in case the computer fails. Morphing wing would be the best solution to the problem as once the wing is locked for a geometry, it won't change even if the control system fails completely.

5. Conclusion

The BWB aircraft tends to reduce the air pollution because of its aerodynamic efficiency. The technology used to build this aircraft is still under research phase hence the exact feasibility and economic trade-off is not available but as the technology is new, manufacturing the aircraft will be expensive. Once the new materials and technology hits the market, an accurate estimation of cost as well as environmental trade-off can be carried out.

14. Class II: Landing Gear Design

1. Introduction

This chapter marks the beginning of class II design of the aircraft. Chapter 10 discusses the class I design of the landing gear with all the tip over criteria being satisfied and the dimensions calculated during the class I design procedure are carried for the further detail design. Landing gear must be designed to absorb the shock during landing and take up the taxing load. In this chapter tire size, shock absorber stroke length and strut diameter are determined for the proposed aircraft. The aircraft has retractable landing gears and hence the retraction kinematics needs to be designed.

2. Determination of Allowable Wheel Loads

The landing gear design should account for the following three types of loads:

- Vertical Landing Gear Loads
- Longitudinal Loads
- Lateral Loads

The vertical loads for an aircraft depends on the sink speed. For the proposed aircraft, the FAR 25 requirements constraints the touchdown rate to 12 fps.

$$w_t = 12 \text{ fps}$$

The longitudinal and lateral loads are resisted by drag-brace and side-brace elements respectively. The loads on each landing gear strut as well as the load on each tire should not exceed values that can cause:

- Structural damage to gear or the airplane
- Tire damage
- Cause runway damage

The proposed aircraft is not designed to land on type 1 surfaces which include grassy and gravel surface as the load on the nose gear exceeds 10,000 lb and would induce heavy damage to the surface. The picture below provides the tire pressure to avoid gear induced surface damage.

Description of Surface	Maximum Allowable Tire Pressure	
	kg/cm ²	psi
Soft, loose desert sand	1.8 - 2.5	25 - 35
Wet, boggy grass	2.1 - 3.2	30 - 45
Hard desert sand	2.8 - 4.2	40 - 60
Hard grass depending on the type of subsoil	3.2 - 4.2	45 - 60
Small tarmac runway with poor foundation	3.5 - 5.0	50 - 70
Small tarmac runway with good foundation	5.0 - 6.3	70 - 90
Large, well maintained concrete runways	8.5 - 14	120 - 200

Figure 114 Tire Pressure for Various Types of Runway Surfaces

The aircraft has multiple wheels per strut so the Load Classification Number (LCN) cannot be found directly. According to the layout and number of tires per strut, the Equivalent Single Wheel Load is calculated and then using the chart, LCN is found for the aircraft.

The ESWL depends on the landing gear layout and the number of wheels per strut. The following figure depicts different kind of wheel layouts.

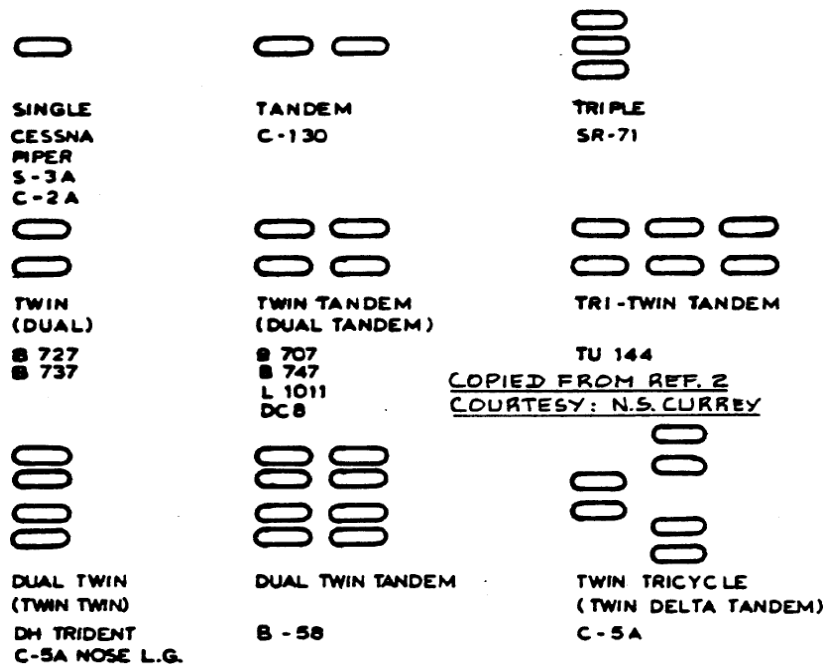


Figure 115 Landing Gear Wheel Layouts

For the proposed aircraft, the nose gear has Twin (Dual) and the main gear has Twin Tandem (Dual Tandem) layouts. As per the layout, the ESWL can be found out using the equations:

Nose Gear:

$$ESWL = P_n/1.33$$

Main Gear:

$$ESWL = P_m/2$$

Where P_n and P_m are the loads on the nose gear and main gear respectively. Borrowing the values of the loads calculated in the Class I design, the ESWL values for the nose gear and main gear results to 25247 lbs. and 37231 lbs. respectively.

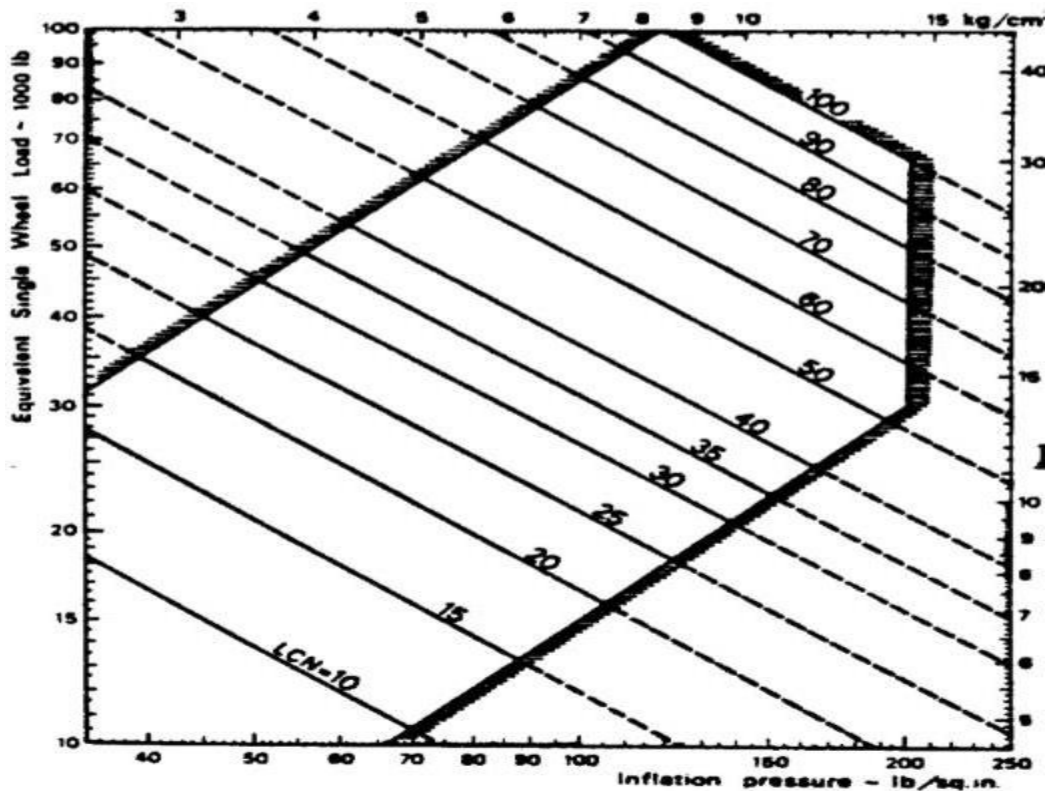


Figure 116 Effect of Tire Pressure and Tire Load on LCN

The figure 116 depicts the relation between the ESWL and LCN. From the figure, the LCN of the aircraft is.

3. Tires: Types, Performance, Sizing and Data

The airplane tires offer a cushioning effect and absorb the shock when the aircraft touch downs the runway. It also supports the entire aircraft weight and loads during taxing, take-off and landing. The aircraft tires are rated in the terms of:

- Ply rating
- Maximum allowable static load
- Recommended inflation pressure
- Maximum allowable runway speed

Mainly there are even different tires are used depending upon the aircraft weight, retraction system and runway type. The following list provides the description of all the types of the aircraft tire.



NEW DESIGN



TYPE I



TYPE III



TYPE VII



New Design: This is a recent design. The outside tire dimensions are reflected in the type designation: D xW. All new tires will be designated with this system.

Type I: Smooth Contour. This type was designed for airplanes with non-retractable landing gears. Although this type is still available, its use in newly designed airplanes is discouraged because this tire type is considered obsolete.

Type II: High Pressure. This type, although still available is also considered obsolete. It was designed for airplanes with retractable gears. It has been replaced by Type VII which has considerably greater load carrying capacity.

Type III: Low Pressure. This type is comparable to Type I but has beads of smaller diameter. It also has larger volume and lower pressure. Any new sizes in this type will be listed under the 'New Design' designation.

Type VI: Low Profile (Inactive). This Type was designed for nosewheel applications only. It was designed to reduce wheel drop following complete deflation of the tire.

Type VII: Extra High Pressure. This Type is almost universal on military and civil jets and turboprops. It has high load capacity and narrow width. Any new sizes in this type will be listed under the 'New Design' designation.

Type VIII: Low Profile High Pressure. This is a new design for very high take-off speeds. Any new sizes in this type will be listed under the 'New Design' designation.

Figure 117 Types of Aircraft Tires

The type VII tire is selected for the proposed aircraft. The nose and main landing gear dimensions are:

Nose gear tire: 13.5 x 5 inches

Main gear tire: 40 x 14 inches

The nosewheel is designed to support the maximum allowable dynamic load. These dynamic loads are obtained as follows:

$$\text{Dynamic Load} = f_{dyn} * (\text{Static Load})$$

For type VII tire, the f_{dyn} factor is 1.5 and static load is 33577.78 lbs.

$$\text{Dynamic Load} = 50366.67 \text{ lbs}$$

As the aircraft is to be FAR 25 certified, the loads are multiplied with the factor of 1.07 and to accommodate weight growth of the aircraft, the loads are again multiplied with the factor of 1.25. The new static load values obtained are divided with the number of tires on the nose gear to calculate the load on each tire, which is used for the selection of tires from the chart provided in the book.

Table 41 Load Values

Loads	Nose gear (lbs.)	Main Gear (lbs.)
Static Load	44910.28	99591.73
Dynamic Load	67365.42	N/A
Load per tire	22455.14	12448.97

Maximum Load per nose gear tire can be calculated using the following equation:

$$P_{n_{dyt_t}} = \frac{W_{TO} (l_m + \frac{a_x}{g(h_{cg})})}{n_t(l_m + l_n)}$$

Where,

$$l_m = 83.49 \text{ inches} \ \& \ l_n = 370.29 \text{ inches}$$

$$\frac{a_x}{g} = 0.35 \text{ for dry concrete with simple brakes}$$

$$\frac{a_x}{g} = 0.45 \text{ for dry concrete with anti - skid brakes}$$

$$h_{cg} = 102.5 \text{ inches} \ \& \ n_t = 2$$

$$P_{n_{dyt_t}} = 16789.77 \text{ lbs}$$

$$\text{Static Load} = \frac{16789.77}{1.5} = 11193.18 \text{ lbs}$$

The maximum value is chosen from the calculated according to both the methods for static as well as dynamic load.

The design maximum static load per nose gear wheel = 22455.14 lbs.
 The design maximum dynamic load per nose gear = 67365.42 lbs.
 The design maximum static load per main gear wheel = 12448.97 lbs.

The data provided in the book of Roskam, the following list of tires meet the load criteria of the aircraft:

Table 42 Sorted Wheel Information

Main Gear							
No	Size	Ply Rating	Load Rating (lbs.)		Inflation Pressure (Psi)	Tire outer dia. (Inches)	Qualification Status
			Static	Dynamic			
1	29x7.7	16	13000	NA	230	28.4	MIL
2	29x7.7	16	13000	NA	220	28.4	MIL
Nose Gear							
3	30x11.5	24	25000	NA	245	28.75	MIL
4	30x11.5	25	25000	NA	245	28.75	MIL

From the above table of the tire data and considering the factors like wheel diameter and inflation pressure, the following tires are chosen for nose and main gear:

Nose Gear: No. 4 30x11.5 25 PR
 Main Gear: No.2 29x7.7 16 PR

4. Strut Wheel Interface, Struts and Shock Absorber

There are two main parameters for strut-wheel interface. The 'rack' is the angle between the wheel swivel axis and a line vertical to the runway surface. The 'trail' is the distance between the runway-wheel contact point and the point where the wheel swivel axis intersects the ground. Both parameters are shown in the figures below:

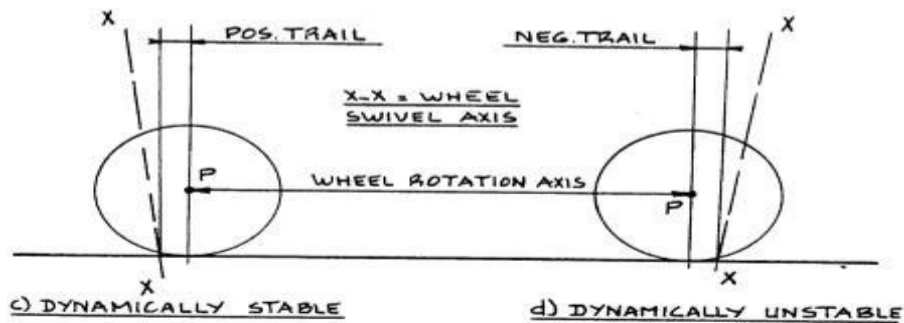
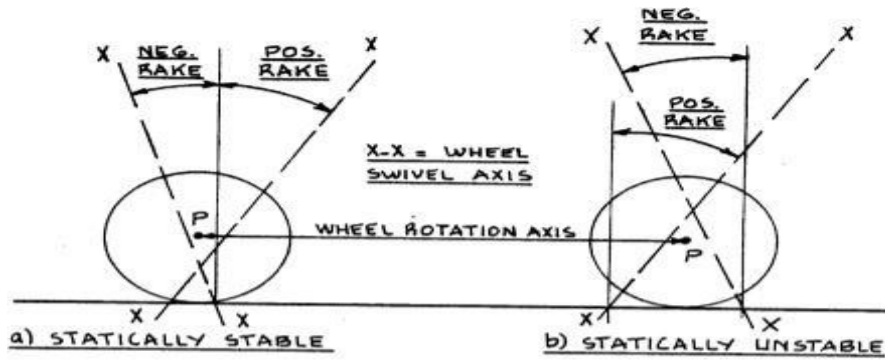


Figure 118 Rake and trail definition

In most airplanes, stable strut-wheel arrangements are used. For the nose as well as the main gear a trailing link with self-locking side brace actuator system is used. The following figure shows the shock absorbing system.

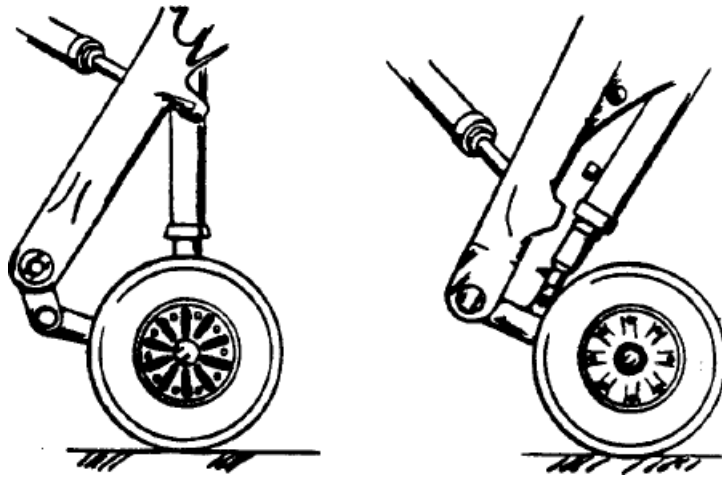


Figure 119 Trailing Link Mechanism

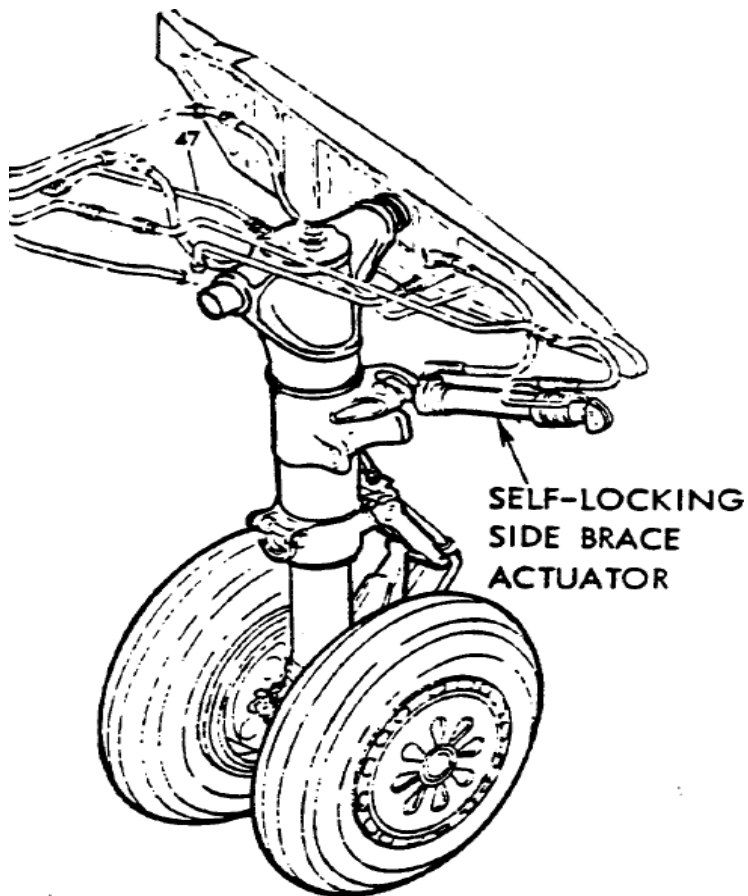


Figure 120 Self Locking Brace Actuator

There are many shock absorbing devices available. The main aim of the device is to dissipate the energy from shock during landing in the form of heat energy. The main devices are tires, shock chords, air spring, cantilever spring, oleo-pneumatic struts and liquid springs. For the proposed aircraft type, liquid spring is the best choice as the shock absorbing efficiency is higher than any of the other devices.

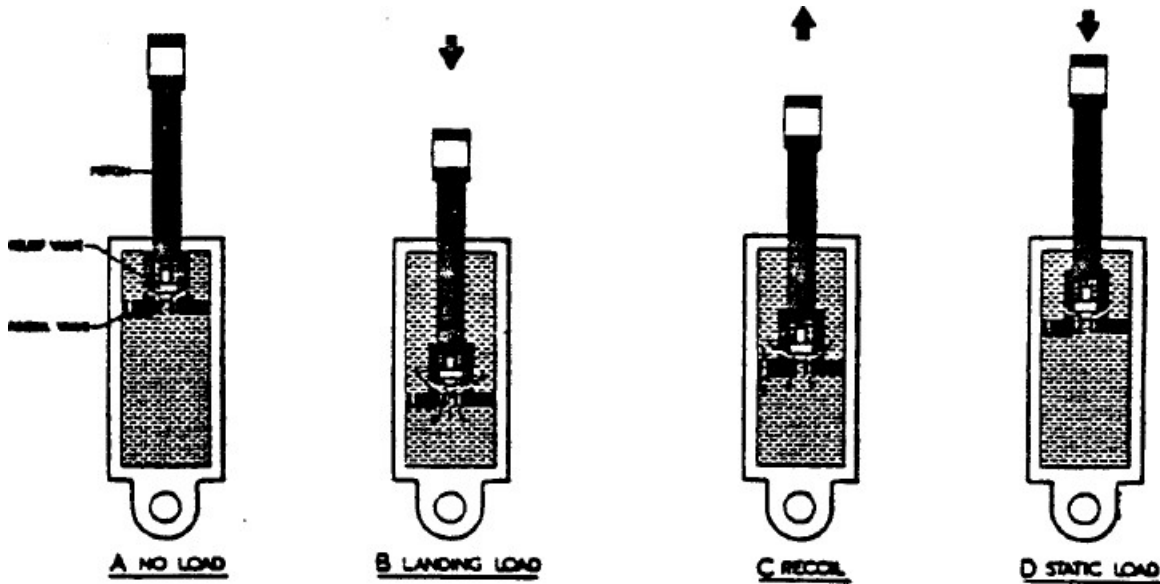


Figure 121 Liquid Spring Shock Absorber

Sizing of Strut:

The maximum kinetic energy which needs to be absorbed when the aircraft touches down is calculated from the following equation:

$$E_t = 0.5(W_L)(w_t)^2/g$$

Where W_L is the landing weight and $w_t = 12$ fps for FAR 25

$$E_t = 0.5(153300)(12)^{32.174}$$

$$E_t = 89453.27 \text{ pound} - \text{force}$$

A) Main Landing Gear: It is convenient to assume that the entire touch-down energy is absorbed by the main landing gear and to design it, following equations are used:

$$E_t = n_s P_m N_g (\eta_t S_t + \eta_s S_s)$$

where n_s is the number of main gear struts = 2
 P_m is the maximum static load per main gear strut

N_g is the landing gear load factor: ratio of maximum load per leg to the maximum static load per leg = 1.8

η_t is the tire energy absorption efficiency = 0.47

η_s is the energy absorption efficiency of the shock absorber = 0.85

S_s is the stroke of the shock absorber

S_t is the maximum allowable tire deflection

$$W_L = 0.84 * W_{T0} = 153300 \text{ lbf}$$

$$S_t = D_0 - 2(\text{loaded radius})$$

$$S_t = 29.40 - 2(12.2)$$

$$S_t = 4.8 \text{ inches}$$

$$S_s = \left[\{0.5(W_L/g) (w_t)^2 / (n_s P_m N_g)\} - \eta_t S_t \right] / \eta_s$$

$$S_s = 17 \text{ inches}$$

It is suggested to add one inch to the calculated length:

$$S_{s_{design}} = S_s + 1 = 18 \text{ inches}$$

Diameter of the shock absorber is estimated from:

$$d_s = 0.041 + 0.0025(P_m)^{\frac{1}{2}}$$

$$d_s = 0.54 \text{ inches}$$

Nose gear: The main gear equations can be used to calculate the stroke of shock absorber for nose gear with some modification:

$$S_t = 4.75 \text{ inches}$$

$$S_s = 21 \text{ inches}$$

$$S_{s_{design}} = S_s + 1 = 22 \text{ inches}$$

$$d_s = 0.7 \text{ inches}$$

15. V-n Diagram

1. Introduction

The V-n diagrams are used to determine design limits and design load factors as well as the corresponding speeds to which airplane structures are designed. This section of the report discusses the procedure to construct a V-n diagram for a FAR 25 certifiable aircraft. A typical V-n diagrams of the for a FAR 25 certified aircraft.

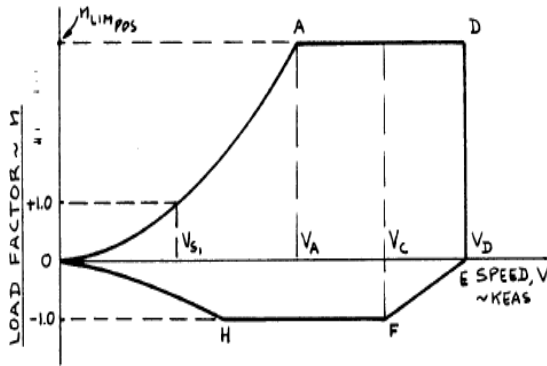


Figure 122 Maneuver V-n Diagram

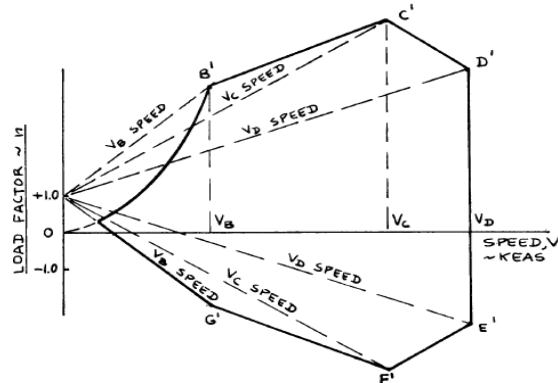


Figure 123 V-n Gust Diagram

2. V-n diagram for the proposed diagram

The proposed aircraft comes under FAR-25 commercial transport category.

Determination of +1g stall speed, V_{s1}

$$V_{s1} = \left\{ 2 * \frac{GW}{\rho * C_{N_{max}} * S} \right\}^{\frac{1}{2}}$$

Where, GW = flight design gross weight in lbs. = 182500

S = wing area in ft^2 = 4136

ρ = air density in slugs/ ft^3

$C_{N_{max}}$ = maximum normal force coefficient = $1.1 * C_{L_{max}} = 1.1 * 1.2 = 1.32$

Determination of design cruising speed, V_c

V_c must be sufficiently greater than V_B to provide inadvertent speed increase likely to occur because of severe atmospheric turbulence.

$$V_C \geq V_B + 43 \text{ kts}$$

Determination of Design Dividing Speed

$$V_D \geq 1.25 V_C$$

Determination of Design Maneuvering Speed

$$V_A \geq V_{S_1} n_{lim}^{1/2}$$

Where, n_{lim} is the limit maneuvering load factor at V_C

V_A should not exceed V_C

Determination of design speed for maximum gust intensity

V_B should not be greater than V_C and should not be less than the speed determined from the intersection of the $C_{N_{max}}$ and the gust line marked V_B .

Determination of negative stall speed line

$$V_{S_{neg}} = \sqrt{2} * \frac{\overline{\left(\frac{GW}{S}\right)}}{\rho C_{N_{maxneg}}}$$

Where, $C_{N_{maxneg}} = 1.1 C_{L_{maxneg}}$

$C_{L_{maxneg}}$ is the maximum negative lift coefficient

Determination of design limit load factor

The positive design limit load factor is given by:

$$n_{lim_{pos}} \geq 2.1 + (24000/(GW + 10000))$$

n_{lim} should not be greater than 3.8

n_{lim} should be greater than 2.5 at all the time

$$n_{lim_{neg}} \geq -1.0 \text{ up to } V_C$$

$n_{lim_{neg}}$ varies linearly from the value at V_C to zero at V_D

Construction of gust load factor lines

For the gust line marked V_B

$U_{de} = 66$ fps between sea level and 20,000 ft

$U_{de} = 47.33 - 0.000933h$ between 20,000 and 50,000 ft

For the gust line marked V_C

$U_{de} = 50$ fps between sea level and 20,000 ft

$U_{de} = 66.67 - 0.000833h$ between 20,000 and 50,000 ft

For the gust line marked V_D

$U_{de} = 25$ fps between sea level and 20,000 ft

$U_{de} = 16.67 - 0.000417h$ between 20,000 and 50,000 ft

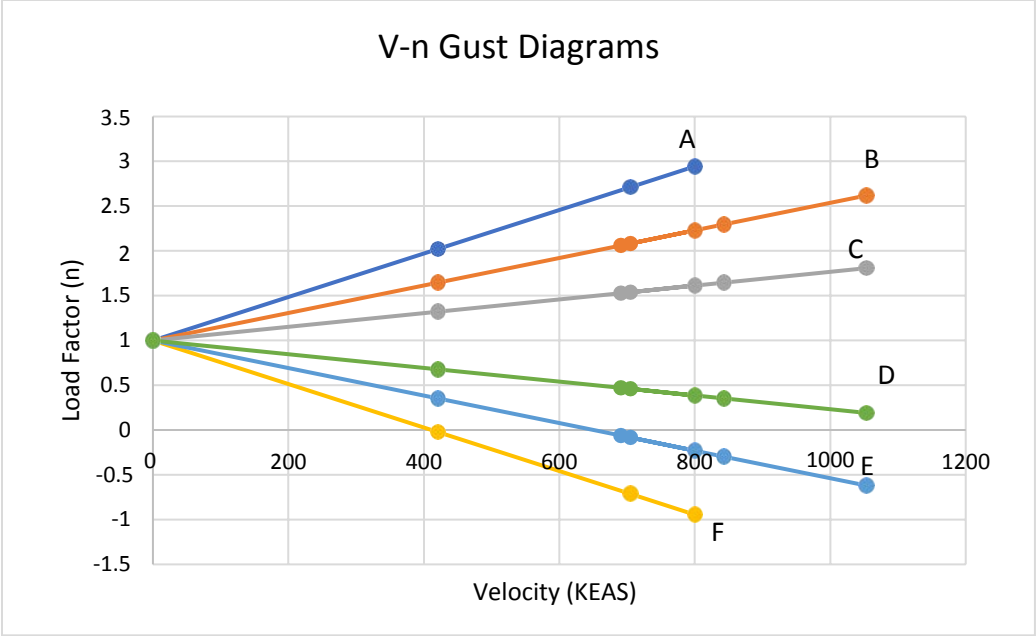


Figure 124 V-n Gust Diagram

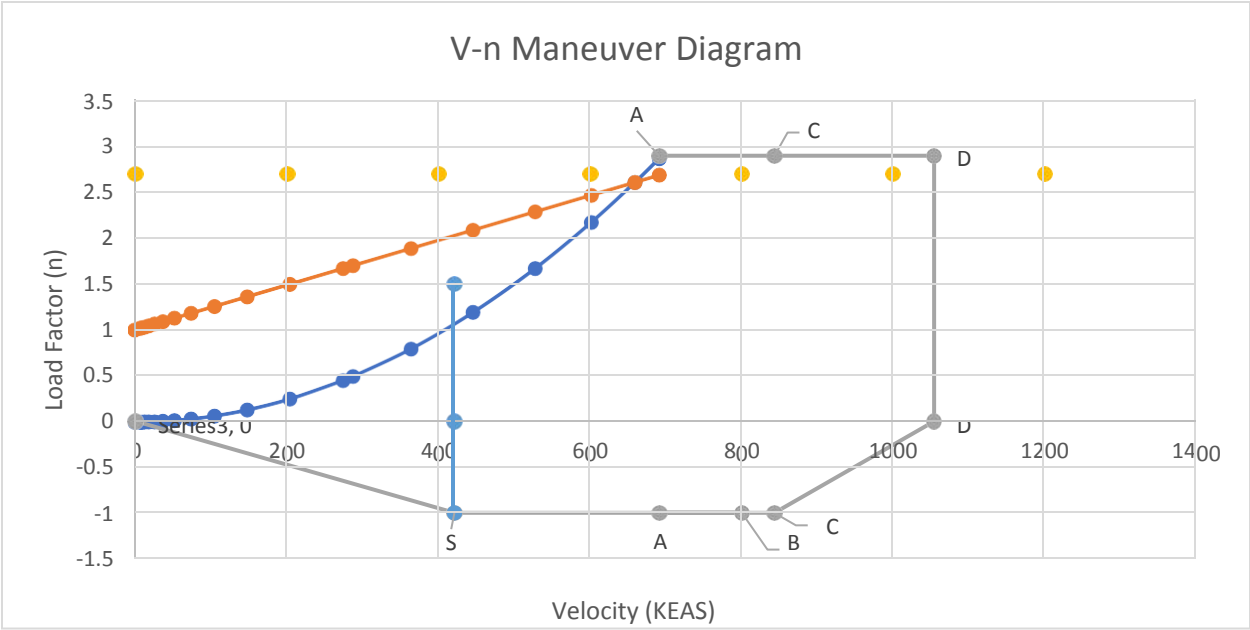


Figure 125 V-n Maneuver Diagram

16. Class II: Weight Estimation

1. Introduction

The Class I method for weight estimation provides you with a fair estimation of weight of the essential structural group of the aircraft. Class II extends the weight estimations by using (i) Cessna Method, (ii) USAF Method, (iii) Torenbeek Method and (iv) GD Method. These methods provide very refined weight estimation of different components. The proposed aircraft has a very novel design and there is no other aircraft of similar kind to compare and set a benchmark plus, some method uses the variables that are not associated with blended wing body design and hence cannot be adopted to calculate the weight estimations.

2. Methodology for Weight Estimation

The book by Roskam adopts 4 different method for weight estimation but for the proposed aircraft on two of them are useful: GD Method and Torenbeek Method as other methods are for light utility aircraft and military purpose aircraft. The methodology is divided into three parts estimating the structural, powerplant and fixed equipment weight respectively.

Structural Weight Estimation

This group of components includes the weight of Wing, adjustment for flower flaps, empennage, fuselage nacelles and landing gear. The weight of all the components are calculated based on either of the two methods discussed earlier.

Estimation of Wing Weight:

The GD method is not used of the calculations as primary assumption for the method is the Mach number of aircraft should not exceed the value of 0.8 hence only Torenbeek method is used. The following equation applies the transport aircraft with take-off weight above 12,500 lbs.:

$$0.0017W_{MFZ} \left(\frac{b}{\cos \Lambda_{\frac{1}{2}}} \right)^{0.75} \left(1 + \left(\frac{6.3 \cos \Lambda_{\frac{1}{2}}}{b^2} \right)^{0.5} \right) n_{ult}^{0.55} \left(\frac{bS}{t_r W_{MFZ} \cos \Lambda_{\frac{1}{2}}} \right)^{0.30}$$

The adjustment for flaps is not required as they are not used in the design.

Estimation of Empennage Weight

The horizontal tail is not incorporated in the design hence there is no added weight of it. The weight of vertical stabilizer is calculated using:

$$W_v =$$

$$0.19 \left(\left(1 + \frac{z_h}{b_v}\right)^{0.5} (W_{TO} n_{ult})^{0.363} S_v^{1.089} M_H^{0.601} l_v^{-0.726} \left(1 + \frac{S_r}{S_v}\right)^{0.217} (A_v)^{0.337} \left(1 + \lambda_v\right)^{0.363} \cos \Lambda_{\frac{1}{4}}^{1.014} \right)$$

Estimation of Fuselage Weight

The estimation of the fuselage weight is based on a specialized study conducted for the design procedure of a BWB aircraft. The following equation is used for calculating the weight:

$$W_f = 5.69885 * 0.316422 (W_{TO}^{0.166652}) S_{cabin}^{1.061158} + (1 + 0.05 * N_{engine}) * 0.53 * S_{aft} W_{TO}^{0.2} (\lambda_{aft} + 0.5)$$

Estimation of Nacelle Weight

The engines proposed to be used in the aircraft are still under research and have not yet been developed for commercial use, hence the data is not available for the engine parameter. The Torenbeek estimates the weight of nacelle based on thrust required:

$$W_n = 0.065 T_{TO}$$

Estimation of Landing Gear Weight

Torenbeek and GD methods both provide a close estimation of the weight of landing gear:

$$GD \text{ Method: } W_g = 62.61 \left(\frac{W_{TO}}{1000} \right)^{0.84}$$

$$Torenbeek \text{ Method: } W_g = K_r (A_g + B_g W_{TO}^{0.75} + C_g W_{TO} + D_g W_{TO}^{1.5})$$

Powerplant Weight Estimation

Weight of Engines

The weight of engines is provided by the manufacturer in the catalog and the same value is used to calculate the further weights that depend on it.

Weight of Fuel System

The weight of the fuel system depends on where the engines are mounted. Though the configuration show that the engines are mounted on the fuselage, but the design does not have any specific bifurcation between wings and fuselage hence equation of wing mounted engines is used to calculate the weight of the fuel system.

$$W_{ec} = 88.46 \left(\frac{(l_f + b) N_e}{100} \right)^{0.294}$$

Weight of Propulsion System

The engines have an electric starting system.

$$W_{ess} = 38.93 \left(\frac{W_e}{1000} \right)^{0.918}$$

Weight of Accessory drives and Ignition System

As the engines use an electric starting system, the equation for estimation of weight of propulsion system includes the weight for accessory drives and ignition system.

Weight of Thrust Reversers

The estimate of the C.G effect due to thrust reverser can be calculated using the following equation:

$$W_{tr} = 0.18W_e$$

Fixed Equipment Weight Estimation

This group includes flight control system, electrical systems, instrumentation, avionics and electronics, air-conditioning, pressurization, de-icing, oxygen system, APU, furnishing, baggage, cargo, operational items and paint.

Weight of Flight Control System

Torenbeek provides a better estimation for weight of the flight control system

$$W_{fc} = K_{fc} W_{f0}^{\frac{2}{3}}$$

K_{fc} = 0.64 for airplanes with powered flight controls

Weight of Electrical System

For jet transport, GD method provides with a much better estimation of the weight

$$W_{els} = 1163 \left\{ \frac{W_{fs} + W_{iae}^{0.506}}{1000} \right\}$$

The Torenbeek method cannot be used as it uses the value of volume of passenger cabin for which the standards are yet to establish for a BWB aircraft.

Weight of Instrumentation, Avionics and Electronics

Torenbeek estimates the value to much better accuracy than GD method

$$W_{iae} = 0.575 W_E^{0.556} R^{0.25}$$

where W_E is the empty weight and R is the range in nautical miles

Weight of Air-conditioning, Pressurization and De-icing system

$$W_{api} = 6.75 p_{ax}^{1.28}$$

Weight of Oxygen System

Torenbeek provides the equation for oxygen system weight estimation.

$$W_{OX} = 40 + 2.4 N_{pax}$$

Weight Estimation of APU

The weight of APU has a range with equation based on aircraft take-off weight. The weight ranges from:

$$W_{APU} = 0.004W_{TO} \text{ to } 0.013W_{TO}$$

Weight Estimation of Furnishing

Torenbeek provides an equation compatible with BWB aircraft.

$$W_{fur} = 0.211(W_{TO} - W_F)^{0.91}$$

Weight of Baggage and Cargo Handling System

The GD method gives for passenger transport:

$$W_{bc} = K_{bc}(N_{pax})^{1.456}$$

Weight of Paint

There is no equation for estimating the weight of paint for a BWB aircraft, but a basic equation associated with density and volume of the paint used can be incorporated to find the weight of paint.

Table 43 Summary of Weight Estimation

Structural Weight		
	GD Method	Torenbeek Method
Wing	NA	33734.46
Empennage	1439.563	NA
Fuselage	Specialized Method	113739.8
Nacelles	NA	3997.663
Landing Gear	NA	6580
Total Structural Weight	159000	
Powerplant Weight		
Engine	Provided	20950
Fuel System	145	NA
Propulsion System	636	NA
Thrust Reverser	2095	
Total Powerplant Weight	23825	
Fixed Equipment		
Flight Control System	NA	2471
Electrical System	2475	NS
Instruments and Avionics	NA	2821
A/C, Pressurization & De-icing	NA	775
Oxygen System	NA	424
APU	Maximum Consideration	2373
Furnishing	NA	9671
Baggage & Cargo System	512	NA

3. Conclusion

The methods defined in the book are meant for conventional design which cannot be directly implemented for a BWB aircraft. With no aircraft for reference, the values calculated cannot be compared nor any approximation be done from the previous aircraft data. This method of calculation tends to accumulate a large error which needs to be rectified by detailed research.

17. Future Work

Stability and control analysis of the proposed aircraft is to be conducted. The inherent design drawback of the blended wing body makes the aircraft laterally unstable. Blended wing body configuration is a very novel design with its inherent drawbacks due to which it is not possible for the aircraft to be introduced in the commercial service sector. The CG tolerances are too big when compared to a conventional aircraft. This can be corrected if a part is integrated which can substitute the elevator without increasing the drag of the aircraft.

The aircraft design poses a danger due to instability without any computer augmented system. There needs to be sufficient research involved regarding the lifting and pitch control systems. There needs to be a research on the body integrated elevator which can provide pitch stability and be deflected for pitch control. The major problem with BWB design is the high angle of attack to provide required lift for landing which can make passengers very uncomfortable. With the use of the elevator, flaps can be employed to generate the required lift without involving high angle of attack.

References

- C Goldber, D. N. (2017). Economic Viability Assessment of NASA's Blended Wing Body N3-X Aircraft. *AIAA/SAE/ASEE Joint Propulsion Conference*. Atlanta: AIAA.
- Denieul, Y. (2017). *Preliminary Design of Control Surfaces and Laws for Unconventional Aircraft Configuration*. INSTITUT SUPERIEUR DE L'AERONAUTIQUE ET DE L'ESPACE (ISAE).
- Government, U. (n.d.). *United States Environmental Protection Agency*.
- Huijts, C., & Voskuil, M. (2015). The impact of control allocation on trim drag of blended wing body aircraft. *Aerospace Science and Technology*, 46, 72-81. Retrieved 12 20, 2017, from <http://sciencedirect.com/science/article/pii/S1270963815002084>
- Kimmel, W. B. (2004). *A Sizing Methodology for the Conceptual Design of Blended-Wing-Body Transports*. NASA.
- Larkin, G., & Coates, G. (2017). A design analysis of vertical stabilisers for Blended Wing Body aircraft. *Aerospace Science and Technology*, 64, 237-252. Retrieved 12 19, 2017, from <http://sciencedirect.com/science/article/pii/S1270963816310434>
- Liebeck, R. H. (2002). Design of the Blended Wing Body Subsonic Transport. *Journal of Aircraft*, 41(1), 10-25. Retrieved 12 20, 2017, from <http://arc.aiaa.org/doi/10.2514/1.9084>
- Lyu, Z., & Martins, J. R. (2014). Aerodynamic Design Optimization Studies of a Blended-Wing-Body Aircraft. *Journal of Aircraft*, 51(5), 1604-1617. Retrieved 12 20, 2017, from <https://arc.aiaa.org/doi/abs/10.2514/1.c032491>
- M. Bradley, K. D. (2011). *Subsonic Ultra Green Aircraft Research: Phase I Final Report*. Huntington Beach: NASA/CR.
- NASA. (n.d.). *NASA MADCAT*. Retrieved from <https://ti.arc.nasa.gov/news/MADCAT/>.
- Qin, N., Vavalle, A., Moigne, A. L., Laban, M., Hackett, K., & Weinerfelt, P. (2004). Aerodynamic considerations of blended wing body aircraft. *Progress in Aerospace Sciences*, 40(6), 321-343. Retrieved 12 20, 2017, from <http://sciencedirect.com/science/article/pii/S0376042104000569>
- Raymer, D. (2004). *Aircraft Design: A Conceptual Approach*. Sylmar: AIAA Education Series.
- Reckzeh, D. (2003). Aerodynamic design of the high-lift-wing for a Megaliner aircraft. *Aerospace Science and Technology*, 7(2), 107-119. Retrieved 12 20, 2017, from <http://sciencedirect.com/science/article/pii/S1270963802000020>
- Regan, C. D. (2008). *In-Flight Stability Analysis of the X-48B Aircraft*. Retrieved 12 20, 2017, from <http://arc.aiaa.org/doi/pdf/10.2514/6.2008-6571>
- Roskam, J. (1985). *Airplane Design*. Ottawa: Roskam Aviation and Engineering Corporation.
- Roskam, J. (1988). *What Drives Unique Configurations*. Retrieved 5 23, 2018, from <http://papers.sae.org/gsdownload/?prodcid=881353>

- Sammi Ammar, C. L.-Y. (2017). Conceptual design, performance and stability analysis of a 200 passengers Blended Wing Body aircraft. *Aerospace Science and Technology*, 325-336.
- Siouris, S., & Qin, N. (2007). Study of the effects of wing sweep on the aerodynamic performance of a blended wing body aircraft. *Proceedings of the Institution of Mechanical Engineers, Part G: Journal of Aerospace Engineering*, 221(1), 47-55. Retrieved 12 20, 2017, from <http://journals.sagepub.com/doi/abs/10.1243/09544100jaero93>
- Torenbeek, E. (2010). *Blended Wing Body Aircraft: A Historical Perspective*. Retrieved 12 20, 2017, from <http://onlinelibrary.wiley.com/doi/10.1002/9780470686652.eae1003/pdf>
- Wohlfahrt, K. N. (1994). *Tailless Aircraft in Theory and Practice*. Washington DC: AIAA Education.